uOttawa

L'Université canadienne
Canada's university

FACULTÉ DES ÉTUDES SUPÉRIEURES ET POSTOCTORALES

uOttawa

L'Université canadienne
Canada's university

FACULTY OF GRADUATE AND POSDOCTORAL STUDIES

Raymond M. Sturgeon
AUTEUR DE LA THÈSE / AUTHOR OF THESIS

M.Sc. (Biochemistry)
GRADE / DEGREE

Department of Biochemistry, Microbiology and Immunology
FACULTÉ, ÉCOLE, DÉPARTEMENT / FACULTY, SCHOOL, DEPARTMENT

Interplay Between Cations, Anionic Lipids, and Lipid-Protein Interactions at the Nicotinic Acetylcholine Receptor

TITRE DE LA THÈSE / TITLE OF THESIS

John Baenziger
DIRECTEUR (DIRECTRICE) DE LA THÈSE / THESIS SUPERVISOR

CO-DIRECTEUR (CO-DIRECTRICE) DE LA THÈSE / THESIS CO-SUPERVISOR

EXAMINATEURS (EXAMINATRICES) DE LA THÈSE / THESIS EXAMINERS

Danielle Carrier

Jean-François Couture

Gary W. Slater
Le Doyen de la Faculté des études supérieures et postdoctorales / Dean of the Faculty of Graduate and Postdoctoral Studies

INTERPLAY BETWEEN CATIONS, ANIONIC LIPIDS, AND LIPID-PROTEIN INTERACTIONS AT THE NICOTINIC ACETYLCHOLINE RECEPTOR

by

Raymond M. Sturgeon

Thesis submitted to the Department of Biochemistry, Microbiology and Immunology in partial fulfilment of the requirements for the degree of Master of Science

University of Ottawa
Ottawa, Ontario, Canada
April, 2009

Your file Votre référence
ISBN: 978-0-494-51658-4
Our file Notre référence
ISBN: 978-0-494-51658-4

ABSTRACT

Mixtures of phosphatidylcholine (PC) and phosphatidic acid (PA) are particularly effective at stabilizing a functional nicotinic acetylcholine receptor (nAChR). To test whether the ability of PA to adopt both monoanionic and dianionic states plays a role in lipid-nAChR interactions, we monitored the ionization state of PA in nAChR-reconstituted membranes. In the presence of the nAChR, PA head groups in PC/PA 3:2 membranes are stabilized in the monoanionic state. Stabilization of monoanionic PA in nAChR-reconstituted membranes accounts for some of the observed increase in membrane gel-to-liquid crystal phase transition temperature (T_m) upon nAChR incorporation, possibly by nAChR-induced pH reduction at the membrane surface. Increasing concentrations of cations at the bilayer surface and diacylglycerol within the bilayer account for the remaining shift in membrane T_m observed upon nAChR incorporation. We conclude that the nAChR, which is a cation-selective ion channel, alters its environment through both cation concentration and enzymatic activity.

ACKNOWLEDGEMENTS

My Master's program would never have been completed without the help, support and encouragement of a number of important people. At this point, I would like to say thank you to those who helped me along my chosen path.

- First and foremost, I want to say thank you to my family members: Mom, Dad, JP, Dave and Jen. Mom & Dad, this document would be a figment of my imagination without you. I can never thank you enough for believing in me. JP, I don't think I could have survived without your help, support and brotherly advice, and especially not without our e-mail conversations. Taking the time to talk about nothing helped me make it through everything. Thank you, brother.
- Dr. Baenziger, thank you for the opportunity to be your student, and the possibility to improve myself as both a student and a scientist. You expect a certain degree of independence from your students, and I may have had a tough time at first, but your continued confidence in me and my research made me more confident about my own work and I feel my ability to work independently has greatly improved under your steady guidance. I'm proud to have been a part of your lab, and I know the experiences I've gained here will help me excel in the next stage of my life.
- Corrie, your lab habits, work ethic and drive for success have been an inspiration over the past 4 years. I have never met anyone with more motivation and drive, Corrie, and anyone who works in our lab (the whole building?) should try and model

their attitude towards science and the enjoyment thereof after your example. The hockey debates, Friday afternoon soccer games, shinny hockey games and your friendship will not be forgotten. Thank you.

- Thank you to all current and past members of the Baenziger lab for putting up with my habits and making my time in the Baenziger lab extremely enjoyable: Casey Carswell, Lopa Dey, Daniel Gagné, Mike Goodreid, Yara Harb, Danny Hill, Yi Huo, Prateek Khatri, Jon Labriola, Roxanne Landry, Nadine Lavigne, Marc Rigden, Wajid Sayeed, Ali Syed and Shuzhi Wang (special thank you for the TLC help and the sample preps).

- Thanks for the morning coffee conversations, Leslie! Take good care of the ol' coffee-maker ☺

TABLE OF CONTENTS

LIST OF FIGURES

Chapter 1

Chapter 3

Chapter 4

Chapter 5

Chapter 6

LIST OF TABLES

Chapter 1

Chapter 5

LIST OF ABBREVIATIONS

1-2-DAG	1-Palmitoyl-2-oleoyl-3-sn-glycerol
1-3-DAG	1-Palmitoyl-3-oleoyl-2-sn-glycerol
α-Btx	α-Bungarotoxin
Å	Angstrom
ACh	Acetylcholine
AChBP	Acetylcholine binding protein
ATR	Attenuated total reflectance
Ca^{2+}	Calcium ion
CAPS	3-(Cyclohexylamino)-1-propanesulfonic acid
Carb	Carbamylcholine
CH_3OH	Methanol
$CHCl_3$	Chloroform
CFPE	1,2-Dioleoyl-*sn*-Glycero-3-Phosphoethanolamine-N-(Carboxyfluorescein)
Chol	Cholesterol
C=O	Carbonyl group
COO^-	Carboxyl group
Da	Dalton
DAG	Diacylglycerol
DB	Dialysis Buffer
Dib	Dibucaine
EDTA	Ethylenediaminetetraacetic acid
Eth	Ethidium bromide
Fln	Fluorescein
FTIR	Fourier Transform Infrared
^1H	Hydrogen
^2H	Deuterium
^2H_2O	Deuterium oxide

HCOOH	Formic Acid
HP-TLC	High Performance Thin-Layer Chromatography
ICD	Intracellular Domain
IRE	Internal Reflection Element
K_D	Dissociation constant
kDa	KiloDalton
λ	Wavelength
LBD	Ligand Binding Domain
M	Molarity
Mg^{2+}	Magnesium ion
M1	1st transmembrane spanning segment of the nAChR
M2	2nd transmembrane spanning segment of the nAChR
M3	3rd transmembrane spanning segment of the nAChR
M4	4th transmembrane spanning segment of the nAChR
MS	Mass Spectrometry
Na^{+}	Sodium ion
nAChR	Nicotinic Acetylcholine Receptor
NCI	Non-competitive Inhibitor
$N\text{-}^{1}H$	Peptide hydrogen
$N\text{-}^{2}H$	Peptide deuterium
NT	Neurotransmitter
O	Open/activated state of the nAChR
PA	1,2-Diacyl-*sn*-glycero-3-phosphate
PC	1,2-Diacyl-*sn*-glycero-3-phosphocholine
PE	1,2-Diacyl-*sn*-glycero-3-phosphatidylethanolamine
PI	1,2-Diacyl-*sn*-glycero-3-phosphoinositide
PL	Phospholipase
POPA	1-Palmitoyl-2-oleoyl-*sn*-glycero-3-phosphate
POPC	1-Palmitoyl-2-oleoyl-*sn*-glycero-3-phosphocholine
PS	1,2-Diacyl-*sn*-glycero-3-phosphoserine
R	Resting state of the nAChR
Rb^{+}	Rubidium ion
SM	Sphingomyelin

T_m	Gel-to-liquid crystal phase transition temperature
TMD	Transmembrane Domain
TRB	*Torpedo* ringer buffer
Tris	Tris (hydroxylmethyl)aminomethane
U	Membrane uncoupled state of the nAChR

Chapter 1: General Introduction

Introduction

The ability of humans to interact with the world around them relies on our nervous system. The nervous system is an intricate network of specialized cells, called neurons, and it is involved in controlling our five senses, as well as higher brain functions, such as attention, learning and memory. The diversity of the types of neurons and the connections between them are responsible for the ability of the nervous system to interpret the innumerable signals that we experience each and every day, and to transmit the information contained in those signals to our brains almost instantaneously (1, 2). An important part of the nervous system is the communication between individual neurons at the junctions between them, called synapses. The conversion of electric signals generated by neurons to a chemical signal sent from one neuron to its neighbor at a synapse is the basis of neurotransmission (3, 4).

Communication throughout the nervous system occurs through electrical signals called action potentials. Action potentials are waves of charged ions that move along neurons (Fig. 1.1). These large concentrations of charged ions are generated by a rapid diffusion of ions into a neuron through gated ion channels. The action potential travels to the end of the neuron along the path to the brain. Upon arrival of an action potential at the nerve terminal, the neuron is depolarized and storage vesicles containing small molecules called neurotransmitters fuse with the pre-synaptic membrane, releasing the neurotransmitters into

Figure 1.1

Neurotransmission and the Players Involved. Signals are transmitted through neurons in the form of action potentials (yellow arrow), which are waves of charged ions (green spheres). At the synapse where neurons meet, the electrical signals are converted to chemical signals following the arrival of an action potential by the release of neurotransmitters (NT) (blue triangles) into the synaptic cleft. On the adjacent neuron, ligand-gated ion channels (green) open pores within the post-synaptic membranes in response to NT binding. The resulting rapid influx of ions into the post-synaptic neuron propagates the electrical signal.

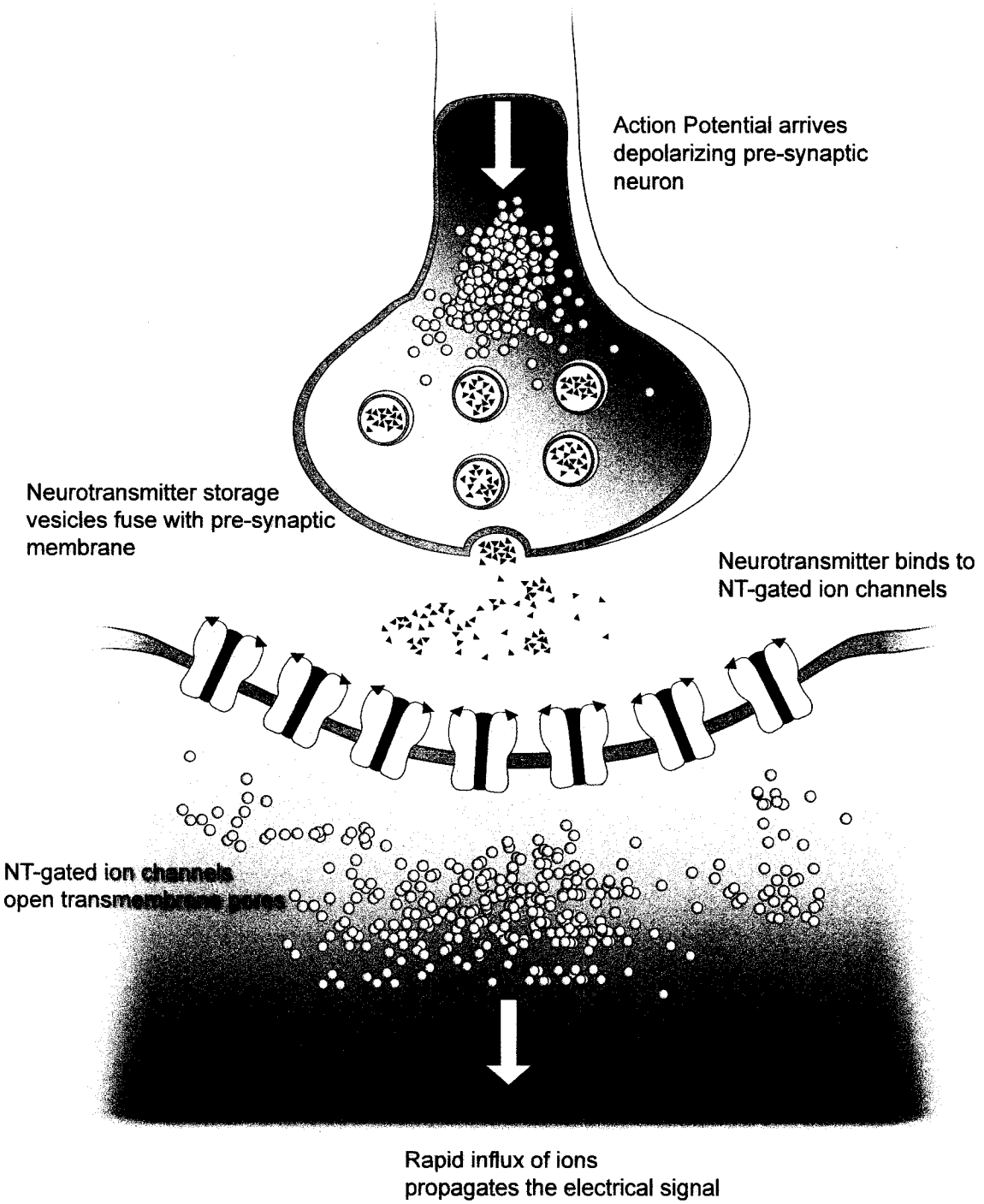
Action Potential arrives
depolarizing pre-synaptic
neuron
Neurotransmitter storage
vesicles fuse with pre-synaptic
membrane
Neurotransmitter binds to
NT-gated ion channels
NT-gated ion channels
open transmembrane pores
Rapid influx of ions
propagates the electrical signal

the synaptic space (5). The neurotransmitters flow through the synaptic space and bind to neurotransmitter receptors within the post-synaptic membrane. These receptors belong to a class of proteins that form pores in the post-synaptic membrane that open in response to external triggers (in this case the binding of neurotransmitters) referred to as ion channels (6). Charged ions will flood through the open pores into the post-synaptic neuron, thereby generating an action potential. The electrical signal is propagated through this neuron and the nervous system.

The process described above is one of many potential responses that can occur at a synapse upon the arrival of an action potential. There exists an expansive number of chemical processes occurring at synapses due to diverse factors: the variety of neurotransmitters that can be released from the pre-synaptic neuron, the diversity of the receptors found at synapses, and their distribution between the pre- and post-synaptic membranes. The synapse is also influenced by external signals, as sensory experiences can affect synaptic function, resulting in the formation of long-term effects (this is the basis for how memories are formed) (7). Deficiencies of any of the processes of neurotransmission results in serious health afflictions, including myasthenic syndromes and other serious diseases (5, 6).

The work presented in this study focuses on one of these ligand-gated ion channels (LGIC) found on the post-synaptic membrane that plays a significant role in neurotransmission. This particular channel gates open its cation-selective pore in the membrane in response to the binding of the neurotransmitter acetylcholine (ACh) (Fig. 1.2), allowing rapid diffusion of cations from the synaptic space into the post-synaptic neuron. The first experiments suggesting the existence of the channel were conducted using nicotine; hence the receptor is referred to as the nicotinic acetylcholine receptor (nAChR). Owing to

Figure 1.2

Nicotinic Receptors Interact with Diverse Agonists and Antagonists. Agonists bind to the nAChR agonist binding site leading to opening of the transmembrane pore. Nicotine was the first agonist found to elicit strong responses, but acetylcholine and carbamylcholine both elicit stronger responses. Antagonists bind to either the agonist binding site or the pore binding site, inhibiting the nAChR by locking it in a non-functional state or blocking the pore of the channel, respectively. Local anesthetics procaine, tetracaine and dibucaine block the channel inhibiting the flux of cations. D-tubocurarine is the active antagonist in curare (9).

Agonists

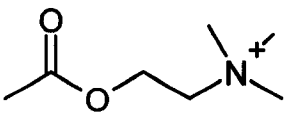

Acetylcholine

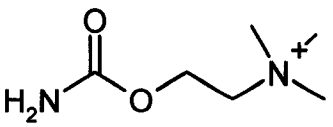

Carbamylcholine

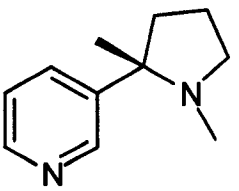

Nicotine

Antagonists

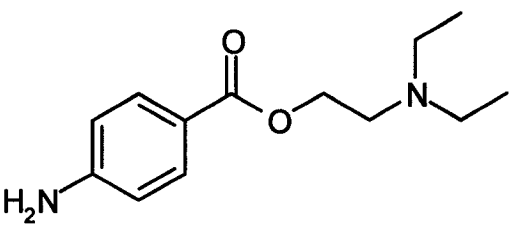

Procaine

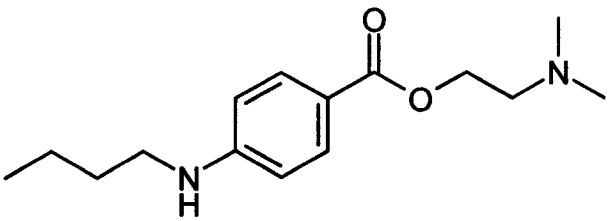

Tetracaine

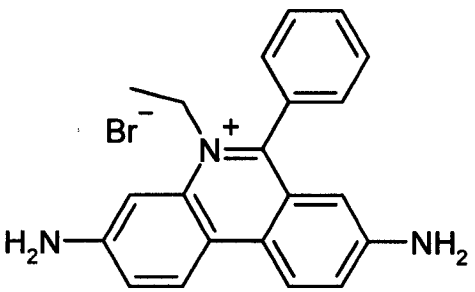

Ethidium Bromide

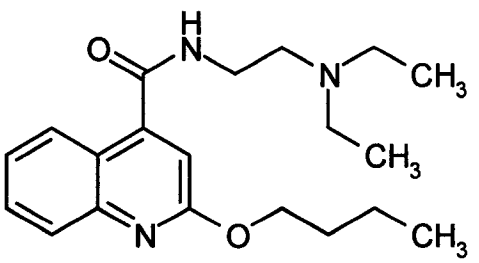

Dibucaine

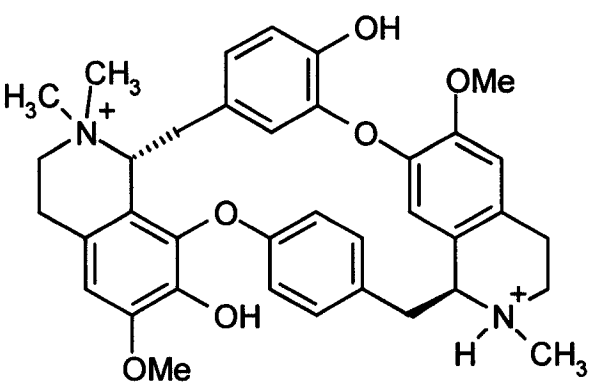

d-Tubocurarine

the availability of an abundant source and the high homology to human forms of the receptor, the nAChR isolated from the electric fish *Torpedo californica* has been studied extensively throughout the past 40 years. The biochemical data acquired throughout this period resulted in further understanding of the mechanism of neurotransmission, but also laid an important foundation upon which a structural model has been built (8). This structural model allows for the proposal of sophisticated hypotheses regarding the mechanism of the nAChR, its role in affecting the strength of synaptic communication and thus its modulation of higher cognitive function.

1.1 – Nicotinic Acetylcholine Receptor: The Early Years

The story of the nAChR unknowingly began in the 2nd half of the nineteenth century with Claude Bernard studying the effects of curare, an extract from poisonous vines of Central America that causes relaxation and paralysis (9). Bernard concluded that curare was acting at the peripheral ending of motor nerves (10). However, following extensive work from 1870 to 1910, John Newport Langley had proven that this was not the case. Langley found that muscle contraction of an anaesthetized fowl could be caused by application of nicotine to the muscle, but the addition of curare prior to nicotine abolished any response. After abolishing the contractions with curare, however, direct electrical stimulation of the muscle cells still resulted in contraction (11). The pertinent conclusion from these experiments is that the curare did not act directly on the contractile cells, but rather on an "accessory substance of the muscle cell." As the observed response was the result of adding nicotine, Langley dubbed the substance a "nicotinic receptive substance" (10, 11). The

experiments conducted by Langley over 100 years ago and the conclusions drawn are the basis of drug-receptor theory that we know today.

At the time, however, the notion of a receptor for small chemical molecules found within tissue was against the traditional rationale of drug action (10). Criticisms of Langley's theory about the "receptive substance" came from noted scientists of the period, citing a lack of evidence for the interactions between a receptive "side chain" and the small chemical compounds. However, support of drug-receptor theory came from work in the 1920s, which indicated that neuronal communication occurred via a chemical messenger released by a neuron exerting its effects on the adjacent neuron. Further support came from Alfred Joseph Clark in 1933 when he published a collection of pharmacological data from multiple sources that had been analyzed or reanalyzed in his book *The Mode of Action of Drugs on Cells*. Calculations within this book suggested that, based on the molecular size and postulated cell surface area, small molecules like adrenaline or acetylcholine likely exert their action by binding, or "uniting with", certain receptors within tissues (10). Despite Clark's publication and its re-assertion of the drug-receptor theory, it remained just that, a theory, until the late 1960s and early 1970s when receptor proteins were first isolated from cell membranes.

In order to validate the concept behind the drug-receptor theory, isolation of the "receptive substance" was ultimately required. However, isolation seemed a daunting task as researchers were unsure how a small chemical, such as acetylcholine, could elicit substantial intracellular changes and orchestrate the complex processes of neuronal communication. However, researchers were resolute in their ability to isolate and identify Langley's "receptive substance." Moreover, in light of recent work on the concept of the ion channel, it was hypothesized that Langley's "receptive substance" was likely a protein that would open

an ion channel within neuronal membranes upon binding of either nicotine or acetylcholine, resulting in the propagation of the electrical signals in the nervous system (12). The next chapter of the story involves the attempts to identify, isolate and purify these hypothesized proteins: nicotine/ACh-responsive ion channels.

1.2 – Nicotinic Acetylcholine Receptor: Identification and Isolation

The search for the nicotine/ACh-responsive ion channel began by trying to identify a source from which large amounts of the receptor could be isolated. Rather than searching by application of acetylcholine to various tissues, Changeux and colleagues used something more specific: snake venom toxin that binds only the receptor. Acetylcholine has the potential to bind to other proteins, including acetylcholine esterase, resulting in specificity issues when searching for the nAChR (13). As a result of this concept, α-Bungarotoxin (α-Btx), from the snake *Bungarus multicinctus* was applied to tissues and exhibited blockage of the effects of cholinergic agonists, with no detectable effects on acetylcholine esterase functions. The tissues used for these experiments were isolated from the electric ray *Torpedo* (primarily *californica*) and the electric eel *Electrophorus electricus* (13-15). These animals have the ability to deliver large electric currents in order to kill prey. The generation of these large currents is a result of a high concentration of cells with high concentrations of nicotinic receptors, called electrocytes, in specialized organs called electroplaques. Application of α-Btx to these tissues led to dramatic binding, indicating these tissues contain a significant concentration of the nAChR. Isolation of the tissue from electroplaques from the *Torpedo*, an abundant source of the nAChR, led to extensive use of the *Torpedo* nAChR for biochemical studies.

By the mid-to-late 1970s, a number of groups had developed methods to purify large quantities of the nAChR from *Torpedo californica* electroplaques (16-18). SDS-Page gel electrophoresis of the purified nAChR indicated that the nAChR was composed of 4 different polypeptides or subunits (18, 19). Due to the migration pattern, the subunits were named α, β, δ and γ, with molecular weights of 40,000, 49,000, 60,000 and 64,000 Da, respectively (15, 19). A number of different characteristics of the subunits, including the subunit responsible for agonist binding (the α-subunit) (19), and the predicted subunit stoichiometry of 2:1:1:1 α:β:δ:γ (molar ratio), were determined, eventually leading up to the primary amino acid sequence of the subunits from the complete DNA sequences of the 4 nAChR subunit genes (20). The full sequencing of the subunit amino acids led Mishina *et al.* to inject *Xenopus* oocytes with the mRNA of the nAChR subunits and examine their expression and electrophysiology (21). In this system, functional nAChR was expressed on the surface, and electrophysiology traces indicated that all 4 subunits, with the proper stoichiometry, were required for expression of functional nAChR. Without the α-subunit mRNA, the receptors lost α-Btx binding ability, further indicating that the α-subunit is responsible for agonist binding.

At this point, a number of groups focused on the functional aspects of the nAChR while other groups worked on determining the structure of the nAChR (22). The structure of the nAChR, however, would remain unsolved until 2005 when a structural model was published. The model incorporates extensive biochemical data as well as the recently published structure of the acetylcholine binding protein (AChBP) to establish the first high-resolution model of the nAChR (for detailed review of biochemical data and the structure, see (9, 23)).

1.3 – Nicotinic Acetylcholine Receptor Structure

Even with almost 30 years of biochemical and biophysical data in hand, there remains the requirement for high-resolution structural data in order to determine the mechanism of how the nAChR translates the binding of a neurotransmitter into gating open its cation-selective pore. In order to fully understand the molecular basis behind the multiple events that occur during the gating process, exquisite detail regarding the structure is required, as has been evidenced by the publication of crystal structures of the potassium channel (24-27). The majority of membrane proteins remain resistant to standard high-resolution imaging techniques, resulting in only a select handful of crystal structures of membrane proteins having been solved prior to 2005. However, the study of the nAChR took its first step into the atomic age with the publication of the crystal structure of a structurally related protein to the nAChR: the AChBP (28, 29). From this point, models, concepts and hypotheses were made regarding the mechanisms by which the nAChR bound agonist and the resulting conformational changes, but the structure of the AChBP would ultimately provide an important part of the determination of the structural model 4 years later (8). At this point, I will review the brief history of the structural information used as the foundation for the structural model and I will also review said model briefly. With the availability of the Unwin model, studies involving the nAChR must address findings in a structural context; therefore an understanding of the structure and its intricacies is crucial.

1.3.1 – Acetylcholine Binding Protein (AChBP) – Prior to 2001, there had been a large amount of research on the ligand binding domain of the nAChR gathered in an effort to

figure out how the agonist bound. In 2001, the study of the ligand binding domain took a huge leap forward with the publication of the structure of the AChBP. The AChBP is a soluble protein found in snails stored in glial cells. In response to ACh release from the pre-synaptic neuron, the AChBP is released into the synaptic space and modulates the transmission of the neuronal signal by binding the ACh, effectively inhibiting the ACh-induced response on the post-synaptic neuron (28). The AChBP is a stable homopentamer that aligns with the N-terminal domain of the LGIC superfamily; the subunits of the AChBP are most closely related to the α-subunits of the nAChR. The AChBP also binds other known agonists and antagonists of the nAChR including nicotine, d-tubocurarine (the effective agent in curare) and α-Btx (29). The crystal structure of the AChBP was solved to 2.7Å and the structure indicates that the AChBP protomer can be used as an example of an α-subunit of the nAChR.

When viewed along the five-fold axis, the AChBP pentamer forms what the authors described as a "windmill toy with petal-like protomers" (Fig. 1.3) (29). From the side, the AChBP forms a cylinder with a vestibule down the center, with dimensions of 62 x 80Å. The individual protomers are arranged around the central pore with a near five-fold symmetry. The protomers each consist of an N-terminal α-helix, two short 3_{10} helices and a core of ten β-strands (Fig. 1.4).

The ligand binding sites of the AChBP are located in cavities that are formed by a series of loops from the principal face of one subunit (A) and the complementary face of the adjacent subunit (B) (Fig. 1.4B). These cavities are located roughly 30Å above the C-terminal, which is the rough location of the beginning of the transmembrane domain of the

Figure 1.3

Structure of the AChBP from *Lymnaea stagnalis*. Top, AChBP viewed from the top, down through the central vestibule. The pentamer is formed by 5 identical subunits (A-E). The binding sites are located at the interfaces between the subunits, on the outer perimeter of the cylindrical pentamer. Bottom, AChBP viewed from the side. Ligands bind at the interface between the principal (+) subunit (blue) and the complementary (-) subunit (yellow) in a pocket formed from contributing loops and residues from both subunits. PDB accession code: 1I9B (29).

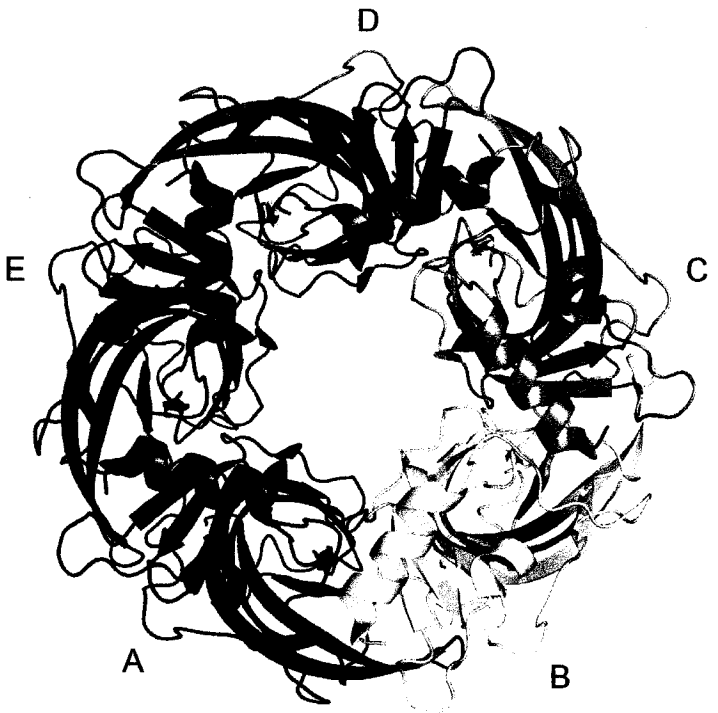

90°

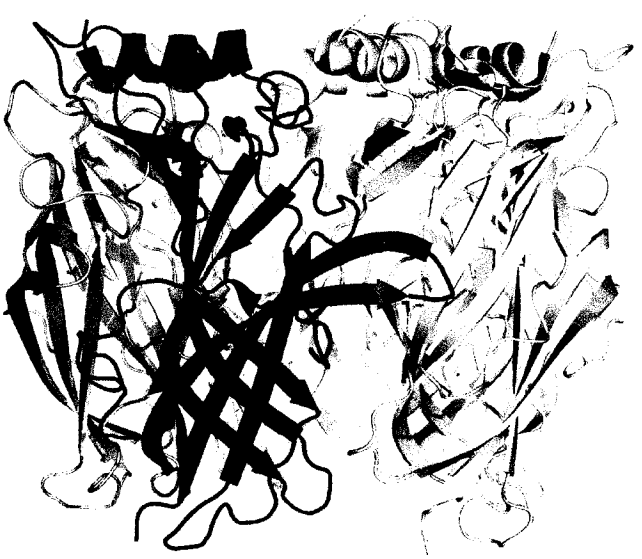

Principal (+) Complementary (-)

Figure 1.4

Individual Subunit of the AChBP Pentamer. A, Single subunit with important structural elements highlighted. The inner sheet (red) and the outer sheet (blue) form the 10-stranded β-sandwich core of each subunit. The C-loop (yellow) has been shown to undergo significant conformational rearrangements upon agonist binding, leading to movements of the Cys-loop (green). B, Subunit shown with the principal (left) binding site residues and the complementary (right) binding site residues highlighted in yellow. The agonist binds to this site, located at the interface of adjacent subunits, and the C-loop closes around the agonist bringing the residues highlighted into closer contact with the agonist. AChBP shown in the HEPES-bound state with C-loop slightly closed over the binding site compared to the unbound state.

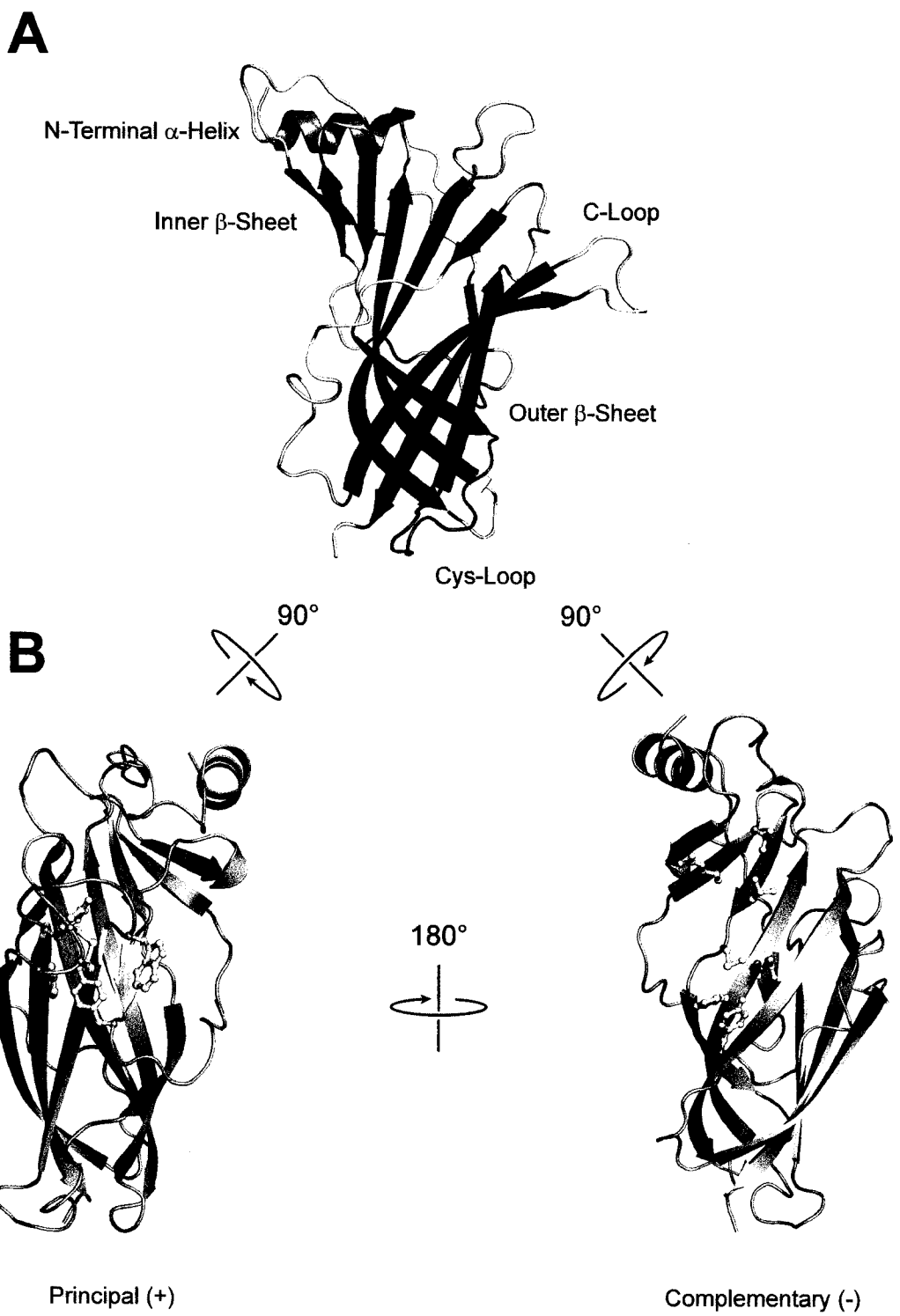
A
N-Terminal α-Helix
Inner β-Sheet
C-Loop
Outer β-Sheet
Cys-Loop
B
90°
90°
180°
Principal (+)
Complementary (-)

nAChR. This distance correlates with previous data regarding the location of the binding site in the nAChR. These cavities are lined by residues that have been shown to be involved in ligand binding in the nAChR through photoaffinity labeling and mutagenesis studies (30-33). The residues in the site are from Loop A (Y89), Loop B (W143, W145) and Loop C (Y185, C187-188, Y192) from the principal subunit. From the complementary subunit, residues contributing to the binding site are from Loop D (W53, Q55), Loop E (R104, V106, L112, and M114) and Loop F (Y164). All the large, aromatic residues in the binding site are thought to coordinate the ligands through cation-π interactions between the quaternary amine groups of the ligands and the π electrons of the aromatic residues (31).

In a recent paper, multiple structures of the AChBP from a saltwater mollusk were solved in the presence of different agonists and antagonists (34). The structures indicated that upon agonist binding, the C-loop (Loop C in the previous section) undergoes a rigid-body motion swinging almost as much as 11Å upon binding of agonist. Like a cap closing over the binding site, the C-loop conformational change moves residues in closer register with the agonist, resulting in tight association between the aromatic residues and the quaternary amine of the agonists. In the presence of antagonists, the C-loop is in an "open" conformation, possibly due to the larger size of the antagonists. In the apo form, the C-loop is also in the "open" conformation, possibly allowing agonist access to the binding site.

The AChBP structures provided the first atomic resolution information regarding the agonist-binding domain of the nAChR. The location of the AChBP residues and the ligand binding sites generally agreed with the nAChR biochemical and biophysical data presented prior to the publication of the AChBP structure. The AChBP would also be an important part of the publication of the structural model in 2005.

1.3.2 – nAChR Transmembrane Domain (TMD) – In 2003, using electron microscopy of crystalline post-synaptic membranes, Miyazawa *et al.* published the structure of the membrane-spanning pore, or the transmembrane domain, of the nAChR (35). The images were refined to 4Å resolution, allowing imaging of the helices within the transmembrane domain as well as some information regarding approximate orientations of the side chains. The helices form a pore through the membrane that taper together towards the intracellular side, with each of the subunit helical bundles forming what appear to be propeller blades. The structure indicates there are effectively 2 structural components to the transmembrane pore of the nAChR: an inner ring of helices that interacts with cations passing through the pore, and an outer ring of helices that interacts with each other and the lipid membrane (Fig. 1.5). The outer ring effectively acts as a barrier between the lipid membrane and the transmembrane pore.

The gate of the nAChR is located within the pore at the center of the membrane, as dictated by the structure. The gate is formed by large, bulky, hydrophobic residues at the center of the pore, at the narrowest point between the helices. The residues involved are αL251, αS252, αF256, and αV255 (Fig. 1.5B). The gap in the pore at this constriction point is roughly 3Å across, which is too narrow for a hydrated ion to pass through without giving up its first hydration shell. It would be energetically unfavorable for the ion to lose any of the associated water molecules in the pore without compensating interactions with the pore (does not seem likely due to the absence of hydrophilic residues at this point). The hydrophobic girdle, therefore, acts as an energetic barrier to the passage ions in the closed state, rather than a physical occlusion. The location and mechanism of the gate reconciled some ambiguous results concerning the specific location of the gate. As well, the notion of

Figure 1.5

The TMD of the nAChR. A, Top: nAChR TMD viewed from the lipid membrane (grey bars). Each individual subunit forms a 4-helix bundle (blue and yellow). Cations (green) can pass through the central pore through the membrane. Bottom: nAChR TMD viewed from the synaptic cleft. M2 helices (red) form the pore through the membrane, and the inner ring of helices (red dashed line). M1, M3 and M4 form the outer ring of helices (grey dashed line), "protecting" the pore from the surrounding lipid membrane (helical rings described in text). B, Individual subunit of the TMD. Transmembrane segment of each helix shown in yellow with grey section protruding from the membrane. The M2 helices line the channel, and the hydrophobic gate residues (red, ball-and-stick) are found at the narrowest point in the middle of the membrane. PDB accession code: 1OED (35).

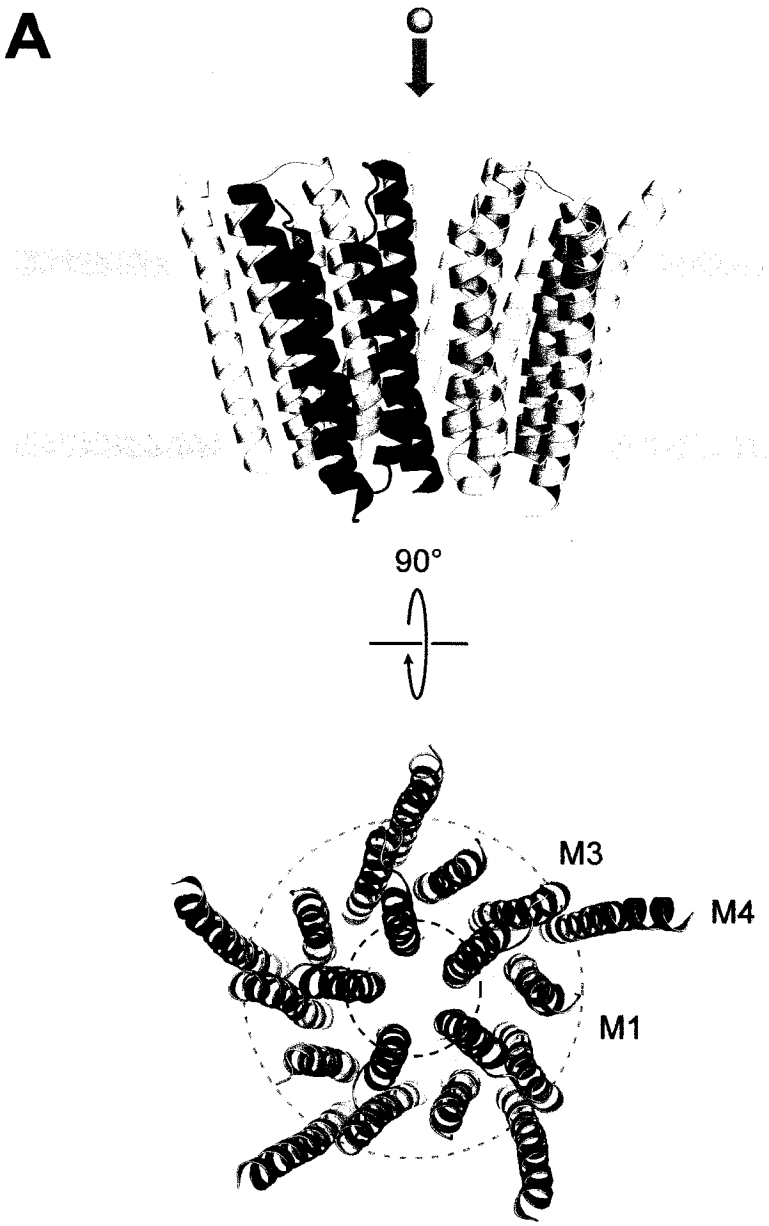
A
i
90°
M3
M4
M1
B
M3
M4
Hydrophobic
Gate Residues
M2
M1

an energetic barrier rather than a simple physical barrier was an intriguing aspect of the nAChR TMD in the closed state.

*1.3.3 – **Refined Structural Model of the nAChR*** – Following the publication of the AChBP and the transmembrane pore of the nAChR, Unwin used these 2 components and was able to refine the images recorded from the nAChR in crystalline membrane tubes used to image the pore and form a structural model of the nAChR (8). The model takes into account the extensive past biochemical data, allowing a detailed description of the entire receptor in the closed-channel form. With a model in hand, it is now possible to visualize the mechanism of how agonist binding is translated into gating the transmembrane pore.

The structural model indicates near five-fold symmetry down the central axis of the channel when viewed from the synaptic cleft, similar to the AChBP (Fig. 1.6). From the membrane, the structure appears wedge-shaped. Each individual subunit contains 3 distinct domains and as a result the protein can easily be sectioned into its 3 domains: the ligand binding domain (LBD), the transmembrane domain (TMD) and the intracellular domain (ICD). Similar to the AChBP, the ligand binding domain consists of an N-terminal helix and a β-sandwich core consisting of ten β-strands, with 2 distinct sheets (inner and outer sheets). The loops that play a role (A-F) in the agonist binding are also identified in each of the subunits, but now with the model of the nAChR structure, more inferences can be made regarding the interface between the ligand binding and transmembrane domains and the potential changes during the gating process (Fig. 1.7).

The ligand binding sites appeared in similar conformations to those identified in the AChBP structure, but the C-loop of the nAChR model was weakly resolved, suggesting that

Figure 1.6

Refined Model of the nAChR. Left, nAChR viewed normal to the membrane. The secondary structure elements divide the nAChR into 3 distinct domains: the ligand binding, transmembrane and intracellular domains. The front 2 subunits are highlighted in blue (α) and yellow (δ). The grey bars indicate approximate location of the membrane leaflets. Right, nAChR viewed from the synaptic space. The 5 subunits (α: blue, β: red, δ: yellow, and γ: green) are oriented around the central pore with near five-fold symmetry. PDB accession code: 2BG9 (8).

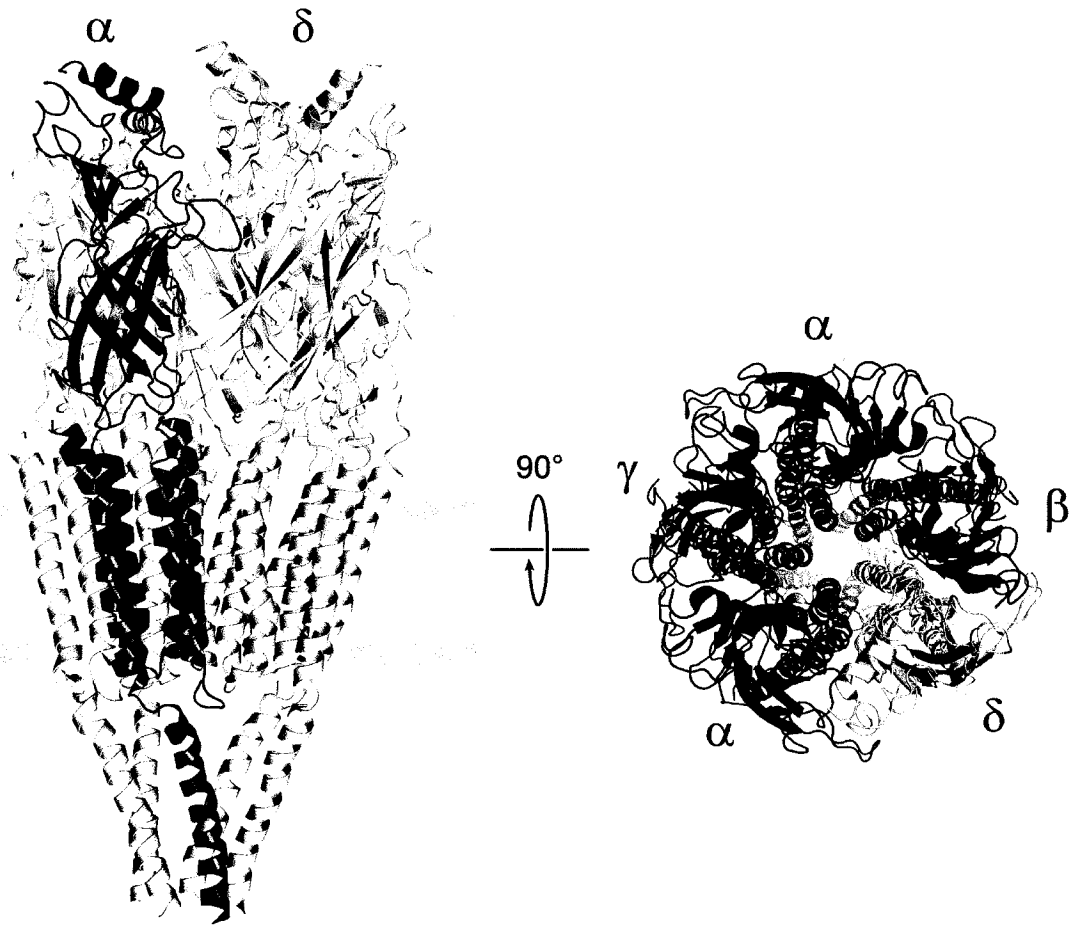
α
δ
90°
γ
α
β
α
δ

Figure 1.7

Individual α-subunit of the nAChR. The LBD, like that of the AChBP, consists of an N-terminal α-helix, an inner β-sheet (blue) and an outer β-sheet (red) (β-sandwich core) and the loops involved in binding. The Cys-loop and the M2-M3 linker are thought to be involved in translating the agonist binding signal to the opening of the transmembrane pore. M2 lines the channel pore, while M1, M3 and M4 occlude lipids from the pore region. Loops A, B and C are involved in agonist binding and undergo similar conformational changes to the AChBP upon binding of agonist. Grey bars indicate approximate location of the membrane.

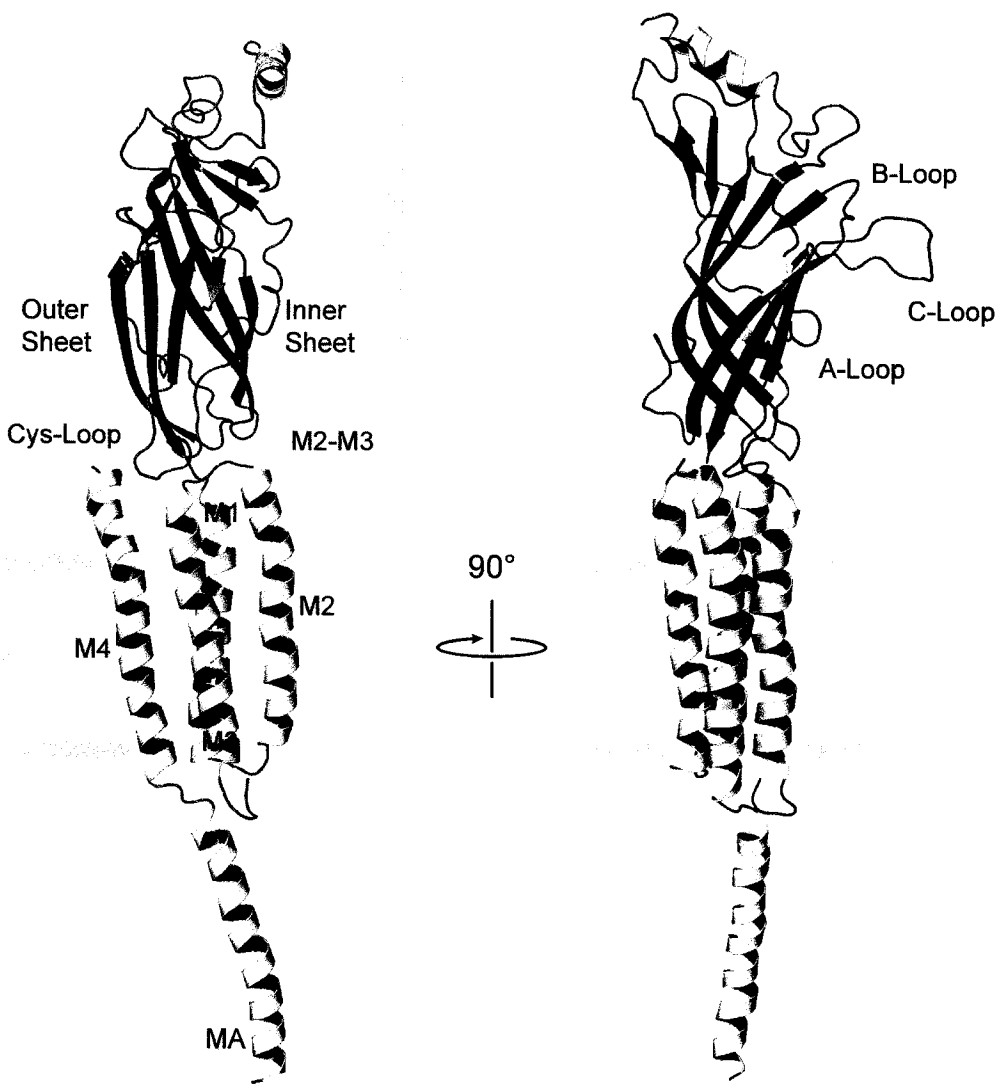
Outer Sheet
Inner Sheet
Cys-Loop
M2-M3
M1
M2
M4
M3
MA
90°
B-Loop
C-Loop
A-Loop

the C-loop is flexible in the absence of ACh (8). The residues, however, that have been shown to be involved in the binding of ACh were visible in the nAChR model binding sites. These side chains include Y190, Y198 and C192 of the C-loop and W149 of the B-loop in the α-subunit. In this closed-channel conformation of the nAChR, the C-loop is projected further away from the binding site pocket, supporting the movements of the C-loop predicted by the AChBP structures with different ligands.

1.3.4 – Agonist Binding to Channel Gating – An important point of the nAChR model is the "distorted" conformation of the α-subunits compared to the non-α subunits. It appears that the conformation of the α-subunits is held in this distorted state wherein the β-sheets are rotated roughly 10° from the non-α subunits relative to an axis normal to the membrane plane. Included with the alternate conformation of the β-sheets in the ligand binding domain, the C-loop exhibits a reduced twist compared to the C-loops of the non-α subunits. A series of interactions between subunits adjacent to the α-subunits are likely responsible for stabilizing the distorted conformation of the α-subunits in the unbound state. The importance of the altered conformation is that the ligand binding domains of the α-subunits likely undergo a conformational transition upon binding of agonist that results in a non-α subunit conformation. The result of agonist binding would likely be that the B-loop rotates clockwise while the C-loop twists and rotates in order to close these loops over the bound agonist.

Based on the AChBP structures with bound agonist (34), it is likely that the rotations of the B- and C-loops result in a rigid-body movement of the inner and outer sheets and the helices that lead to conformational changes of the loops at the domain interfaces. The

movements of the connecting links between the domains result in conformational changes within the transmembrane domain, potentially twisting or rotations of the helices, resulting in opening of the transmembrane pore. Due to the limited resolution of the structural model, the specific gating movements of the domain interfaces and the transmembrane helices are not immediately clear. However, potential mechanisms of the gating movements resulting in channel opening have been proposed (5, 36-41). The likely candidates involved in the coupling of binding to gating involve the loops connecting the structures between the 2 domains that are located at the interface of the ligand binding and transmembrane domains. The β1-β2 loop, located at the domain interface, contains the residues E45 and V46. These 2 residues are thought to "straddle" P272 in the M2-M3 linker, and the concerted movements in the ligand binding domain are propagated to the channel via the interaction of these residues (42). Mutation of these residues results in impaired function of the channel. However, as mentioned, the specific residues involved could ultimately be different than the residues listed above, or the gating conformational changes could involve additional residues as future structural information is solved.

The interface between the 2 domains is the location where the conformational changes that occur in the ligand binding domain are transmitted to the transmembrane domain, resulting in gating of the pore. While the specific mechanism of the interactions occurring between the contributing loops at this interface is not clear, it is evident that these 2 domains must remain in proximity in order for the physical or electrostatic interactions to govern the translation of binding to gating. Analysis of the overall charge of the 2 domains indicates that there are overall opposite charges found on the extracellular and intracellular domain residues that comprise the domain interface. In the α-subunit, the extracellular

domain carries an overall negative charge at the domain interface while the transmembrane domain carries an overall positive charge (Fig. 1.8) (40). Rather than specific salt bridges or electrostatic interactions, mutant cycle analysis indicated that maintaining the overall attraction between the 2 domains stabilized the functional properties of the nAChR. In light of the extensive research indicating the requirement of anionic lipids for proper nAChR function, the potential interactions between these charged interfaces and anionic lipids and the possibility that anionic lipids maintain the proximity of the domains merits further investigation.

Now that there is a structural model of the nAChR, the events that occur upon agonist binding and the conformational changes that occur in distinct regions of the receptor can be visualized. Following the publication of the structure, the ability to reconcile data in terms of the model allows for detailed mechanistic interpretations, eventually leading towards a full understanding of the mechanism of action of the nAChR.

1.4 – Nicotinic Acetylcholine Receptor and the Lipid Membrane

Initial studies on the nAChR described in section 1.2 were primarily carried out on the receptor-rich membranes isolated from *Torpedo* in its native environment, with the surrounding accessory proteins and components of the membrane. In order to examine the nAChR at the level of single molecular events, an important step in the isolation procedure involves reconstitution of the nAChR into the lipid bilayer. Establishing a consistent and reproducible purification and reconstitution protocol required examining the functional properties of the nAChR at each step of the protocol to ensure that function was largely unaffected. The reconstitution protocol of the nAChR was heavily modified and optimized

Figure 1.8

Electrostatic Interactions Govern the Coupling of the LBD to the TMD. The overall negative charge on the LBD is due to negatively charged residues (red, ball-and-stick) within loops 2, 7 and 9. The TMD carries an overall positive charge at the interface due to the positively charged residues (blue, ball-and-stick) on the Pre-M1, M2-M3 linker and Post-M4. The opposite charges in these domains result in an overall attraction between the domains, effectively ensuring coupling between the 2 domains (40).

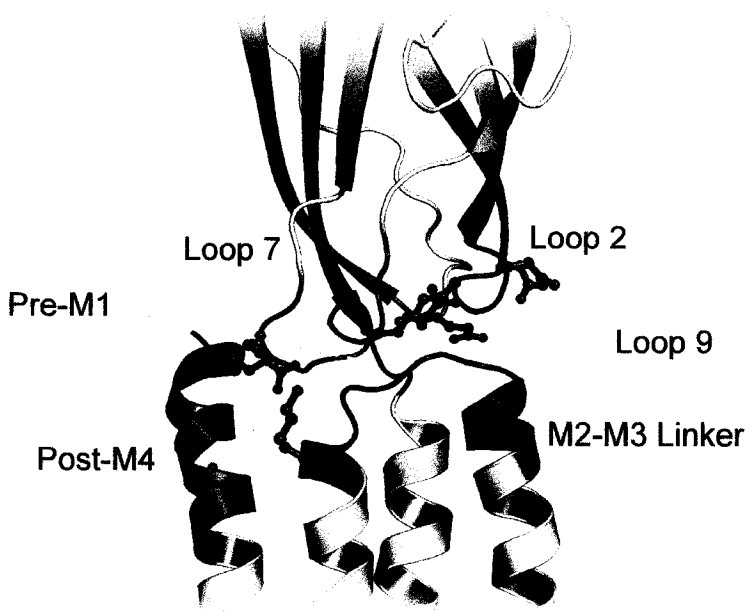
Loop 7
Loop 2
Pre-M1
Loop 9
M2-M3 Linker
Post-M4

throughout the late 1970s, with multiple groups attempting to establish the first reproducible and effective reconstitution protocol.

*1.4.1 – **Membrane Solubilization*** – Establishing the reconstitution protocol first involved finding the appropriate detergents to use for removing the nAChR from its native *Torpedo* membrane prior to affinity purification. Early studies used a variety of detergents to remove the nAChR from its native membrane. The retention of the nAChR agonist binding properties was found using several detergents, both anionic and non-anionic, but the degree to which the agonist binding properties were retained was different depending on the detergent (43). In some cases, large-scale purifications were carried out using Triton X-100 to solubilize the membranes, removing the nAChR. In the majority of these particular reconstitutions, the ability of the nAChR to bind agonist was retained, but cation flux ability of the nAChR was lost (44, 45). The issue would be resolved with the publication of a reconstitution protocol using cholate, an anionic detergent, to solubilize the membrane, but there was one aspect that was key in retaining both agonist binding and the ability to flux cations. The protocol used a mixture of cholate and 2.5% soybean phospholipids to solubilize the membrane (46). Purified nAChR following this solubilization exhibited a rapid, agonist-dependent cation flux that was inhibited by α-Btx. Following the publication of this protocol, focus of research became identifying those lipid mixtures that when included with the detergent during solubilization and purification would result in functional nAChR.

*1.4.2 – **Reconstitution and Exogenous Lipids*** – The protocol published by Epstein and Racker highlighted the functional relationship between the nAChR and its membrane environment. With purification in the absence of phospholipids, their measurements indicated no cation flux or the desensitization of the nAChR in the prolonged presence of agonist. However, upon inclusion of even a small percentage of lipids in the solubilization mixture, cation flux and desensitization were observed (46). With the retention of the functional properties of the nAChR, a protocol had been established that consistently resulted in functional nAChR, and this marked the starting point for future studies aimed at optimizing the protocol. The Changeux group included an even greater amount of lipids within their reconstitution procedures, and found similar results: agonist-induced flux that was abolished in the presence of α-Btx, indicative of a functional nAChR following reconstitution (47). Further work based on the protocol established by Epstein and Racker led to early electrophysiology traces on the nAChR. Nelson and colleagues used the reconstitution protocol to obtain functional nAChR in lipid vesicles and spread the vesicles into planar bilayers to measure the conductance. Again, the nAChR exhibited pharmacological specificity, Carb-induced activation and in the continual presence of the agonist, the receptor became desensitized (48).

The presence of exogenous cholesterol during the purification/reconstitution procedure was examined as an effector of stabilizing function of the nAChR. However, rather than using soybean asolectin, which contains various phospholipid species, 3:1 mixtures of phosphatidylethanolamine (PE) and phosphatidylserine (PS) were used. This report indicated that the nAChR was non-functional without cholesterol, but the presence of cholesterol resulted in significant increases in the functional behavior (49). Further studies

determined different aspects of the functionality of the nAChR depending on the lipids present, and the general orientation of the nAChR in these functional proteoliposomes (50). Throughout these reports, the constant finding was that the presence of lipids during purification was essential to retaining the function of the nAChR following reconstitution.

The activity of many integral membrane proteins is intricately related to the surrounding lipid environment. There is extensive information showing that the membrane environment affects the function of membrane proteins (51, 52). The nAChR is dependent on the presence of either endo- or exogenous phospholipids in order to retain functionality following the reconstitution procedure. The question becomes: Are there specific lipids that are required throughout the reconstitution procedure, or does the nAChR simply require the presence of phospholipids? The native *Torpedo* nAChR-rich membranes are quite diverse in terms of the phospholipids present (Table 1.1) (53-55). The values in Table 1.1 indicate a large amount of cholesterol (Chol) within the membrane, as well as a diverse group of phospholipids including phosphatidylcholine (PC), PS, PE, sphingomyelin (SM), and phosphatidic acid (PA) (Fig. 1.9). One characteristic of the *Torpedo* nAChR-rich membranes is the large amount of negatively charged lipids suggesting that these membranes are generally negatively charged. Attempting to deduce precisely which lipids were responsible for the stabilization of the functional nAChR was difficult at first as the protocol used soybean asolectin (46), which is a mixture of various phospholipids in different amounts (55). From here, phospholipids within the *Torpedo* membranes were systematically examined for their role, if any, in stabilizing the functional state of the nAChR.

1.4.3 – Reconstitution into Defined Lipid Mixtures – The functional dependence of the nAChR on the surrounding lipid membrane generated a large amount of attention. Multiple

Table 1.1 - Approximate Percentages of Lipids in Membranes

Lipid	*Torpedo californica*		Soybean Asolectin
Reference	Schiebler and Hucho (54)	Gonzalez-Ros *et al*. (53)	Demel *et al*. (55)
Cholesterol	20	20-30	-
PC	32	38.4	24
PE	22	35.8	39
PS	10	10.9	19
PI	4	-	1
SM	1.5	2.3	-
PA	-	2.9	6
Other	10	-	11

Figure 1.9

General Structure of Lipids Found within the nAChR-rich *Torpedo* Membranes. Phospholipids consist of long, hydrophobic acyl chains, a glycerol connecting segment and a phosphate head group. The lipid acyl chains shown here are palmitoyl (16:0) and oleoyl (18:1). The different R-groups on the phosphate head group result in the variety of phospholipid species found in the *Torpedo* membranes. A number of these phospholipids are anionic leading to an overall negative membrane. Cholesterol is also found in large quantities within these membranes.

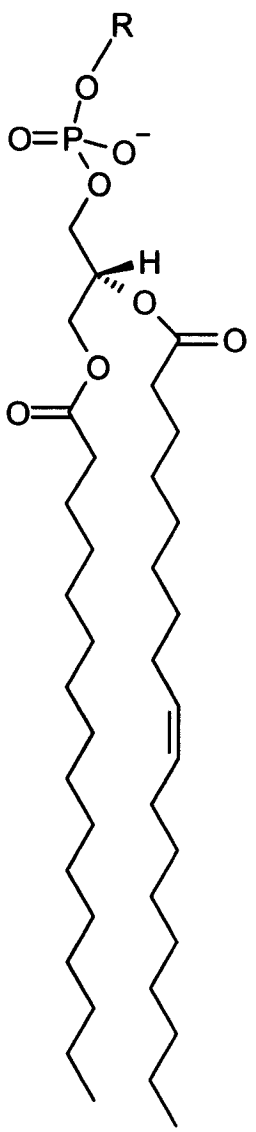

Generic
Phospholipid

R = H

Phosphatidic Acid (POPA)

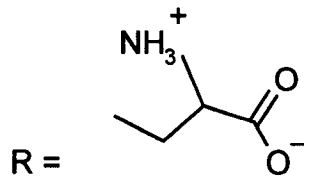

Phosphatidylserine (POPS)

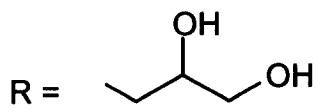

Phosphatidylglycerol (POPG)

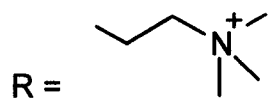

Phosphatidylcholine (POPC)

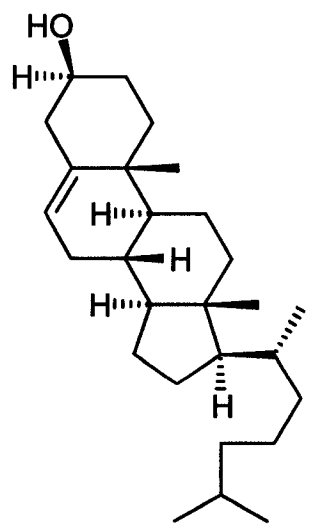

Cholesterol

groups began to examine how specific lipids interact with the nAChR, resulting in functional or non-functional conformations. Early studies examined lipid mixtures containing PC as the primary component with different amounts of other phospholipids, including PE, PS and PA, as well as neutral lipids such as Chol and androstane (56, 57). Reports indicated that Chol was necessary in order to stabilize the functional nAChR (49, 58). This finding seems logical as the *Torpedo* membranes generally contain 20-30% Chol. However, other studies found that the presence of anionic lipids was sufficient to stabilize function of the nAChR following reconstitution (56, 59). These studies examined the cation flux ability of the nAChR using radio-labeled cations ($^{22}Na^{+}$ or $^{86}Rb^{+}$) measuring the amount of these cations found within the proteoliposomes following an incubation period. Flux studies, however, exhibit artifacts that result in the inconsistencies between studies. There are some issues, including vesicle size and morphology and the rates of flux of the nAChR in the different membranes, which leads to variation within the data. As a result, groups used a normalized response measurement that takes into account the concentration of the nAChR and the vesicle size, and a threshold was set below which any response levels are considered non-functional (58). This "all-or-nothing" approach resulted in some lipid mixtures being considered by some researchers to be non-functional, while other researchers found response levels indicative of a functional nAChR. The inconsistencies led to different considerations of what was considered a "functional membrane" and ignore the possibility that the presence of different lipids results in different levels of functional nAChR within a reconstituted membrane.

Despite disagreements regarding the specific lipid requirements of the nAChR, there was a general consensus regarding the importance of anionic lipids and Chol. Studies examining the function of the nAChR by various methods found that there was an inherent

requirement for anionic lipids (59-68), and while Chol is generally considered important there remains some controversy over the effects of Chol. An emerging hypothesis was that there were specific lipid binding sites on the nAChR and these sites were key for the stabilization of function in the reconstituted proteoliposomes. Fluorescence quenching studies using brominated lipids, both phospholipids and Chol, found that these lipids were quenched by the nAChR in such ways that the phospholipids were located in the lipid annulus, the ring of lipids surrounding the nAChR, while the Chol was located in non-annular sites on the nAChR, or specific binding sites on the transmembrane domain of the nAChR (57, 68). While these sites have not specifically been located and/or proven, the possibility remains that the nAChR binding specific lipids is vital to stabilization of nAChR function. The binding of specific lipids to the nAChR has also been implicated in stabilizing particular aspects of the structure, thereby indicating that the presence of different lipids should result in different structural conformations of the nAChR (69, 70). The presence of Chol, for example, was suggested to stabilize the α-helical content of the nAChR, specifically in the transmembrane domain, while PA was thought to stabilize the β-sheet content. However, subsequent studies indicated that the overall secondary structure of the nAChR remains relatively similar in various lipid membranes (71).

1.4.4 – Lipids Modulate the nAChR – A consistent finding is that PA, an anionic phospholipid with a small, negatively charged head group, is effective at stabilizing the nAChR in a functional conformation. Early reports indicated that PA was particularly effective, but the presence of Chol was also required in order to stabilize the functional nAChR (58). Confusion still existed, though, as there were reports that PA was not

sufficient to stabilize the nAChR function without Chol (60), while still other reports indicated that PA alone stabilized a functional nAChR and Chol did not (67). Some reports indicated that rather than specific lipid requirements, there were optimal membrane physical parameters that needed to be met in order to stabilize the functional nAChR (58). Still other reports indicated that rather than the physical conditions of the bilayer the membrane composition was the most important aspect of the membrane in stabilization of nAChR function (62). Despite the continual contradiction, one consistency was that the nAChR was found to be optimally functional in membranes containing PA and Chol, rather than any other anionic lipid or neutral lipids.

In an attempt to address the inconsistent reports regarding the specific lipids required rather than mixtures of lipids, nAChR-reconstituted membranes with a wide variety of lipid compositions were analyzed using FTIR difference spectroscopy (61). FTIR difference spectroscopy examines the ability of the nAChR in planar bilayers to undergo conformational change following the application of agonist (65, 66). The results from FTIR difference measurements indicated that PA and Chol were able to independently modulate the proportion of the functional nAChRs to the non-functional nAChRs. First, the nAChR was examined in pure PC bilayers, which have been shown to result in a non-functional conformation of the nAChR. Difference spectra were then recorded from the nAChR in PC membranes with increasing amounts of PA or Chol (72). The degree to which the nAChR was stabilized in the functional resting state increased with increasing amounts of PA or Chol, eventually reaching a plateau in each different system. The results indicated that the conformational equilibrium between the functional, resting state of the nAChR and the non-functional state of the nAChR is modulated by the lipids present, with PA being more effective at shifting this equilibrium towards the functional state.

In light of the effectiveness of PA, further studies were performed in order to assess the influence of PA, and the requirement of Chol. By reconstituting the nAChR into membranes containing PC and PA at a molar ratio of 3:2, daCosta *et al.* found that the nAChR was stabilized in a functional conformation that appeared to be almost as functional as the native membranes or PC/PA/Chol 3:1:1 membranes (73). By further examining the nAChR in these membranes, the same group confirmed that PS, another anionic phospholipid, was not able to stabilize the nAChR in a functional conformation in the absence of Chol (74). In the membranes containing PS, without Chol, the conformational equilibrium of the nAChR was similar to the equilibrium observed in the pure PC bilayers. Still further studies examined the nAChR in membranes containing other anionic lipids rather than PA, and found that some lipids could substitute for PA and stabilize a functional nAChR (75). In contrast, a recent report found that the nAChR exhibited only moderate functionality in a binary membrane mixture of PC/PG 3:2; the only binary mixture containing an anionic lipid, phosphatidylglycerol (PG), with PC that resulted in any degree of functional nAChR (76). In the end, the general consensus is that PA is the most effective anionic lipid at retaining full function of the nAChR following reconstitution.

There were additional observations in the PA-containing nAChR membranes that suggested PA was unique in its interactions with the nAChR. In PC/PA 3:2 membranes, the presence of the receptor led to changes in certain physical properties of the lipid bilayer. When compared to PC/PA 3:2 membranes without the nAChR, the PC/PA-nAChR reconstitutions underwent the transition from the liquid crystal phase to the rigid gel phase at significantly higher temperatures. An increase of ~13°C in the gel-to-liquid crystal phase transition was observed in PC/PA 3:2 membranes upon incorporation of the nAChR (73). Other anionic lipids, such as PS and PG, exhibit subtle shifts in the phase transition

temperature (74), but not nearly as significant as in PC/PA-nAChR reconstitutions. It appeared that membranes containing anionic lipids able to modulate the nAChR functional conformation (PA, for example) were susceptible to changes in physical properties upon the incorporation of the receptor. This bi-directional coupling, observed in PA-containing membranes, indicates potential unique interactions occurring between the nAChR and PA.

However, despite the intense focus on determining the role of anionic lipids in stabilizing optimal nAChR function, the mechanism of how PA modulates the conformational equilibrium of the nAChR has yet to be resolved. PA appears to be unique among the anionic lipids in its ability to stabilize the functional nAChR in binary membranes with PC; focus was directed towards traits of PA that could be responsible for its modulation of the nAChR functional conformation. One possibility that was examined is the unique chemical trait of PA, the ability of PA to exist in 2 different head group ionization states within the membrane, and its role in modulating the functional conformation of the nAChR. The ability of the PA head group to exist in different ionization states at near-physiological pH values is a unique chemical trait among the lipids that are commonly found in the nAChR-rich *Torpedo* membrane. A paper published in 1993 examining the effects of PA on nAChR function suggested that the ability of PA to exist in the dianionic state was responsible for the modulatory role of PA on nAChR conformational equilibrium (64). However, based on the FTIR data presented and their interpretations thereof, there were some issues regarding the accuracy of their conclusions. Interpretation of FTIR data from a previous paper from the McNamee group also led to inaccurate conclusions, therefore reducing their credibility regarding the quality of their FTIR data as well as the conclusions drawn from the spectra. Based on these reasons, the dianionic hypothesis described in the

1993 paper, which is an interesting idea regarding PA modulation of the nAChR functional conformation, still warrants an in-depth investigation.

Statement of Objectives

I began a project oriented towards the ultimate goal of understanding the mechanism of how PA effectively stabilizes the functional conformation of the nAChR, while other anionic lipids require the presence of Chol. Specifically, I wanted to examine the potential role of the dianionic PA head group in modulation of the nAChR, and the possibility that the nAChR preferentially associates with the dianionic state of the PA head group. My research began with the following hypothesis:

- The dianionic state of the PA head group is essential in stabilizing the functional conformation of the nAChR in reconstituted membranes, and this dianionic state of PA is stabilized by the presence of the nAChR.

My initial objective was to confirm that FTIR spectroscopy could be used to monitor ionization state of PA head groups within lipid membranes. By systematically examining the FTIR spectra recorded from lipid membranes without the nAChR and the spectral changes observed upon changing the pH, I wanted to establish a reproducible protocol applicable to monitoring PA head group ionization in nAChR-reconstituted membranes.

As my project progressed, the focus of my thesis shifted based on the results obtained while addressing my first hypothesis. My results indicated that the dianionic state of the PA head group was not involved in stabilizing the functional nAChR. In fact, it appeared that in the presence of the nAChR, the monoanionic state of the PA head group was stabilized by the nAChR, rendering the dianionic state inconsequential in affecting the nAChR conformational state. Based on these findings, I began to investigate how the monoanionic state of PA is stabilized in the nAChR-reconstituted membranes. The stabilization of the

monoanionic state appeared to be related to the bi-directional coupling highlighted in section 1.4.4. The 2nd section of my thesis was based on the following hypothesis:

- The stabilization of the monoanionic state of the PA head group is partly responsible for the altered physical properties of lipid membranes upon reconstitution of the nAChR.

Towards this end, my work began to examine the influence of different factors on the physical properties of the bilayer, ultimately aimed at providing a deeper understanding of lipid modulation of the nAChR, and the role of the lipid membrane in influencing the strength of synaptic communication.

Chapter 2: Materials & Methods

Materials. Frozen *Torpedo californica* electroplax tissue was obtained from Aquatic Research Consultants (San Pedro, CA). 1-Palmitoyl-2-Oleoyl-*sn*-Glycero-3-Phosphocholine (POPC), 1-Palmitoyl-2-Oleoyl-*sn*-Glycero-3-Phosphate (POPA), 1,2-Dioleoyl-*sn*-Glycero-3-Phosphoethanolamine-N-(Carboxyfluorescein) (CFPE), and 1-Palmitoyl-2-Oleoyl-*sn*-Glycerol (DAG) were from Avanti Polar Lipids, Inc. (Alabaster, AL). High purity Burdick & Jackson chloroform ($CHCl_3$) and methanol (CH_3OH) were obtained from Honeywell (Morristown, NJ). Carbamylcholine Chloride (Carb), dibucaine (Dib), ethidium bromide (Eth) and fluorescein (Fln) were from Sigma (St. Louis, MO).

nAChR Purification and Reconstitution. The nAChR was affinity purified on a bromoacetylcholine bromide-derivatized Affi-Gel 102 column (Bio-Rad; Richmond, CA) as described elsewhere (73). For each reconstitution, crude nAChR membranes from roughly 300 g of *Torpedo* electroplax tissue were solubilized for 1 h at 4°C in a total volume of 100 mL of dialysis buffer (100 mM NaCl, 10 mM Tris-HCl, 0.1 mM EDTA, 0.02% w/v NaN_3, pH = 7.8) containing 1% cholate. The solubilized membranes were centrifuged for 30 min at 87,000 X *g* to pellet insoluble material and the supernatants were applied to a 10 mL affinity column at a flow rate of 1 mL/min. The column-bound nAChR was first washed with a 3.2 mM lipid solution in 1% cholate dialysis buffer (Lipid A). The column-bound nAChR was then washed with 32.5 mL of a 1.3 mM lipid solution in 1% cholate dialysis buffer (Lipid B). The column-bound nAChR was further washed with 32.5 mL of a 0.13 mM lipid solution in

0.5% cholate dialysis buffer (Lipid C). The nAChR was then eluted from the column with a 0.13 mM lipid solution in 250 mM NaCl, 0.1 mM EDTA, 0.02% NaN_3, 5 mM phosphate, pH = 7.8, with 0.5% cholate and 10 mM Carb (Lipid D). After elution from the column, nAChR fractions were pooled and then dialyzed 5 times against 2 L of dialysis buffer with buffer change approximately once every 12 hours. The dialyzed membranes were centrifuged at 120,000 X *g* for 2 h to pellet the reconstituted membranes, which were resuspended in 2 mM phosphate buffer (pH = 7.8). Purity of nAChR aliquots from elution fractions was analyzed by 12% SDS-PAGE with Coomassie Blue staining. For the delipidated sample (see Chapter 4), the column was washed with buffer containing 15 mM cholate and no exogenous lipids. The sample was eluted from the column using a similar elution buffer again containing no exogenous lipids, leaving the purified nAChR solubilized in cholate with no lipids. The absence of lipids was confirmed using FTIR spectroscopy (see below).

Lipid Extraction. The final lipid composition of the reconstituted membrane samples was determined using high-performance thin layer chromatography (HP-TLC) on lipids extracted from reconstituted membrane samples. Lipids were extracted from the reconstituted membrane samples using a modified Bligh & Dyer extraction protocol (77). Lipid standards were dried down under N_2 from stocks in $CHCl_3$, dissolved into aqueous buffer and extracted using the same protocol as the nAChR-reconstitutions. For each sample, 500 μg of PC (as checked by Phospholipids C assay; Wako Chemicals USA; Richmond, VA), (and the corresponding masses of other lipids, if present, and nAChR), were extracted from the nAChR-reconstituted membranes and standards. The samples were diluted to a total volume of 1.6 mL in Tris dialysis buffer and the diluted sample was added to 6 mL of high purity

Burdick & Jackson organic solvent (1:2 $CHCl_3$:CH_3OH) and the mixture was shaken vigorously. An additional 2 mL of $CHCl_3$ and 2 mL dialysis buffer were added to the mixture (final ratio 1:1:0.9 $CHCl_3$:CH_3OH:sample in dialysis buffer; total 11.8 mL). Extraction tubes were then centrifuged at 500 X *g* for 10 minutes to separate the aqueous and organic $CHCl_3$ phases. Using a stretched glass Pasteur pipette, the bottom organic $CHCl_3$ phase (total 4 mL) containing extracted lipids was removed and transferred to a small glass vial. An additional 4 mL of $CHCl_3$ was added to the extraction tube, and the extraction tube was shaken and centrifuged again (same settings). The organic $CHCl_3$ phase was removed using a new stretched Pasteur pipette and added to same glass vial as the first 4 mL of organic $CHCl_3$ phase. The extra 4 mL of $CHCl_3$ and repetition of the shaking/centrifugation ensures complete extraction of the lipids. The 8 mL of $CHCl_3$ (with the extracted lipids) was evaporated under a stream of N_2 drying the lipids on the bottom of vial. Lipids were resuspended in 500 μL $CHCl_3$ to obtain final lipid concentration of 1 mg/mL PC in $CHCl_3$ (and corresponding concentration of other lipids, if present). Lipids in $CHCl_3$ were stored under N_2 in -20°C freezer until used for HP-TLC.

High Performance Thin-Layer Chromatography (HP-TLC). The extracted lipids were run on HP-TLC Silica gel plates (60Å 4.5 μM particle size 200 μM thickness) from Whatman Laboratory Products, as previously described elsewhere (78). Plates were washed twice in a TLC tank using 100 mL 1:1 $CHCl_3$:CH_3OH as solvent system. Tanks were then washed with distilled water prior to solvent equilibration. Tanks were allowed to equilibrate for 1 h with the following TLC solvent system: $CHCl_3$:CH_3OH:$HCOOH$:H_2O (50:37.5:3.5:2 vol:vol). Plates were spotted with 15 μg PC of each sample (with corresponding masses of

other lipids, if present). Washed and spotted plates were then placed in the equilibrated tank until the solvent front reached 0.5 cm from the top of the plate. Plates were dried for 45 minutes before being immersed in 50 mL of staining solution (0.03% G250 Coomassie Blue in 30% CH_3OH in 0.1 M NaCl) and placed on shaker for 30 minutes or until adequately stained. Plates were then transferred into fresh destaining solution (30% CH_3OH in 0.1 M NaCl) for 15 minutes. Destaining step was repeated twice, or until background staining had been reduced while sample bands remained stained. Stained HP-TLC plates were then photographed immediately, and dried overnight prior to wrapping in plastic wrap for preservation.

The HP-TLC plate standard analysis was performed using a similar protocol to the HP-TLC analysis described above. The lipid standards were prepared in aqueous buffer by mixing PC and PA in the desired molar ratio. The concentration of PC was assayed by Phosphocholine assay prior to extraction. The lipids in each standard were extracted using the same method as the reconstituted membranes (see above). The extracted lipid standards were dried down and resuspended in $CHCl_3$ at a PC concentration of 1 mg/mL, with the corresponding PA concentration based on the lipid molar ratio. For each standard, 10 μg of PC (and the corresponding amount of PA) was spotted on the HP-TLC plate and run with the lipids extracted from the nAChR-reconstituted membranes. Densitometry was used to obtain an estimate of the amount of PA vs. intensity of the band on the TLC plate, and interpolation used to determine amount of PA in the lipids extracted from the reconstituted membranes. Data presented herein are averages from at least 2 standard HP-TLC plates.

Lipid samples to be analyzed by Mass Spectrometry were run on a single 10 cm X 20 cm aluminum TLC plate (Whatman) in a Benzene:Isopropanol:Ethyl Acetate:Formic Acid (72.5:3.5:22:2 vol:vol) solvent system. Large quantities, 250 μg per half plate, of the lipid samples were spotted across an entire plate (20 cm plate width, with 19 cm lane width leaving small space on each side). Following the run of the plate, a section of the plate was stained to locate the sample bands of interest. The remaining portion of the plate was cut and the Silica gel, where the lipid bands were located, was scraped and the silica was suspended in $CHCl_3$. Lipids on the Silica gel dissolved from the Silica into the $CHCl_3$. The $CHCl_3$ was aspirated off of the top of the silica and placed in a glass vial and the $CHCl_3$ was evaporated under a stream of N_2. The lipids removed from the silica by the $CHCl_3$ were dried in the bottom of the glass vial, and the lipids were resuspended in aqueous buffer for MS-MS analysis (performed by Jeff Smith, at the Ottawa Institute of Systems Biology, University of Ottawa).

Transmission FTIR Spectroscopy. All FTIR spectra were recorded on a FTS-40a, FTS-575 or FTS-7000 spectrometer (Varian; Randolph, MA). All spectrometers were equipped with a DTGS detector. For the analysis of lipid thermotropic phase behavior, 250 μg of nAChR was incubated at 4°C in ^2H_2O phosphate buffer for precisely 72 hours in order to exchange peptide N-^{1}H for N-^{2}H. Samples were then stored at -80°C until used for FTIR spectroscopy (no longer than one week in freezer prior to use). Prior to FTIR analysis, samples were individually thawed, centrifuged and resuspended in 30 μL of ^2H_2O phosphate buffer, and subjected to five freeze thaw vortex cycles. Samples were then deposited on a 1 cm diameter CaF_2 window and the excess buffer evaporated with a gentle stream of dry N_2. The nAChR

film was then rehydrated with 8 μL of *Torpedo* Ringer buffer (250 mM NaCl, 5 mM KCl, 2 mM $MgCl_2$, 3 mM $CaCl_2$ and 20 mM Tris) in ^2H_2O (pD 7.0) and sandwiched between a second CaF_2 window with a 12 μM Teflon spacer. The sandwich was placed in a thermostatically-controlled transmission cell from Harrick Scientific (Ossining, NY) and spectra recorded at 2 cm^{-1} resolution signal averaging 4000 scans. Pure lipid samples (no nAChR) were not exchanged for 72 hours. For these samples, dried lipids were dissolved in a 10% dispersion w/v in *Torpedo* ringer buffer in ^2H_2O at a desired pD, and the pD verified by litmus paper. For the pure lipid samples, 8 mL of the sample was placed on the CaF_2 window and sandwiched wet between a second CaF_2 window with a Teflon spacer. After the "sample sandwich" was prepared for both the lipids alone and the nAChR-reconstituted samples, spectra were recorded from both using similar technical protocols.

The data acquisition protocols for assessing the thermotropic phase behavior of membranes with and without the nAChR have been described elsewhere (73). In brief, the sandwich was placed in the thermostatic transmission cell equilibrated with an RTE-110 or RTE-117 water bath/circulator (Neslab; Newington, NH). Spectra (2 cm^{-1} resolution and 128 scans) were recorded at 1°C intervals as the sample was cooled from 35 to -15°C. The actual temperature of the sample cell was monitored using an electronic thermometer (Barnant; Barrington, IL) with a type J thermocouple probe. All spectral deconvolution was performed using GRAMS/AI v.7.01 software (Galactic; Salem, NH).

FTIR Difference Spectroscopy. FTIR difference spectra were recorded at 22.5°C using the attenuated total reflectance technique as described in detail elsewhere (61). Briefly, two

spectra were recorded with *Torpedo* Ringer buffer flowing past a nAChR film that was deposited on the surface of a germanium internal reflection element. The flowing buffer was switched to an identical buffer containing 50 μM Carb and a spectrum recorded of the Carb bound state of the nAChR. The nAChR film was then washed with *Torpedo* Ringer buffer to remove the nAChR-bound Carb, and the data acquisition protocol was repeated, for a total of 30 cycles. All spectra were recorded at 8 cm^{-1} resolution signal averaging 512 scans/spectrum. Each presented spectrum is the average of at least 55 spectra from at least 3 different films from at least 2 different reconstitutions. The difference spectra were baseline corrected between 1800 and 1000 cm^{-1} and were interpolated to an effective resolution of 4 cm^{-1}.

pH Titration Spectroscopy. FTIR spectra at varying pH values were recorded at 22.5°C using the attenuated total reflectance technique similar to a modified difference spectroscopy protocol. The film of either pure lipids or nAChR-reconstituted membrane samples were deposited on the surface of a germanium internal reflection element and placed in a thermostatically-controlled cell and this cell placed in the spectrometer. *Torpedo* Ringer buffer with additional buffers for the high and low pH ranges (Standard *Torpedo* Ringer with 10 mM Tris, 10 mM sodium acetate and 10 mM CAPS) flowed past the sample continuously. The sample was allowed to equilibrate for 20 minutes at each pH value. Spectra (2 cm^{-1} resolution and 512 scans) were recorded after the 20 minute equilibration. In trial experiments, spectra (2 cm^{-1} resolution and 64 scans) were recorded throughout the equilibration period to determine adequate equilibration time. The *Torpedo* Ringer buffer was then removed using a syringe. The flowing buffer was then switched to the *Torpedo*

Ringer buffer at the next pH value. After 20 minutes, the protocol was repeated until the end of the titration. The pH value of the *Torpedo* Ringer buffer was checked prior to addition to the cell and following the removal of the buffer using the syringe to ensure that no changes in buffer pH occurred. Experimental limitations prevented pH values below pH 2 and above pH 12. For these samples, aqueous buffer spectrum and residual water vapor were subtracted from final spectra when needed.

FTIR Spectroscopy using the Golden Gate accessory. Spectra were acquired using a single-reflection attenuated total reflectance apparatus with a diamond internal reflection element (Specac; Kent, England, or ASi/SensIR; Warrington, England) as described previously (79). The attenuated total reflectance apparatus was installed in a FTS-40 spectrometer. In brief, 2-5 μL of sample was deposited on the attenuated total reflectance (ATR) apparatus and excess solvent was evaporated completely with a stream of N_2 (absorption of ^1H_2O at 3500 cm^{-1} monitored to ensure complete evaporation). Spectra (4 cm^{-1} resolution and 512 scans) were then recorded. Spectra were analyzed using GRAMS/AI software.

Fluorescence Spectroscopy. Spectra were acquired on a Cary Eclipse fluorescence spectrometer from Varian (Randolph, MA). Samples of nAChR-reconstituted membranes were diluted in *Torpedo* Ringer buffer at a concentration of 0.15 mg/mL nAChR. In a fluorescence cuvette (10 mm light path, quartz glass; Hellma (Canada) Limited; Concord, ON), 1.8 mL *Torpedo* Ringer buffer was pre-mixed with 2 μL of 300 μM ethidium bromide in a Peltier Multicell Holder in the spectrometer (final concentration of ethidium bromide 300 nM), with a Cary Temperature Control apparatus set at 22.5°C. The sample in the

cuvette was mixed continuously during experiment. The excitation wavelength of the spectrometer was 500 nm and the emission wavelength was set to 590 nm. Kinetics run started after short mixing period and fluorescence recorded at 590 nm. At 100 seconds, 200 μL of the nAChR in *Torpedo* Ringer solution (total 30 μg nAChR) was added to the cuvette. Addition of solution was coupled with mixing using the pipette. At 750 seconds (following equilibration), 10 μL of 100 mM Carb in *Torpedo* Ringer buffer was added (mixed with pipette) to the cuvette. At 1000 seconds, 10 μL of 100mM dibucaine was added (mixed with pipette) to the cuvette. Final Carb and Dibucaine concentrations were ~500 μM, in large excess to the K_D values. All spectra were analyzed using GRAMS/AI software.

Chapter 3: Characterization of the nAChR-Reconstituted Membranes

3.1 - Introduction

The initial objective of my thesis was to examine why the anionic lipid PA, when mixed with PC in a nAChR-reconstituted membrane, is more effective at stabilizing the nAChR in a functional state than all other lipids, including other anionic lipids. In this vein, I set out to test the hypothesis that the efficacy of PA at stabilizing a functional nAChR is due to its ability to adopt different ionization states. It had been suggested prior to this study that the nAChR stabilizes PA in the dianionic ionization state, and that the dianionic form is responsible for the stabilization of a functional nAChR in PA-containing reconstituted membranes. The dianionic state of PA could be essential for creating favourable lipid-protein interactions with cationic residues on the lipid-exposed surface of the nAChR, or act on the nAChR via an indirect mechanism through alteration of the nAChR membrane environment.

The first stage of this study consisted of a detailed analysis of the ability of PA in a reconstituted membrane to influence the nAChR function. The nAChR was affinity-purified and reconstituted into membranes composed of PC (PC-nAChR), PC/PA 3:2 (PC/PA-nAChR) or PA (PA-nAChR). The molar ratio of 3:2 for the PC/PA mixture was used because a previous study indicated that 40% PA within a PC membrane (mol%) is the optimal level of PA in a PC bilayer for stabilizing the nAChR in a functional state (72). The PA-nAChR reconstitutions were performed primarily for examining the ionization state of

the PA head group within nAChR-reconstituted systems (see below), though we assessed the functional properties of the nAChR within this membranes as well. For each of the experiments, the reconstitutions were performed at least twice.

In this chapter, I analysed the affinity-purified, nAChR-reconstituted membranes in terms of protein purity and lipid composition. I also characterized the functional conformation of the nAChR in the different reconstitutions. I used two different techniques to examine functional capabilities of the nAChR in reconstituted membranes: FTIR difference and ethidium fluorescence spectroscopy. These two approaches examine subtly different functional aspects of the nAChR, but the combination of these two techniques provides an in-depth analysis of the effects of PA on the function of the nAChR in reconstituted membranes (66, 80).

The results of the analyses confirmed the ability of PA to stabilize a near-native proportion of functional nAChR in the reconstituted membrane systems. The results of the PA-nAChR reconstitutions indicate a moderate level of functional nAChR; this is the first instance of a single lipid nAChR-reconstitution able to stabilize any degree of functional nAChR. The lipid composition analysis by HP-TLC revealed new complexities of the nAChR-reconstitutions. Specifically, the TLC showed that DAG forms during the PC/PA-nAChR reconstitutions, suggesting that the nAChR may possess some phospholipase activity in these reconstituted systems. The latter could be an important in vivo function of the receptor.

3.2 – Results

3.2.1 – Characterization of the nAChR-Reconstitutions in terms of Protein Purity and Lipid Composition

3.2.1.1 – nAChR Purity – The purity of the nAChR in each of the reconstituted membranes was examined by SDS-PAGE. A representative gel for the nAChR in each of the 3 reconstituted membrane environments shows that the affinity purification protocol leads to high-purity nAChR samples with only 4 bands, each corresponding to one of the 4 subunits: α, β γ and δ (Fig. 3.1). The enhanced staining suggests a greater proportion of the α-subunit, consistent with the expected 2:1:1:1 α:β:γ:δ subunit stoichiometry for the *Torpedo* nAChR pentamer. The calculated molecular weights for the subunit bands are 43, 57, 64, and 72 kDa for the α, β, γ and δ subunits, respectively, in all of the reconstituted systems, which correspond to molecular weights of glycosylated versions of the nAChR subunits.

3.2.1.2 – nAChR-Reconstituted Membrane Composition – The lipid composition of each reconstitution was examined by HP-TLC after extracting the lipids using a modified Bligh and Dyer protocol (see Chapter 2). A representative HP-TLC of lipids extracted from the PC-nAChR and PC/PA-nAChR reconstituted membranes is shown in Fig. 3.2. The lipids extracted from reconstituted PC-nAChR run on the HP-TLC as a single lipid band showing that these reconstitutions contain only PC. The extracted lipids from reconstituted PC/PA-nAChR run mainly as 2 bands corresponding to PC and PA. The PA band, however, is significantly less intense than the PA band in the PC/PA 3:2 standard. The HP-TLC suggests the PA level in our reconstituted PC/PA-nAChR is lower than the expected 40 mol%. I estimated the amount of PA in the PC/PA-nAChR reconstitutions using HP-TLC as shown in

Figure 3.1

SDS-PAGE of the nAChR from each of the 3 Reconstitutions. Lanes: 1, Molecular weight standard ladder (molecular weights, in kDa, noted along left edge); 2, PC-nAChR reconstitution; 3, PA-nAChR reconstitution; 4, PC/PA-nAChR reconstitution. nAChR subunit bands identified along right edge. For each reconstitution, 5 μg nAChR was loaded in the well.

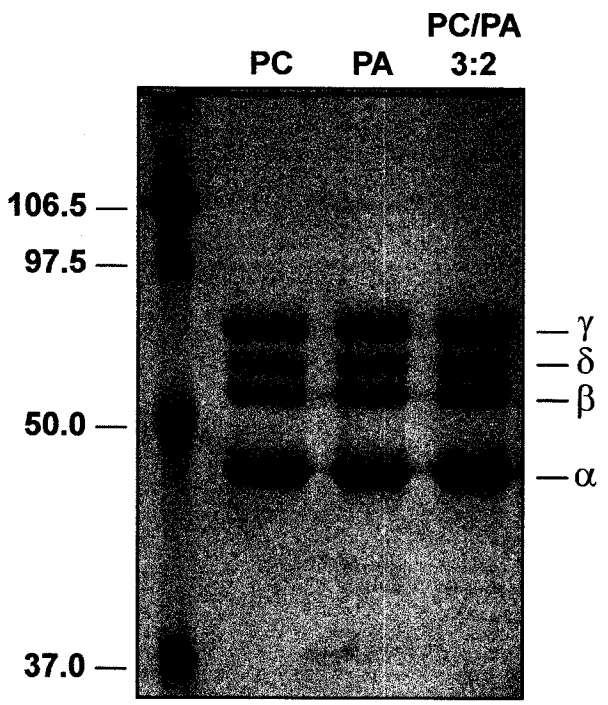
PC
PA
PC/PA
3:2
106.5
97.5
50.0
37.0
γ
δ
β
α

Figure 3.2

HP-TLC of Lipids Extracted from nAChR-reconstitutions. Lanes: 1, PC standard; 2, PC/PA 3:2 standard; 3, Lipids extracted from PC-nAChR reconstitution; 4, Lipids extracted from a PC/PA-nAChR reconstitution; 5, Lipids extracted from a second PC/PA-nAChR reconstitution; 6, PA standard. Lipid standards used for HP-TLC extracted from aqueous dispersions formed from stock lipids in $CHCl_3$ (See Chapter 2). Solvent system for running the HP-TLC: $CHCl_3$:CH_3OH:HCOOH:H_2O (50:37.5:3.5:2 vol:vol). O: Origin. S: Solvent front. Location of lipid standard bands marked along left edge.

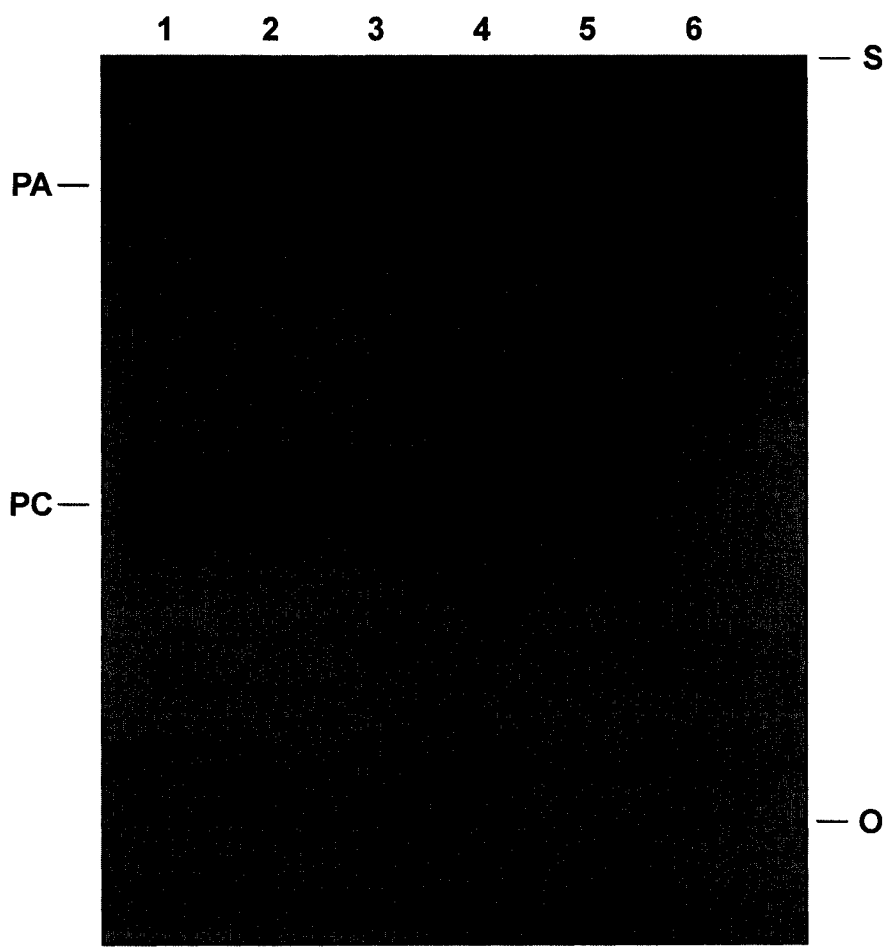
1
2
3
4
5
6
S
PA
PC
O

Fig. 3.3. The lipids extracted from the reconstituted membranes from 2 different reconstitutions were run on an HP-TLC plate along with a series of PC/PA standards, each with different PC:PA ratios. The actual amount of PA in these two reconstitutions was determined as ~10 mol% and 15 mol%, significantly reduced from the 40 mol% desired from the reconstitution protocol. It is important to note that these samples were purified/reconstituted during my 4th year honours project and were analyzed by HP-TLC after a significant amount of time (see below). Note also the intense staining near the solvent front; this staining will be discussed in more detail below.

To determine why the levels of PA in these PC/PA-nAChR reconstitutions were lower than expected, I first examined, using FTIR spectroscopy, whether the PA was extracted effectively using the Bligh and Dyer protocol (Fig. 3.4A). FTIR spectra recorded from the organic phase of the extraction procedure, the phase expected to contain the lipids, exhibit strong bands in the methylene stretching region (3000-2800 cm^{-1}; spectral region not shown) as well as a strong lipid ester carbonyl band centered at 1736 cm^{-1}, which suggests the presence of phospholipids (*top*, B). The phosphate region of the spectra recorded from the organic phase also shows a pattern consistent with phospholipids, specifically bands at 1236 and 970 cm^{-1} and the 1090/1070 cm^{-1} doublet. In contrast, FTIR spectra recorded from the aqueous phase of the extraction (containing the aqueous Torpedo Ringer buffer and the methanol) show no bands in the lipid ester carbonyl region, though there is a large peak in the phosphate region likely due to the aqueous buffer which is the primary component of this phase (*middle*). The lack of lipid-indicator bands shows that no lipid has been lost to the aqueous phase in our extractions. The extraction procedure also produced a white precipitate. FTIR spectra recorded from the precipitate exhibit strong protein amide I (1600-1700 cm^{-1}) and II bands (*bottom*, C), characteristic of a denatured nAChR (81). No peaks in

Figure 3.3

HP-TLC of Lipid Standards Compared with Lipids Extracted from PC/PA-nAChR Reconstitutions. Lanes 1-6: Lipid standards of PC/PA with decreasing amount of PA. Ratios: 1, 3:2; 2, 2:1; 3, 3:1; 4, 4:1; 5, 9:1; 6, 19:1. Lanes 7 and 8: Lipids extracted from 2 different PC/PA-nAChR reconstitutions. Location of lipid standard bands marked along left edge.

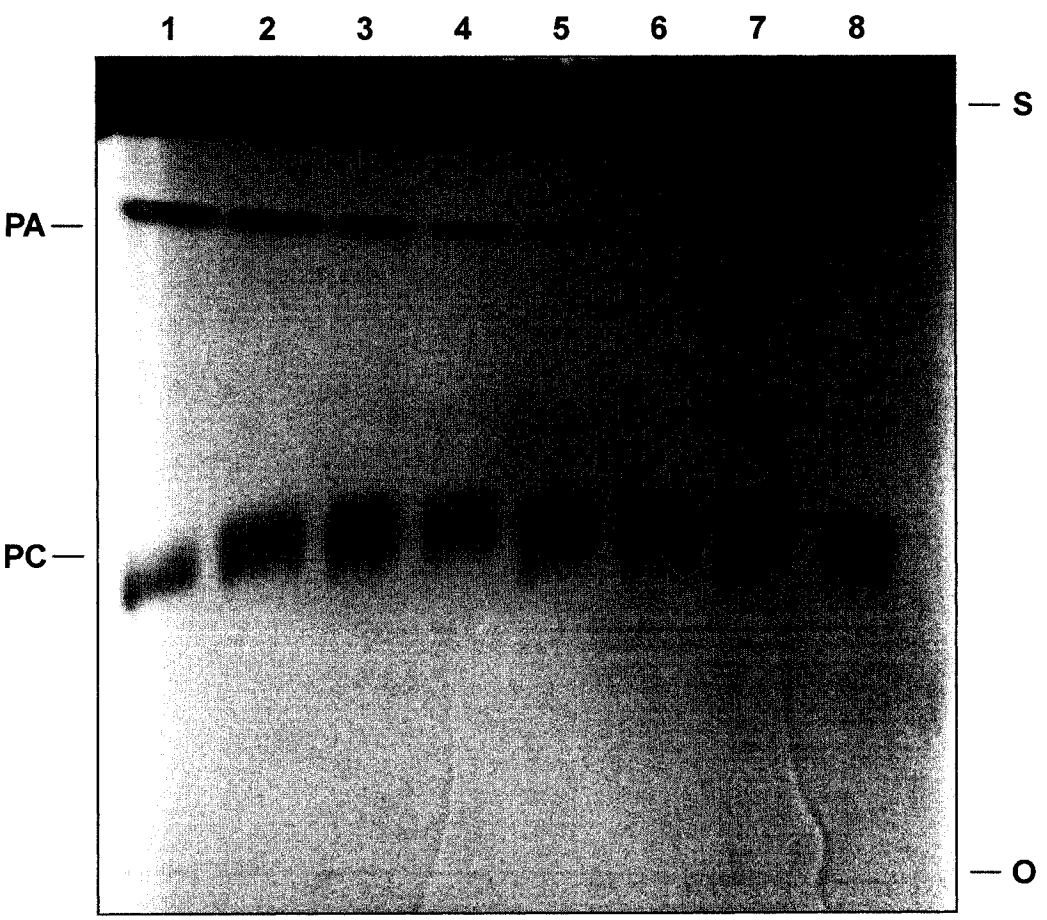
1
2
3
4
5
6
7
8
S
PA
PC
O

Figure 3.4

FTIR Spectra Recorded from the Organic and Aqueous Phases and the Precipitate from the Extractions. A, Spectra from each phase of lipid extraction. Top, Spectra recorded from 5 μL of the organic phase of the lipid extraction. Middle, Spectra recorded from 5 μL of the aqueous phase of the lipid extraction. Bottom, Spectra recorded from a sample of the precipitate dried onto the golden gate IRE. For bottom spectrum, a Pasteur pipette was used to isolate a sample of the precipitate large enough to cover the golden gate IRE, thus amount not specifically known. Spectral region shown from 1800-900 cm^{-1}. Shaded region indicates lipid ester carbonyl absorption region, an indicator of the presence of lipids. B, PC structure showing prominent structural features and the frequencies of the corresponding IR bands. Highlighted frequencies from B found only in A-Top. C, Peptide bond and the 2 main frequencies of the corresponding IR bands. Highlighted frequencies in C found mainly in A-Bottom.

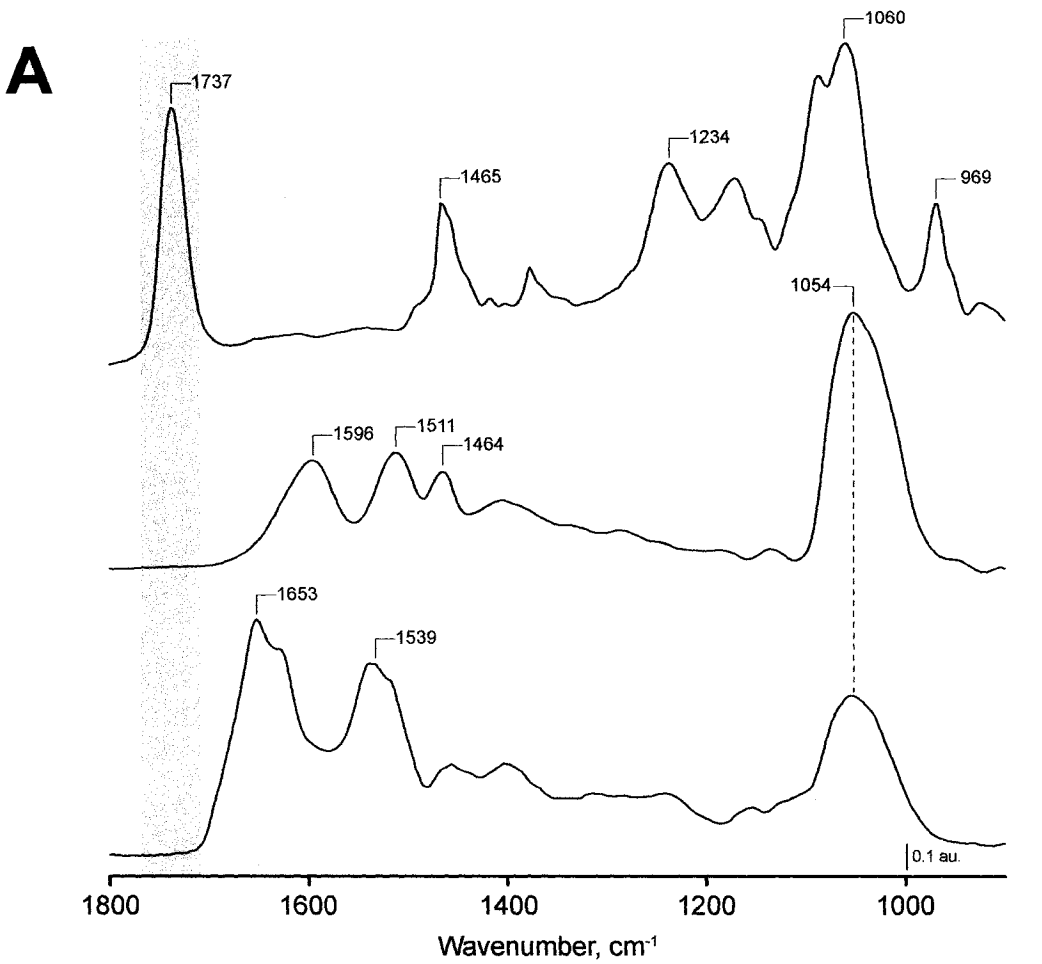
A
1737
1465
1234
1060
969
1054
1596
1511
1464
1653
1539
0.1 au.
1800
1600
1400
1200
1000
Wavenumber, cm-1

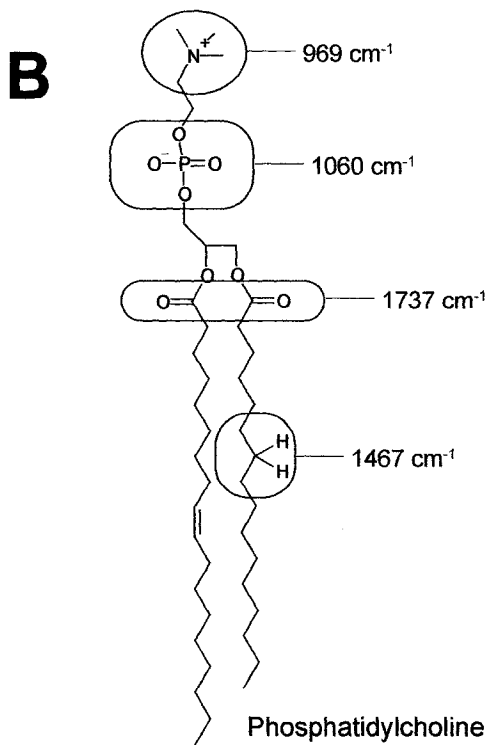
B
969 cm-1
1060 cm-1
1737 cm-1
1467 cm-1
Phosphatidylcholine

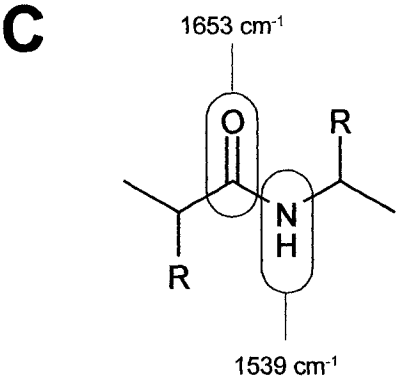
C
1653 cm-1
R
R
1539 cm-1
Peptide Bond

the precipitate could be attributed to the presence of lipids. These 3 spectra indicate that the lipids were extracted efficiently into the organic phase. The lower level of PA in our reconstituted PC/PA-nAChR systems is therefore not due to a loss of PA during the extraction procedure.

A more detailed examination of the HP-TLCs shown in Fig. 3.2 and Fig. 3.3 suggested an alternative explanation for the loss of PA. An interesting feature of these TLC runs was the presence of an additional darkly stained smear, which runs within or just below the dark solvent front in the lanes of the lipids extracted from our PC/PA-nAChR reconstitutions. However, over the course of my TLC experiments, I often found the smear to appear sporadically and at varying intensity levels, leading to difficulty in isolating and removing the smearing effect. Improved pre-washing of the HP-TLC plate led to a reduction in the staining intensity of the smear near the solvent front, due to enhanced removal of impurities. The original tubes used for extractions had lids with Teflon glued in them, and the glue from the lids apparently leeched from the lids, contaminating our extractions leading to increased intensity of the smear. As well, some of the solvents contained impurities that, when dried down from large quantities, lead to intensity of the smear staining. Changing the extraction tubes, organic solvents, and washing techniques resulted in almost complete removal of the smear, and I found that lipids extracted from nAChR-reconstituted PA-containing membranes contained a 3rd lipid species, possibly a neutral lipid (see below). The intensity of this "extra" band correlates with the drop in PA band intensity, however, suggesting that it could represent either an alternate form of PA or degradation of PA into a hydrophobic, neutral product.

Given that PA can exist in multiple ionization states, I examined whether the additional band could represent a neutral form of PA due to variation in the pH of the

surrounding environment. Previous data has also indicated that the nAChR has the ability to concentrate cations at the membrane surface (74), thus I also examined if the additional band was a result of PA complexed with cations due to the high concentration. To test these possibilities, PC/PA 3:2 membrane vesicles were prepared in varying buffer conditions including at low pH and at elevated cation concentrations. These different membrane mixtures were then extracted and run on HP-TLC plates to assess the presence of the additional band, and if the staining intensity of the additional band correlated with a decreased staining of PA (Fig. 3.5). Compared with lipids extracted from PC/PA 3:2 membranes in *Torpedo* Ringer buffer at pH 7 (*lane 1*), lipids extracted from membranes in *Torpedo* Ringer buffer at pH 4 (*lane 2*) and pH 4 with increased cations (*lanes 3-9*) showed similar staining of PA, with no correlated increased staining of the smeared band beneath the solvent front (Fig. 5A). The TLC presented in Fig. 3.5A indicates the variability of the staining of the smear due to the technical issues of the protocol noted above. However, changing the pH of the membrane environment did not result in consistent increased staining of the smear due to a decreased amount of PA within the pure lipid membranes.

Increased levels of cations within the sample buffer also did not result in increased staining of the smear coupled with a decrease in the amount of PA (Fig. 3.5B). Drastic increases in the concentrations of divalent cations (lane 2) or individual divalent cations (*lanes 3 and 4*) did not lead to decreased amount of PA in the lipid membranes without the nAChR. These data suggest that the additional band is not an alternative form of PA due to PA-cation complexes. Note, however, that the intensity of the additional lipid band in the PC/PA-nAChR lipid extractions run on the HP-TLC in Fig. 3.5B (*lanes 5 and 6*) had increased since the first lipid extraction for HP-TLC analysis, shown in Fig. 3.1. The increased staining of the additional lipid species in these TLC plates suggests it could

Figure 3.5

HP-TLC of Lipids in Varying Buffer Conditions. A, HP-TLC of PC/PA 3:2 membranes at different pH values. Lanes: 1, pH 7 *Torpedo* Ringer buffer; 2, pH 4 *Torpedo* Ringer buffer; 3, pH 4 *Torpedo* Ringer buffer with 30 mM Ca^{2+}; 4, pH 4 *Torpedo* Ringer buffer with 20 mM Mg^{2+}; 5, pH 4 *Torpedo* Ringer buffer with 50 mM K^{+}; 6, Same as lane 2; 7, same as lane 3; 8, Same as lane 4; 9, Same as lane 5. In all lanes, 25 μg of PC was spotted on the plate, with corresponding amount of PA (~15 μg). B, HP-TLC of PC/PA membranes at increased cation concentrations. Lanes: 1, pH 7 *Torpedo* Ringer buffer with 10x the standard cation concentrations; 2, pH 7 *Torpedo* Ringer buffer with 10x monovalent cations and 100x divalent cations; 3, pH 7 *Torpedo* Ringer buffer with 10x monovalent cations and Ca^{2+}, and 200 mM Mg^{2+}; 4, pH 7 *Torpedo* Ringer buffer with 10x monovalent cations and Mg^{2+}, and 300 mM Ca^{2+}; 5, Lipids extracted from a PC/PA-nAChR reconstitution; 6, Lipids extracted a different PC/PA-nAChR reconstitution. For standard concentrations of *Torpedo* Ringer buffer, see Chapter 2. Solvent system used for A and B same as Figure 3.2. Location of lipid standard bands marked along left edge.

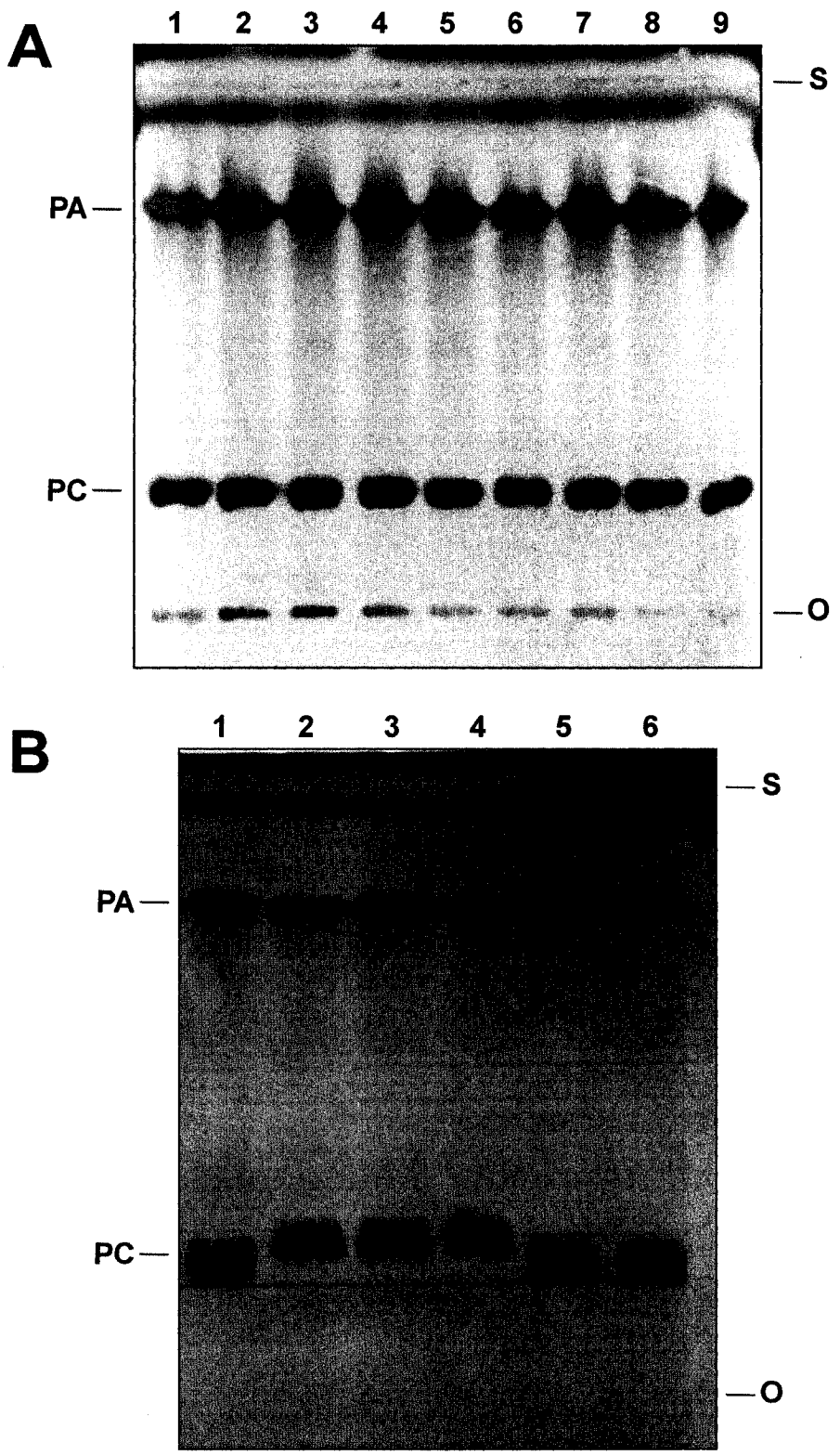
A
1 2 3 4 5 6 7 8 9
S
PA
PC
O
B
1 2 3 4 5 6
S
PA
PC
O

possibly be a degradation product of PA that appears in a time-dependent manner in nAChR-reconstituted membranes.

To determine the identity of the additional lipid band, possibly a neutral lipid, in the nAChR-reconstituted membranes, we used a more hydrophobic solvent system that can resolve neutral lipids, which migrate further in our original solvent system. The additional lipid band was revealed as 2 distinct bands, though with different intensities (Fig. 3.6). The staining above the 2 distinct bands could be due to the presence of amylene, but the level of staining suggests a very low amount, most likely from the solvents (picture presented in Fig. 3.6 darker than TLC plate, an artefact of the camera used to photograph TLC plate). Following the HP-TLC in the hydrophobic solvent system, the 2 bands were extracted from the TLC plate and identified using mass spectrometry (MS) (Fig. 3.7). The primary product found by MS was the Na^+-POPA molecule lacking the phosphate group, both with the double-bond in the oleoyl chain oxidized (633.7 m/z) and unoxidized (617.7 m/z). Further breakdown of the main product ions confirm these findings as the scans contain product ions for the palmitate and oleate chain ions (data not shown). The additional peaks on MS spectrum (539.6 and 507.6) are complexes of the palmitate and oleate chain ions both oxidized and unoxidized, as evidenced by breakdown spectra of these peaks. Although the 2 bands migrated to different points on the TLC plate, MS analysis indicated the 2 bands were comprised of the same lipid species: 1-palmitoyl-2-oleoyl-diacylglycerol (DAG).

With a potential identity of the additional neutral lipid another HP-TLC plate was run in the hydrophobic solvent system with a standard racemic mix of the 1-2-DAG and 1-3-DAG and the lipids extracted from the PC/PA-nAChR reconstitutions (Fig. 3.6). The 2 bands arising from our lipids extracted from the PC/PA-nAChR reconstitutions run to the same point as the 2 bands from the racemic mix of DAG (*lane 1*), while the lower of the 2

Figure 3.6

HP-TLC Analysis of Lipid Bands using Hydrophobic Solvent System. Lanes: 1, 1:1 racemic mix of 1-2-Dipalmitin and 1-3-Dipalmitin standard; 2, 1-2-Dipalmitoyldiacylglycerol standard; 3, 1-palmitoyl-2-oleoyl-Diacylglycerol (1-2-DAG) standard; 4, PC standard; 5, PA standard; 6, PC/PA 3:2 standard; 7, Lipids extracted from a PC/PA-nAChR reconstitution. In all lanes, 25 μg of primary lipids were spotted on plate. In lanes 6 and 7, the corresponding amount of PA was also present (~10 μg). Solvent system for running the TLC: Benzene:Isopropanol:Ethyl Acetate:Formic Acid (72.5:3.5:22:2 vol:vol). Location of lipid standard bands marked along right edge.

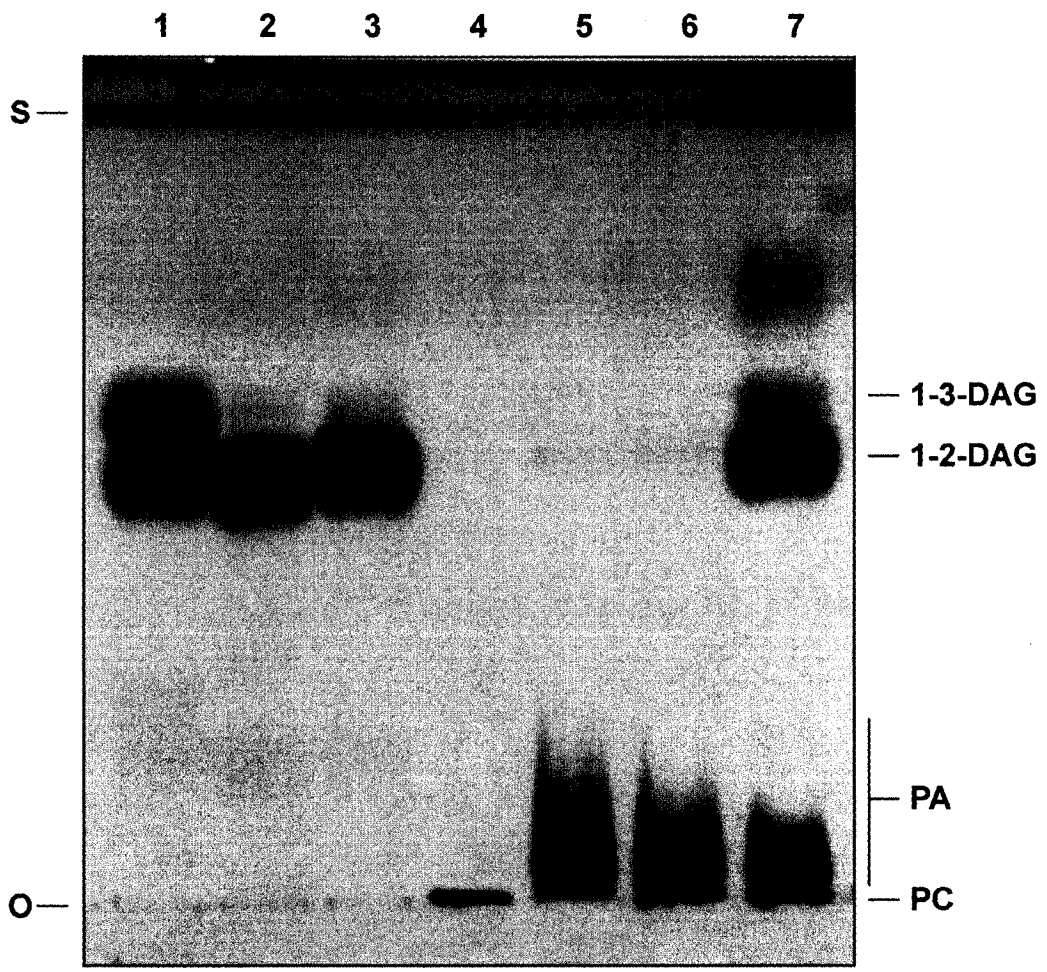
1
2
3
4
5
6
7
S
O
1-3-DAG
1-2-DAG
PA
PC

Figure 3.7

Mass Spectrum Recorded from Unknown Band removed from TLC Plate. The 2 different, unidentified bands from the HP-TLC plates produced near-identical Mass Spectra, thus only one Mass Spectrum shown. Unknown band dissolved from the silica using $CHCl_3$ and prepared for MS analysis (see Chapter 2).

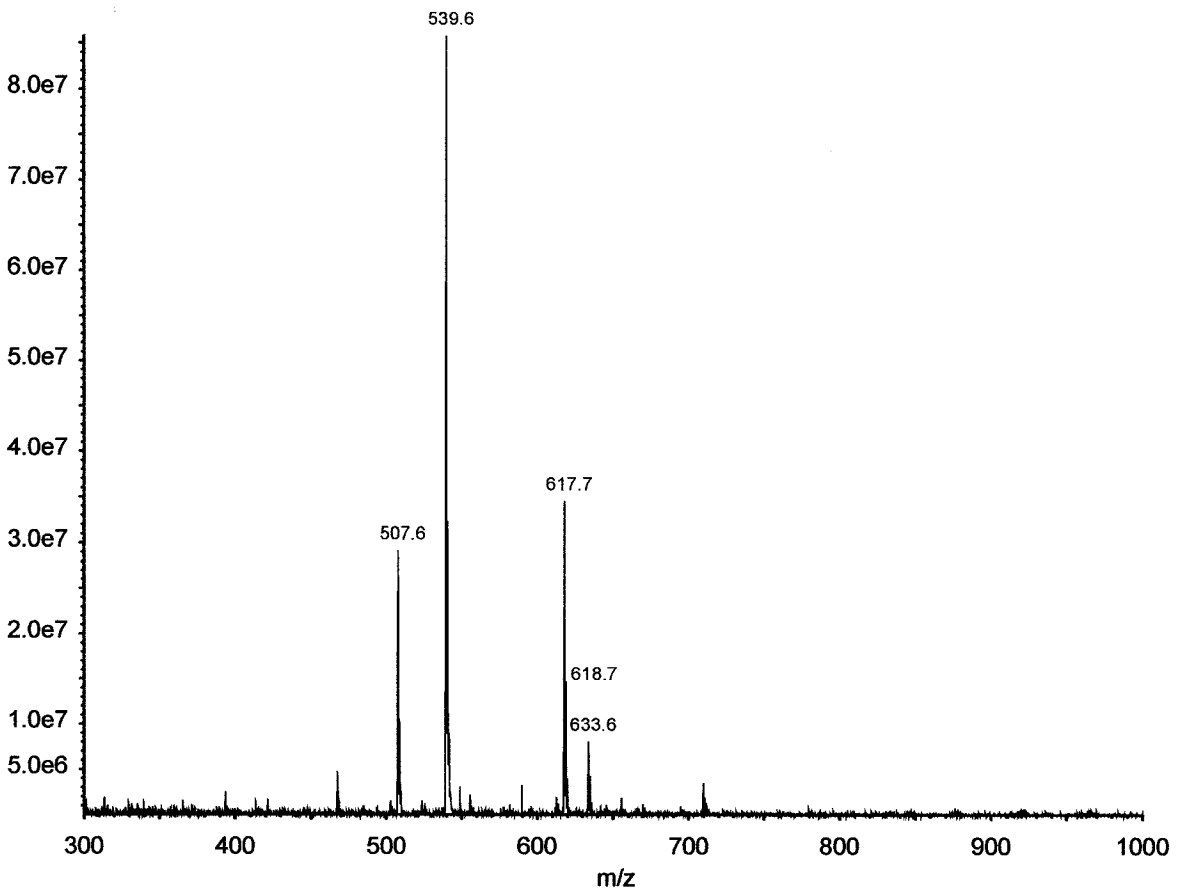
539.6
8.0e7
7.0e7
6.0e7
5.0e7
4.0e7
617.7
3.0e7
507.6
2.0e7
618.7
1.0e7
633.6
5.0e6
300
400
500
600
700
800
900
1000
m/z

bands runs to the same point as the 1-2-DAG isomer (*lanes 2-3*). The lipids we use for our reconstitutions are 1-2-POPA, thus the conversion of PA to DAG results in primarily the 1-2-DAG isomer. Over time in a glass vial, 1-2-DAG will isomerize to 1-3-DAG (Personal communication; Avanti Polar Lipids), thus the presence of the 1-3-DAG isomer, a PA-degradation product, in our lipids extracted from nAChR-reconstituted membranes.

A final HP-TLC plate was run with lipids extracted from 3 freshly-prepared, reconstituted membranes and a standard of PC/PA/DAG (7.5:4:1 mol %). For comparison, the TLC also contained lipids extracted from the Lipid A solutions – the solution used to wash the nAChR on the column and thus determines the final lipid composition of the affinity-purified reconstituted membranes (Fig. 3.8). The reconstituted PC-nAChR lane again exhibits only one lipid band, suggesting no formation of DAG within PC membranes reconstituted with the nAChR. However, both PC/PA-nAChR and PA-nAChR reconstitutions exhibit a DAG band, though the band in the PC/PA-nAChR reconstitution is similar in intensity to the standard lane. All of the Lipid A solution lanes show no presence of DAG, suggesting that DAG is formed in PA-containing membranes upon reconstitution with the nAChR. Based on this analysis, there appears to be induced hydrolysis of the PA head groups in nAChR reconstituted membranes in a time-dependent manner resulting in the presence of DAG within the final reconstituted systems.

The HP-TLC analysis provides sufficient evidence that the ratios of lipids within our nAChR-reconstituted samples are generally as expected, though the analysis also led to the discovery of DAG within the reconstituted membranes containing PA. The presence of DAG in these nAChR-reconstituted systems, even in small amounts, must be considered in the future. The discovery of the time dependence on the formation of DAG within the nAChR-reconstituted systems resulted in increased stringency for our protocols, ensuring

Figure 3.8

HP-TLC of Lipids Extracted from nAChR-Reconstitutions. Lanes: 1, PC/PA/DAG 7.5:4:1 standard; 2, Lipid A solution for PC/PA-nAChR reconstitution; 3, Lipids extracted from PC/PA-nAChR reconstitution; 4, Lipid A solution for PA-nAChR reconstitution; 5, Lipids extracted from PA-nAChR reconstitution; 6, Lipid A solution for PC-nAChR reconstitution; 7, Lipids extracted from PC-nAChR reconstitution. For each reconstituted system, 15 μg of PC were spotted (and corresponding amount of PA and DAG, if present), as determined by phospholipid concentration assay. Solvent system used same as Figure 3.2. Location of lipid standard bands marked along left edge.

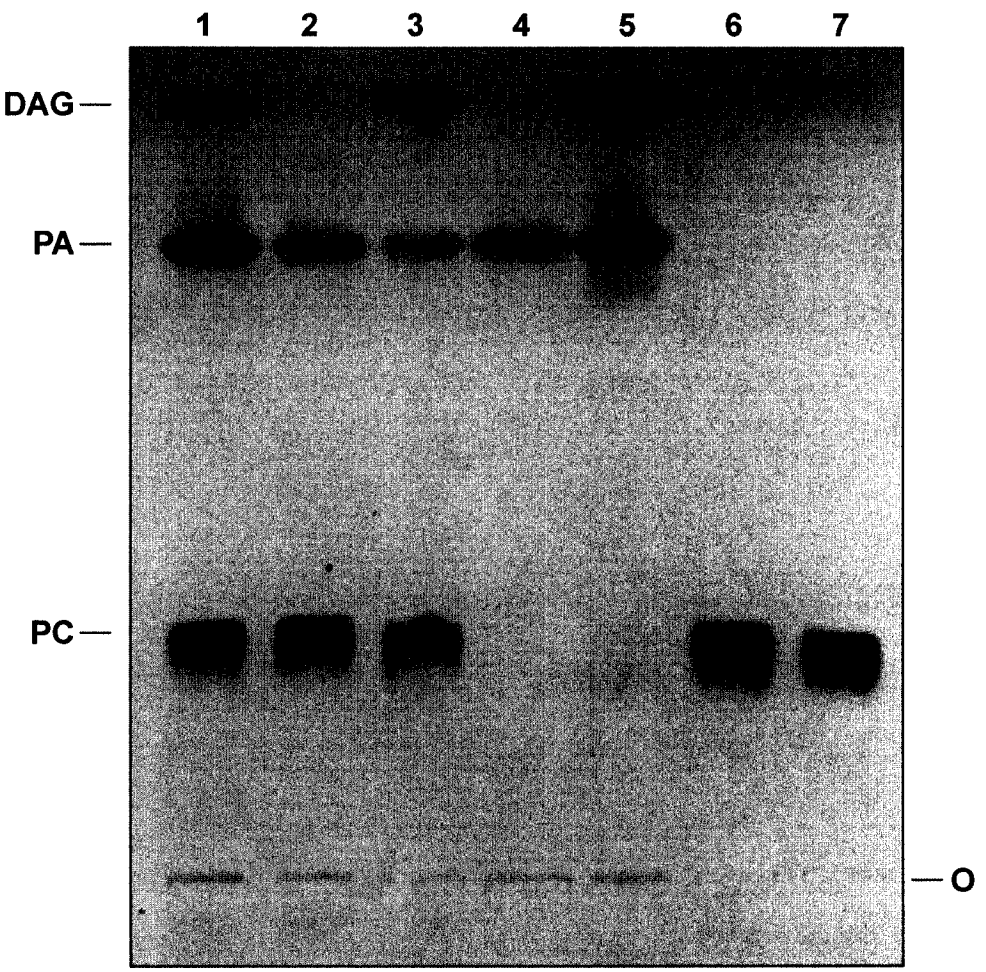
1
2
3
4
5
6
7
DAG
PA
PC
O

using only freshly-prepared nAChR reconstitutions with less than a week spent in the -80°C freezer prior to use. The significance of DAG on the functional conformation of the nAChR and the physical properties of the bilayer could be an important factor of the lipid-protein interactions between the nAChR and its surrounding membrane environment.

3.2.2 – Functional Characterization of the nAChR-Reconstitutions

3.2.2.1 – Difference Spectroscopy of nAChR-Reconstitutions – FTIR difference spectroscopy has been used extensively to examine the ability of the nAChR to undergo the agonist-induced conformational transition (61, 72-74). FTIR spectra of the nAChR recorded in either the presence or absence of the agonist Carb exhibits a pattern of broad, overlapping vibrational bands (Fig. 3.9) (61, 63, 66). The two spectra appear almost identical as the vibrational changes in the FTIR spectrum resulting from a protein conformational change generally represents less than 0.1% of the overall protein intensity. In order to detect the subtle vibrational changes, the spectra recorded in the absence of Carb (R state) is subtracted from the spectra recorded in the presence of Carb (D state), yielding a difference spectrum (referred to as a *Carb difference spectrum*). The Carb difference spectrum exhibits bands from only those residues whose structure and/or environment change upon conformational transition between the 2 states (*bottom*). Detailed analysis of Carb difference spectra from native and various reconstituted membranes led to the identification of bands arising from vibrations of the nAChR-bound Carb (1722 cm^{-1}) (63), the vibrational shifts that occur upon the formation of physical interactions between the agonist binding site and Carb (ex. Cation-π interactions) (1620 and 1515 cm^{-1}) (82), and the vibrational changes that can be specifically attributed to the nAChR conformational changes between the resting and desensitized states (1655, 1547, and 1430 cm^{-1}) (61). A schematic representation of the

Figure 3.9

FTIR Difference Spectroscopy. A, Spectral subtraction procedure shown with actual spectra recorded from a PC/PA-nAChR reconstitution. Top, Spectra recorded in the absence of agonist. Middle, Spectra recorded in the presence of agonist (Carb). Bottom, Difference spectrum obtained by subtracting top (absence) spectrum from middle (presence) spectrum (an individual cycle from single experiment). Positive marker bands highlighted have been shown in previous studies to be due global alterations in structure of the nAChR, though 1722 cm^{-1} is due to agonist binding to nAChR. Top and Middle spectra presented on same scale. Note the difference in intensity between the 2 recorded spectra (Top, Middle) and the resulting difference spectrum (Bottom). B, Schematic representation of the conformational change occurring in the difference spectroscopy experiment. R: Resting state (absence of agonist). D: Desensitized state (presence of desensitizing concentration of agonist). Triangles: Carb. C, Schematic representation of difference spectroscopy in the continual presence of dibucaine. Stars: dibucaine.

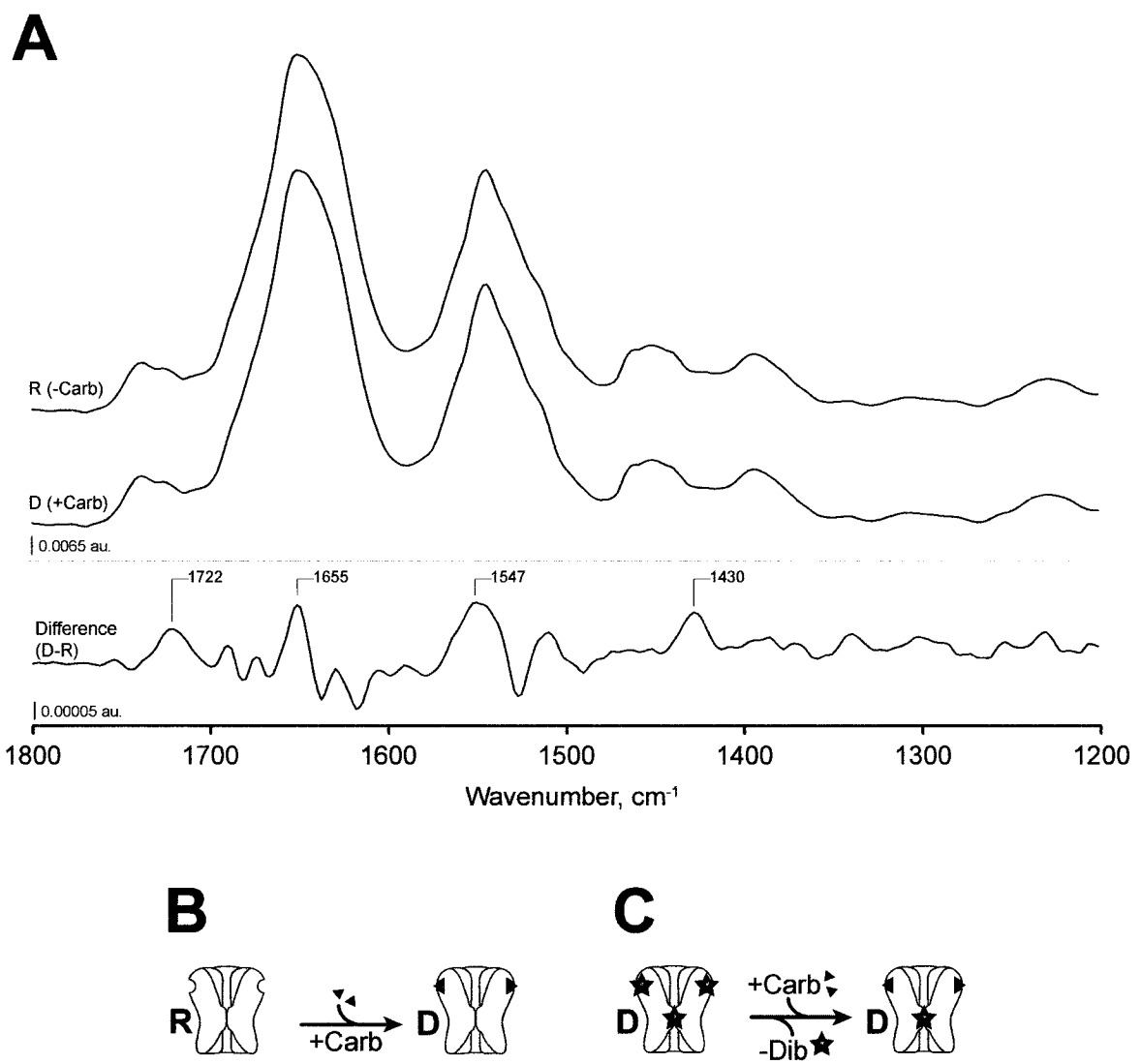
A
R (-Carb)
D (+Carb)
0.0065 au.
1722
1655
1547
1430
Difference
(D-R)
0.00005 au.
1800
1700
1600
1500
1400
1300
1200
Wavenumber, cm-1
B
R
+Carb
D
C
D
+Carb
-Dib
D

nAChR conformational change from the R state to the D state in response to Carb, analyzed with difference spectroscopy, is presented in figure 3.9B. By using FTIR difference spectroscopy, I can first assess the ability of the nAChR to undergo the conformational change from R to D in response to Carb binding.

Carb difference spectra recorded from affinity-purified nAChR reconstituted into membranes composed of PC/PA 3:2 exhibit patterns similar to those recorded in native *Torpedo* membranes and PC/PA/Chol 3:1:1 membranes (Fig 3.10, *trace i*) (63, 73). Positive intensity in the Amide I (1640-1670 cm^{-1}) and the Amide II (1520-1580 cm^{-1}) regions reflect structural and/or environmental changes of functional groups of the polypeptide backbone. As the intensity at these regions (shaded in Fig. 3.10) is lost in the presence of desensitizing concentration of the local anaesthetic dibucaine (Fig. 3.10, *trace iii*), we conclude that these bands in the difference pattern reflect protein structural changes associated with the Carb-induced conformational change from the R to D state. The reproducible patterns obtained in PC/PA 3:2 membranes are evidence that the nAChR undergoes agonist-induced conformational change in these membranes, which suggests the nAChR is functional in PC membranes supplemented with 40% PA (mol %), the optimal ratio of PC to PA in binary membranes (72). Carb difference spectra recorded from the nAChR reconstituted into pure PC membranes, which have been shown to be unresponsive to agonist in flux studies (58, 59, 62, 67), exhibit negative intensities at the 5 marker bands as well as a correlated negative intensity at 1668 cm^{-1} (partially due to decreased intensity at 1663 cm^{-1}) (Fig. 3.10, *trace iv*), similar to the difference spectra obtained in the presence of dibucaine. The absence of intensity at the protein marker bands indicates the PC-nAChR reconstitutions stabilize an agonist-unresponsive conformation of the nAChR. A recent study from our lab examined this particular state in further detail (83).

Figure 3.10

Functional Conformational State Analysis of the nAChR in Reconstituted Membranes using Difference Spectroscopy. Carbamylcholine (Carb) difference spectroscopy of the nAChR in PC/PA 3:2 membrane (trace i), PA membrane (trace ii), PC/PA 3:2 membrane in the presence of 200 μM dibucaine (trace iii), and PC membrane (trace iv). Positive intensities at highlighted marker bands reflect agonist-induced conformational change, indicative of functional nAChR. Negative intensity due to dibucaine peak highlighted at 1620 cm^{-1}. Peaks at ~1512 cm^{-1} suggestive of differences within the binding sites (described in text). Control spectra shown (grey background spectra) to indicate baseline for each experiment – difference spectra resulting from subtraction of 2 spectra recorded in the absence of agonist prior to addition of agonist. Spectra shown are averages of at least 55 difference spectra recorded from at least 2 different reconstitutions (each different membrane).

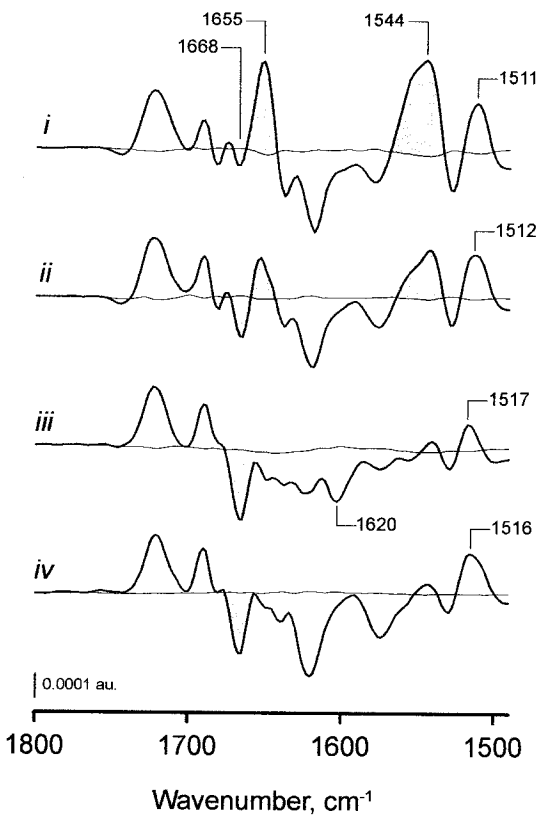
1655
1668
1544
1511
i
1512
ii
1517
iii
1620
1516
iv
0.0001 au.
1800
1700
1600
1500
Wavenumber, cm-1

Interestingly, Carb difference spectra of the nAChR recorded in membranes composed of PA exhibit a similar pattern to PC/PA 3:2 membranes, though the intensities of the positive marker bands are decreased (Fig. 3.10, *trace ii*). Moderate intensity at the marker bands suggest a smaller proportion of the receptors in the pure PA membranes are stabilized in a functional conformation. It is also possible that moderate intensities indicate that some residues in the nAChR are stabilized in an intermediate conformation in PA membranes. The Carb difference spectra of the nAChR in PA membranes also display moderate intensity of bands attributed to physical interactions between the agonist and the agonist-binding site at ~1511 cm^{-1}, similar to PC/PA-nAChR reconstitutions but right-shifted from the frequencies observed in the PC-nAChR reconstitutions. These results are intriguing as the nAChR appears to be stabilized in a functional conformation in this reconstituted membrane containing only one species of lipid, a result previously unseen in nAChR-reconstitution experiments.

3.2.2.2 – Ethidium Fluorescence and the nAChR-Reconstitutions – To further examine the effects of PA on the function of the nAChR, I examined the fluorescence of ethidium binding to the nAChR in the 3 reconstituted membranes (Fig. 3.11). Ethidium fluorescence spectroscopy of the nAChR provides further functional information, specifically about the allosteric communication between the non-competitive inhibitor (NCI) and agonist binding sites of the nAChR (80). Ethidium binds with high affinity to the hydrophobic NCI site within the ion channel pore of the desensitized (K_D = 0.36 μM), but not the resting (K_D = 1 mM), nAChR (22). Addition of agonist to suspensions of the nAChR reconstituted into native and PC/PA/Chol 3:1:1 membranes in the presence of ethidium results in ethidium

Figure 3.11

Functional Analysis of Coupling between the Agonist and NCI Binding Sites of the nAChR in Reconstituted Membranes. A, Schematic representation of the conformational and fluorescent changes occurring within the membrane suspensions with the nAChR. States and symbols similar to Figure 3.9 schematics. B, Ethidium fluorescence kinetic scans of nAChR-reconstituted membranes. Traces: i, PC/PA-nAChR reconstitution; ii, PA-nAChR reconstitution; iii, PC/PA-nAChR reconstitution in the presence of 200 μM dibucaine; iv, PC-nAChR reconstitution. Bar along bottom indicates time points where each suspension was added to cuvette (denoted by black circle): 100s, nAChR reconstituted membrane suspension; 750s. C, Dibucaine displaceable fluorescence of nAChR-reconstituted membranes (mean ± S.D., n = 6). Traces identified as in B. Blue: fluorescence intensity at 590 nm yield in absence of agonist (-). Red: Increased fluorescence quantum yield with addition of Carb (+).

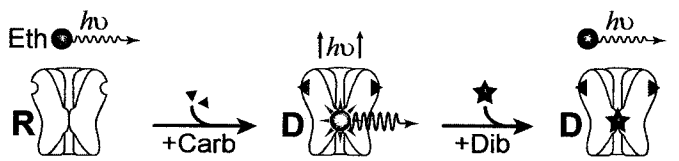
A
Eth
hυ
R
+Carb
D
↑hυ↑
+Dib
D
hυ

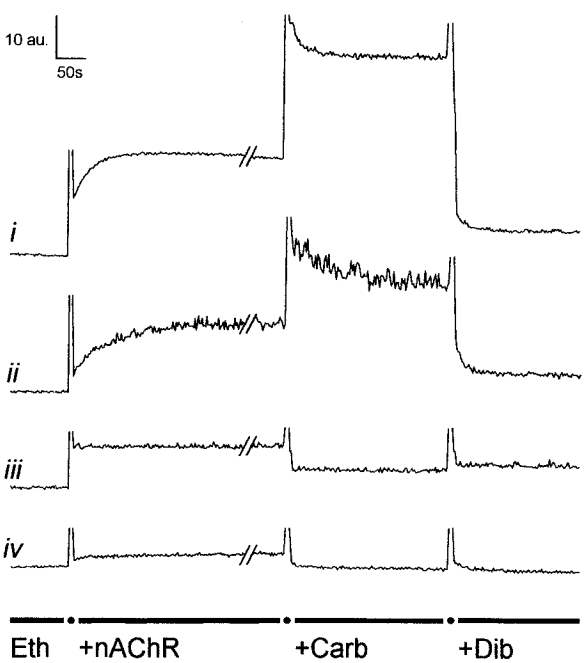
B
10 au.
50s
i
ii
iii
iv
Eth
+nAChR
+Carb
+Dib

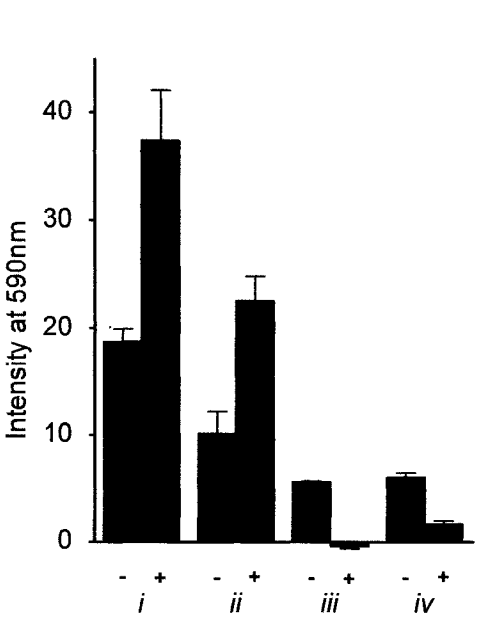
C
Intensity at 590nm
40
30
20
10
0
- + - + - + - +
i
ii
iii
iv

binding to the agonist-induced desensitized state of the nAChR. The bound ethidium exhibits greater fluorescence intensity compared to ethidium free in aqueous solution, a shift in the fluorescence emission maximum from 605 nm (aqueous solution) to 590 nm (nAChR-bound), and a significantly longer fluorescent lifetime. A schematic representation of these events is presented in figure 3.11A. The ethidium fluorescence in the presence of the nAChR reconstituted into various membranes has suggested altered interactions between the sites within the nAChR, providing details about the functional communication within the nAChR in reconstituted membranes.

Addition of PC/PA-nAChR reconstituted membranes to an aqueous solution of ethidium led to a slow increase in the fluorescence intensity. The increased fluorescence level is partly dibucaine-displaceable, possibly suggesting a portion of the increased intensity is due to ethidium binding to a pre-existing population of desensitized nAChRs. The remaining intensity could be due to ethidium partitioning into the membrane vesicles or light scattering from the proteoliposomes in suspension. The addition of 500 μM Carb leads to a significant increase in the dibucaine-displaceable ethidium fluorescence (Fig. 3.11B, *trace i*). In the PC/PA-nAChR, the increased fluorescence upon Carb addition suggests the nAChR is converted to a state with a high affinity for ethidium; the D state. In the PC/PA-nAChR reconstitutions, the nAChR is stabilized in a functional conformation, with retained allosteric communication between sites.

Addition of PC/PA-nAChR reconstituted membranes to an aqueous solution of ethidium containing 200 μM dibucaine leads to different ethidium fluorescence traces (*trace iii*). In these samples, addition of the proteoliposomes does not induce any increased fluorescence, nor does the addition of 500 μM Carb. The likely scenario is that the nAChR-

bound dibucaine cannot be removed by the ethidium, despite the nAChR being stabilized in the D state. The nAChR reconstituted in the PC membranes is also unresponsive to the addition of agonist (*trace iv*). The addition of PC-nAChR to the aqueous ethidium solution does not lead to an increase in the ethidium fluorescence, suggesting the nAChR is not desensitized in these membranes. Addition of 500 μM Carb does not result in ethidium binding to the nAChR in PC membranes, evinced by a lack of increase in the ethidium intensity.

The PA-nAChR reconstitutions produce similar, though less intense, ethidium fluorescence traces as the PC/PA-nAChR reconstitutions, supporting the findings from the Carb difference spectra (*trace ii*). Addition of the PA-nAChR proteoliposomes to the aqueous ethidium solution resulted in a similar slow increase to a moderate intensity compared to the PC/PA-nAChR. The fluorescent traces of these membranes exhibit a high degree of noise, most likely attributable to cloudiness of the reconstituted membrane suspensions. Addition of 500 μM Carb resulted in an increase in the dibucaine-displaceable fluorescent intensity, though not as intense as the PC/PA-nAChR reconstitutions. These results, coupled with the Carb difference spectra, indicate that the nAChR is indeed stabilized in a functional conformation in PA membranes, the only single-lipid reconstituted membrane that can support nAChR function following reconstitution.

3.3 – Summary & Conclusions

The affinity purification of the nAChR and reconstitution into different membranes were characterized by SDS-PAGE and HP-TLC. The SDS-PAGE analysis indicated that the reconstitutions used herein yielded high-purity nAChR, with the appropriate subunit stoichiometry of the *Torpedo* nAChR. HP-TLC analysis of the lipid composition of the nAChR-reconstitutions proved more complex than originally anticipated. Early HP-TLC plates exhibited decreased amounts of PA in lipids extracted from the PC/PA-nAChR reconstitutions, as well as an intense smear at or below the solvent front. The darkly stained smear was removed following rigorous assessment of the origin of these contaminants and how to optimize our HP-TLC analyses by removing as many impurities as possible. After switching to high purity solvents, using alternative extraction tubes and increasing the stringency of our washing protocols, the majority of the stained smears on our TLC plates were eliminated and revealed additional lipids extracted from nAChR-reconstituted membranes.

HP-TLC analysis of lipids extracted from nAChR-reconstitutions containing PA indicates that there is a time-dependent formation of DAG from the PA molecules. The DAG was identified by both mass spectrometry and HP-TLC analysis of extracted lipids compared to DAG standards. Interestingly, lipids extracted from both PC/PA- and PA-nAChR reconstitutions contained increased amounts of DAG, coupled with decreased PA, after the reconstitutions were kept at -80 °C for extended periods of time. The presence of DAG was not detected in any pure lipids extracted from $CHCl_3$ nor was it detected in any of the PC-nAChR reconstitutions. The HP-TLC data suggest the nAChR may possess inherent phospholipase activity, which could alter the lipid composition of the membrane surrounding

the nAChR by producing DAG from PA head groups proximal to the nAChR. This phenomenon has not been seen before and suggests an alternative explanation for the relationship between PA and the nAChR. As a corollary to the finding of possible time-dependent, phospholipase activity in the nAChR-reconstituted membranes, our lab now ensures prompt use of any freshly prepared nAChR samples to ensure a minimal amount of DAG formation. The reality, however, is that DAG could potentially alter the functional conformation of the nAChR and the effects of DAG on the conformational equilibria of the nAChR requires further attention.

The results of the Carb difference spectroscopy confirm the ability of PC/PA 3:2 membranes to stabilize the nAChR in a functional conformation similar to native *Torpedo* membranes (72, 73). Various other anionic lipids have been assessed in previous studies (58, 59, 61, 67, 75), but PA remains unique in its ability to influence the nAChR conformational equilibria in binary mixtures with PC to almost the same degree as the native *Torpedo* membranes. While a recent study determined that PG, which possesses structural and chemical properties similar to PA, is able to stabilize a functional conformation of the nAChR upon reconstitution, the PG-containing membranes only stabilize a moderate functional conformation of the nAChR (76). A further intriguing aspect of the aforementioned study is that HP-TLC plates containing lipids extracted from PC/PG-nAChR reconstitutions exhibit no presence of DAG in these reconstitutions. The effect of DAG on the ability of the nAChR to undergo agonist-induced conformational change in PC/PA membranes specifically is currently being addressed. As previously reported (61), Carb difference spectra recorded from the nAChR in PC membranes indicate that the nAChR is unable to undergo agonist-induced conformational change (Fig. 3.10).

Ethidium fluorescence of the nAChR in PC/PA 3:2 membranes supports the Carb difference spectroscopy and previous reports: Addition of agonist leads to increased fluorescence intensity, indicative of ethidium binding to the NCI site of the nAChR due agonist-induced R to D transition (Fig. 3.11B, C). In the presence of a high concentration of an anaesthetic, ethidium fluorescence does not change significantly upon addition of agonist to PC/PA-nAChR reconstitutions. The dibucaine stabilizes the desensitized state of the nAChR by binding to the NCI site, thus preventing ethidium binding. Interestingly, the PC-nAChR reconstitutions show low fluorescence intensity in the absence of dibucaine both prior to and following Carb addition, suggesting the nAChR is not desensitized in PC-nAChR reconstitutions. Recent data indicates that the nAChR adopts a novel conformation in PC-nAChR reconstitutions, highlighting the role of lipids in modulating the conformation of the nAChR (83).

Carb difference spectra and ethidium fluorescence traces of the PA-nAChR reconstitutions indicate the nAChR is stabilized in a moderate functional state in these reconstituted membranes containing a single anionic lipid. While the level of functionality is not optimal, the functional analyses indicate that the nAChR undergoes agonist-induced conformational change and displays allostery in these PA membranes. These data indicate, for the first time, that a reconstituted membrane containing a sole lipid species is able to stabilize a functional conformation of the nAChR. Previous studies suggest that the nAChR requires the presence of zwitterionic PC along with anionic lipids in order to remain in a functional conformation (58, 61). The data contained herein further supports the notion that PA is unique in its effects on the conformational state of the nAChR in reconstituted membranes. The specificity of PA compared to other anionic lipids that share structural features with PA hints at specific PA head group-nAChR interactions, though these annular

lipid binding sites have not yet been identified, despite the 4Å model of the nAChR (see Chapter 6). However, the formation of DAG in these PA-containing membranes and the absence of DAG in nAChR-reconstituted membranes containing other anionic lipids suggest the mechanism may not be PA-specific, but a result of the nAChR altering its lipid environment through lipid head group modification.

Chapter 4: Monitoring Ionization State of PA Head Groups

4.1 – Introduction

It is clear that PA is effective at stabilizing a functional conformation of the nAChR in reconstituted systems alone with PC, yet it also appears that the PA-nAChR reconstitutions are also able to stabilize function to a moderate degree. While previous studies have suggested the requirement of Chol and/or other anionic lipids, these other lipids are not as efficient as PA in stabilizing a functional nAChR, nor has it been shown that any other single lipid system can retain nAChR function following reconstitution. The efficacy of PA must be attributed to a unique aspect of the lipid that gives it the ability to provide an environment with appropriate physical or chemical properties required for stabilizing a functional nAChR. There are 2 structural features of PA which have been suggested as being responsible for the efficacy of stabilizing the nAChR: the small head group, and the anionic charge. However, other anionic lipids in combination with PC have been shown to be unable to retain the ion flux capability of the nAChR in reconstituted membranes (58), suggesting that the negative charge alone is not the key behind the efficacy of PA in modulating the nAChR function. A recent study examined the possibility of the importance of the small head group size of PA by assessing the structural/functional effects of PG, which possesses a small head group, on the nAChR conformational state. PG is able to moderately mimic the effects of PA in nAChR-reconstituted membranes (76). Other anionic lipids can stabilize function, but not to the same degree as PA and often require the presence of a

neutral lipid. Thus a unique chemical feature could be the reason that PA is so important to the nAChR conformational equilibria.

The ability to exist in different head group ionization states at physiologically relevant pH values within a lipid membrane is a unique chemical characteristic of PA among the anionic phospholipids typically found in *Torpedo* membranes (Fig. 4.1). It has been suggested that the nAChR stabilizes the dianionic form of PA and that the dianionic PA head group is essential for nAChR function (64). In this chapter, I first set out to test whether FTIR spectroscopy is capable of monitoring PA head group ionization state changes within a lipid membrane. Then I used the developed approach to monitor PA head group ionization state in reconstituted membranes. The results indicate that the nAChR does not stabilize the dianionic state of PA in reconstituted membranes, suggesting that the dianionic state is not the key feature of modulation of the nAChR functional conformation by PA. The results herein eliminate the possibility that specific interactions between the unique dianionic state of PA and the nAChR play a role in the bi-directional coupling between PA-containing membranes and the nAChR conformational equilibria.

Figure 4.1

The Different Ionization States of PA. The PA head group experiences ionization state changes in response to pH, even when in a lipid membrane. The bonds in each ionization state give rise to different peaks in the phosphate vibrational region of FTIR spectra (see text). R, the acyl chains of the lipids (1, palmitoyl chain; 2, oleoyl chain).

Phosphatidic Acid (POPA)

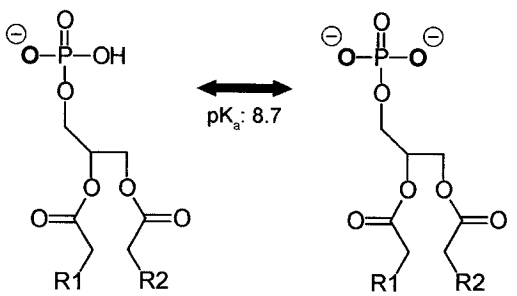

Monoanionic PA Dianionic PA

4.2 – Results

4.2.1 – FTIR Spectra of Pure Bilayers

FTIR spectra of PC, PA, and PC/PA 3:2 membranes exhibit a variety of IR bands that have been assigned to the various functional groups common to phospholipid molecules, as well as those specific to the individual head groups (Fig. 4.2). For example, all 3 membranes exhibit a strong peak at roughly 1735 cm^{-1} assigned to the lipid ester carbonyl vibration, which experiences frequency shifts depending on the hydrogen bonding experienced by the carbonyl oxygen (see Chapter 5). Also, each membrane exhibits a peak at 1467 cm^{-1} that is attributed to the $-CH_2$ groups on the acyl chains of the phospholipids. The broad overlapping peaks from 1100 to 1050 cm^{-1} consist primarily of vibrations of phospholipid head groups, which appear at different frequencies depending on the functional groups of the phosphate head groups within the membranes (84). Specifically, the phosphate group of PC vibrates at 1234 and 1087 cm^{-1}, with a component at 1067 cm^{-1}. Of particular interest for the current study are the peaks from the single-negatively charged monoanionic phosphate group of PA that vibrates at 1178 and 1070 cm^{-1} at low pH, and the double-negatively charged dianionic PA that vibrates at 1090 and 1023 cm^{-1} (64, 85, 86). The dual peaks from each ionization state are a result of symmetric and asymmetric modes of bond stretching occurring simultaneously producing two peaks, with the asymmetric stretching frequency corresponding to the higher of 2 frequencies (85). In PA membranes, the PA head groups experience pH-dependent changes of peak frequencies and intensities resulting in the different appearance from that of PC-containing membranes, as discussed below. The phosphate bands appear similar in each membrane but they are comprised of some similar

Figure 4.2

FTIR Spectra Recorded from Lipid Membranes without the nAChR. Top, PC membranes; Middle, PA membranes; Bottom, PC/PA 3:2 membranes. Spectra from each membrane were scaled at the lipid ester carbonyl peak (~1735 cm^{-1}) to an absorbance intensity of 1. All spectra recorded at pH 4. Highlighted wavenumbers indicate peaks representing different parts of the phospholipid molecules present (see text). Dashed lines indicate common peaks found in each membrane.

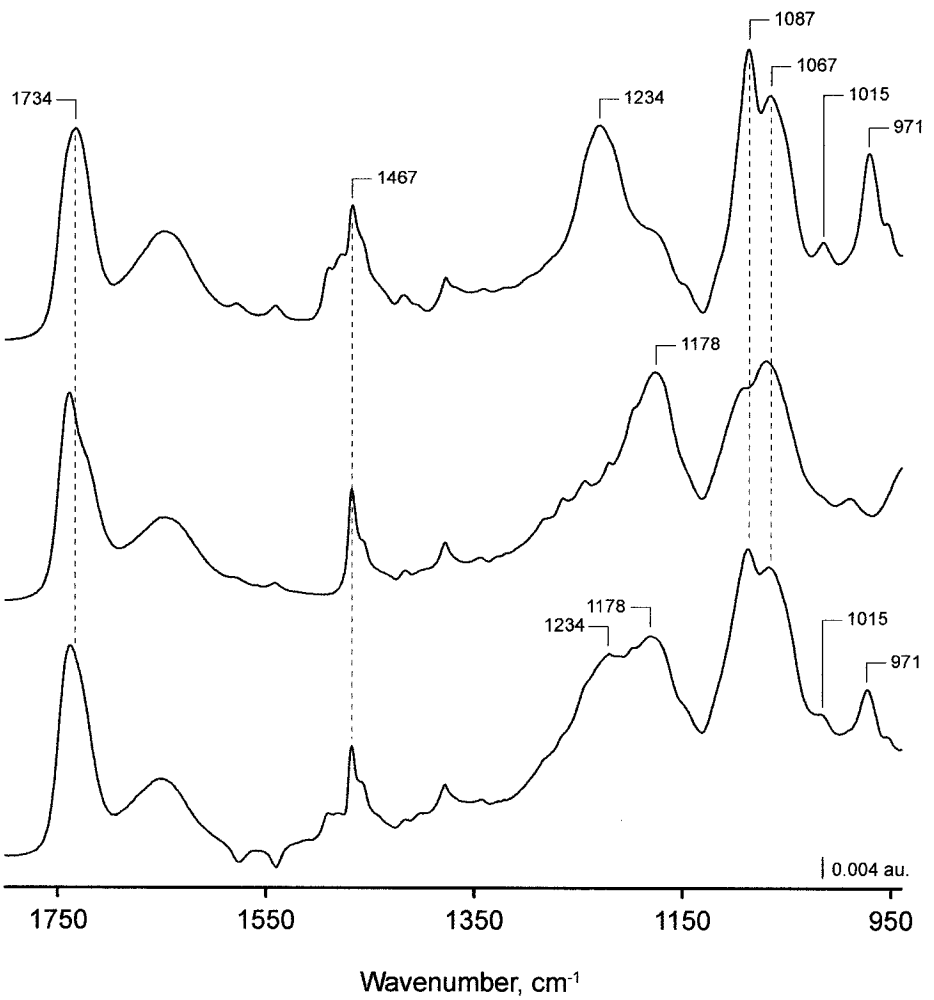
1087
1067
1734
1234
1015
971
1467
1178
1178
1234
1015
971
0.004 au.
1750
1550
1350
1150
950
Wavenumber, cm-1

underlying, component peaks but also contain membrane-specific elements (see below). PC/PA 3:2 membranes contain both PC and PA head groups, thus these spectra are essentially composites of the 2 pure membrane spectra. FTIR spectra of the different membranes exhibit peaks consistent with common phospholipid structural vibrations, as well as head group-specific peaks that can be used to monitor head group alterations in pure or mixed membranes.

4.2.2 – Monitoring Ionization State of PA Head Groups in Bilayers without the nAChR

As a control, FTIR spectra were recorded from PC membranes over the range of pH 4 to 10 (Fig. 4.3A). PC head groups have no ionizable groups in this pH range, thus the spectra should be superimposable in the phosphate region of the spectrum (1300-940 cm^{-1}). The lack of band shape changes indicates neither alteration of the PC head groups nor any changes in phospholipid organization in the bilayer over the large pH range tested. As well, the absence of spectral changes in the lipid ester carbonyl region of the spectra suggests no pH-dependent changes in the physical properties of the PC membranes (see below). Overall PC membranes show no changes in the FTIR spectra that can be attributed to pH-dependent phospholipid head group or bilayer changes.

In contrast, the phosphate head groups of PA are ionizable with a pK_a between the monoanionic and dianionic states of 8.7 (87, 88). In contrast to PC, there are significant changes in the intensity of the phosphate stretching peaks in FTIR spectra of PA membranes recorded over the pH range 4 to 10 (Fig. 4.3B). Significantly, increasing pH leads to an increase of dianionic stretching peaks at 1091 and 1023 cm^{-1} coupled with decreases at monoanionic stretching peaks at 1177 and 1070 cm^{-1}, indicating a change from

Figure 4.3

Phosphate Vibrational Region of Spectra Recorded at Varying pH values in Lipid Membranes without the nAChR; pH titration: 4 to 10. A, Stacked spectra of PC membranes. B, Stacked spectra of PA membranes. C, Stacked spectra of PC/PA 3:2 membranes. In each titration, spectrum at each pH value recorded at increasing pH from front to back (pH 4: front; pH 10: back). Spectra in each titration were scaled at the lipid ester carbonyl peak (~1735 cm^{-1}, not shown) to an absorbance intensity of 1. Spectra offset slightly to create stacking effect. Titration shown for each membrane is a representative series of spectra. Each titration was repeated at least 3 times with different membrane films, and data shown are reproducible, representative titrations.

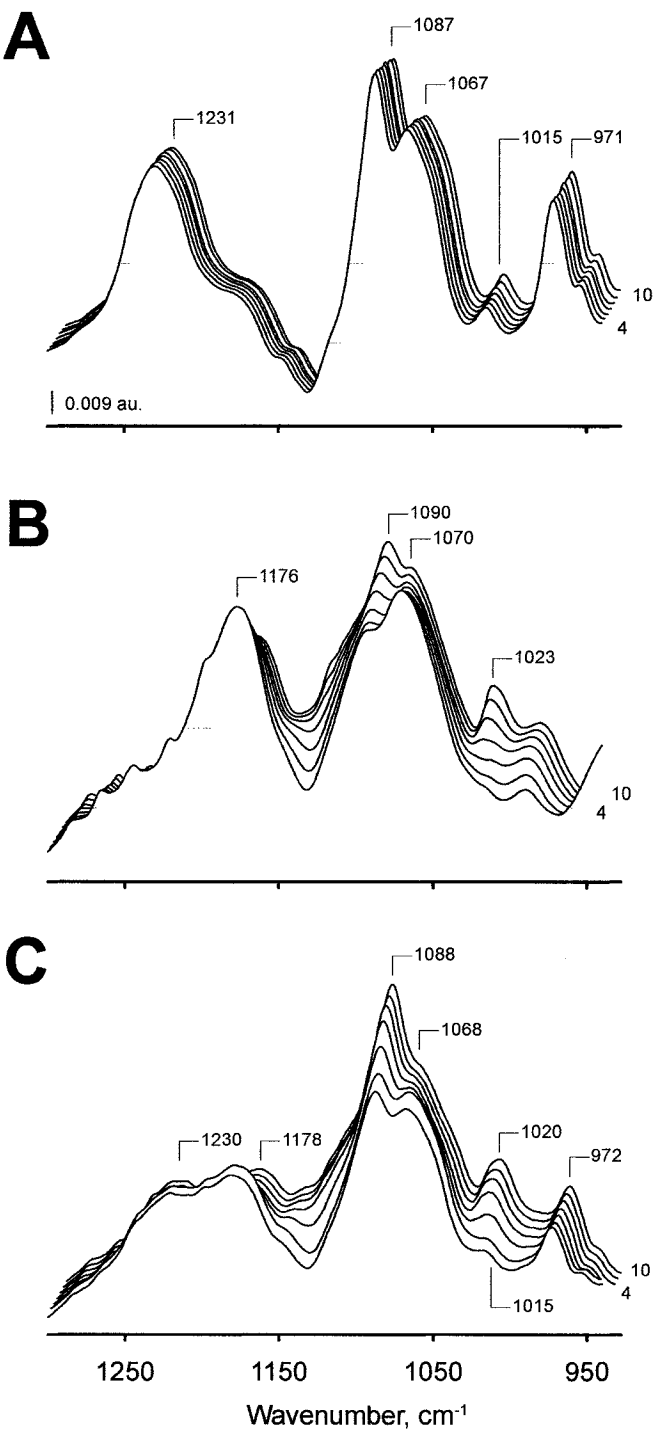
A
1087
1067
1231
1015
971
10
4
0.009 au.
B
1090
1070
1176
1023
10
4
C
1088
1068
1230
1178
1020
972
10
4
1015
1250
1150
1050
950
Wavenumber, cm-1

predominantly monoanionic PA head groups to dianionic head groups (64, 86). Although some of the larger bands have underlying components from common phospholipid structures, increased intensity from the dianionic PA head group bands can increase the intensity at specific frequencies within the broader peaks. Analysis of the area under the dianionic stretching peak at 1023 cm^{-1} provides a curve that indicates a pK_a of 8.7 ± 0.1 (n = 2) (Fig. 4.4, *open squares*), which is the same as the literature value (8.7). Reverse titrations of PA membranes from pH 10 to 4 exhibit band shape changes consistent with PA head group ionization from dianionic to monoanionic, but full monoanionic spectral characteristics only return at pH 4. From these titration experiments, it appears that FTIR spectroscopy can be used to monitor phospholipid head group ionization state changes in response to pH change and obtain an accurate pK_a within a PA membrane.

I next examined the possibility of monitoring PA ionization state in a mixed membrane with only 40% PA. FTIR spectra were recorded from PC/PA 3:2 membranes over pH range 4 to 10 (Fig. 4.3C). The spectral changes observed in the PC/PA 3:2 membranes are not as intense as the changes in PA membranes since the PC head groups in these membranes also contribute intensity in this spectral region and there is less PA present. However, increases at the dianionic PA head group peaks (1088 and 1020 cm^{-1}) coupled with decreases at the monoanionic PA peaks (1178 and 1068 cm^{-1}) corresponding to PA head group ionization within these mixed membranes are easily visible. At low pH, there is a small peak at 1015 cm^{-1} that superimposes with the same peak in PC membranes, but as the pH increases, the dianionic PA head group peak begins to appear to the left of this peak by ~5 cm^{-1} (1020 cm^{-1}) due to increasing amount of dianionic PA head groups. The presence of the small contributing peak from PC causes the dianionic PA peak to appear broader in PC/PA 3:2 membranes than in PA membranes. In PA membranes, the left-shifted dianionic

Figure 4.4

Ionization Curves Measured at the Dianionic PA Symmetric Stretching Peak in PA-containing Membranes. Boltzmann-Sigmoidal curves produced for PC/PA 3:2 membranes (open diamonds) and PA membranes (open squares). Intensity of the peak attributed to the dianionic stretching peak (~1023 cm^{-1}) calculated from integration using GRAMS AI software. All spectra used to produce curves were scaled at lipid ester carbonyl bands to an absorbance intensity of 1. Curves shown are representative curves from individual titrations. Each titration used to produce curves were repeated at least 2 times, with different membrane films each time, and the nAChR-reconstituted membranes were from at least 2 different membrane films from 2 different reconstitutions. Intensity at 1015 cm^{-1} (a PC component; see text) increases in a pH-independent manner in PC (open circles), PC-nAChR reconstitutions (filled circles) and PC/PA-nAChR reconstitutions (filled diamonds). Inset, Zoomed-in view of the PC and nAChR-reconstituted membranes showing pH-independence.

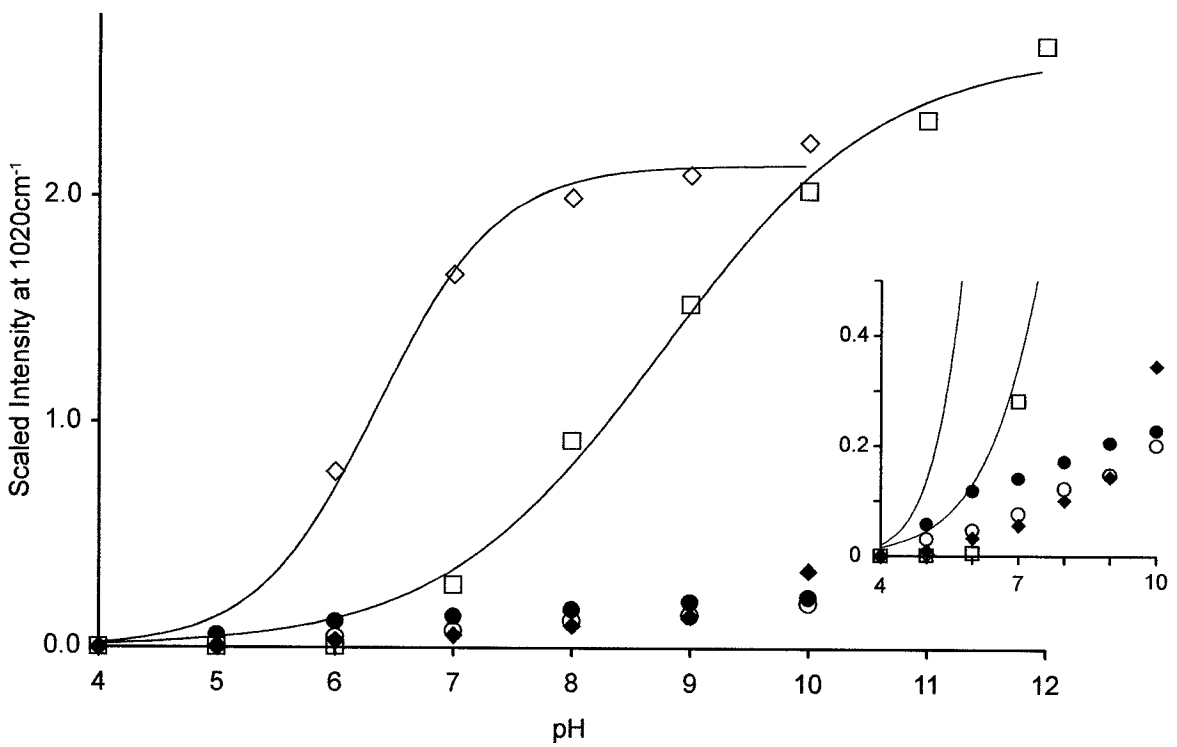
Scaled Intensity at 1020cm-1
2.0
1.0
0.0
4
5
6
7
8
9
10
11
12
pH
0.4
0.2
0
4
7
10

peak (1023 cm^{-1}) is consistently higher than in PC/PA 3:2 membranes (1020 cm^{-1}). The dianionic PA peak, however, is far enough to the left to be discernable from the small PC peak in this region (1015 cm^{-1}) in PC/PA 3:2 membranes, and analysis of the peak in PC/PA 3:2 membranes indicates a pK_a of 6.5 ± 0.2 (n = 3) for the PA within the membrane. The spectra recorded from the mixed membranes exhibit qualitative and quantitative evidence of PA head group ionization within lipid membranes.

The pH-induced changes from both PA and PC/PA 3:2 membranes appear similar qualitatively, but the analysis from both membranes indicated that the pH-induced changes occur within different pH ranges (Fig. 4.4). The dianionic symmetric stretching peak in PA membranes begins to increase in intensity as the pH reaches 7 and appears to plateau at or above pH 12 (Fig. 4.4, *open squares*). In PC/PA 3:2 membranes, there is an increase in peak intensity of the dianionic PA symmetric stretching peak (1020 cm^{-1}) beginning at roughly pH 5 (*open diamonds*). The most significant changes in the peak intensity occur over the pH range of 5 to 8, which indicates a lower pK_a value of PA. The different pK_a values found here are indicative of the different membrane environments created by the presence of PC, which dilutes the PA head groups, weakening the inter-head group repulsion between dianionic PA head groups.

Taken together, the spectra recorded from the 3 membranes without the nAChR in this study indicate peaks due to the vibration of functional groups common to general phospholipids, though they also indicate phospholipid-specific peaks that can be used to identify each individual species. From the titration experiments, it is clear that FTIR spectroscopy can be used to monitor the ionization state of PA head groups within pure and binary PA-containing membranes. The different pK_a values obtained from the analysis of the spectra recorded from the titrations of PA and PC/PA 3:2 membranes are indicative of

the sensitivity of FTIR spectroscopy and validate the designed technical approach for monitoring head group ionization state within lipid membranes over a broad pH titration.

4.2.3 – FTIR Spectra of nAChR-Reconstitutions

Prior to investigating the ionization state of PA in nAChR-reconstituted membranes, I compared spectra of PC/PA-nAChR reconstitutions and PC/PA 3:2 membranes with a delipidated nAChR sample. To ensure the possibility of observing any ionization state changes, I needed to ensure that the nAChR would not interfere with or mask any of the PA head group ionization spectral marker bands. FTIR spectra recorded from PC/PA-nAChR reconstitutions and PC/PA 3:2 membranes without the nAChR were compared with spectra recorded from the delipidated nAChR sample (Fig. 4.5). The large peaks in the amide I and II regions are due to vibrations of the nAChR polypeptide backbone carbonyl and amide hydrogen bonds, respectively, and are absent in the spectra of the PC/PA membrane without the nAChR. Likewise the lipid ester carbonyl vibration at ~1734 cm^{-1} is essentially absent in the delipidated nAChR spectra, indicating almost complete removal of the endogenous nAChR lipids membrane during the purification. The nAChR spectra exhibit some broad peaks in the phosphate vibrational region of the spectra that lead to apparent intensity increases of the phosphate head group bands relative to spectra of pure lipids. The broad nAChR band at 1234 cm^{-1} increases the intensity of this particular section of the phosphate region. The increased intensity can be seen in the PC/PA-nAChR reconstitution compared to the pure PC/PA 3:2 membrane spectra. There is a broad absorbance around 1070 cm^{-1} that increases the intensity of this region and can affect the 1090/1070 cm^{-1} doublet, but this increased intensity does not significantly affect or hide the dianionic PA head group

Figure 4.5

Comparison of FTIR Spectra of Lipid Membranes and the nAChR. Top, Spectra recorded from PC/PA-nAChR reconstitution. Middle, Spectra recorded from nAChR in the absence of lipids. Bottom, Spectra recorded from PC/PA 3:2 membranes. Highlighted wavenumbers primarily attributed to presence of lipids. Dotted lines indicate peaks found in different samples. Amide I peaks in top and middle spectrum scaled to each other. Lipid ester carbonyl peak in top and bottom spectrum scaled to each other. Aqueous solvent subtracted from top and bottom spectrum; middle spectrum recorded dried, in the absence of aqueous buffer. For comparison details see text.

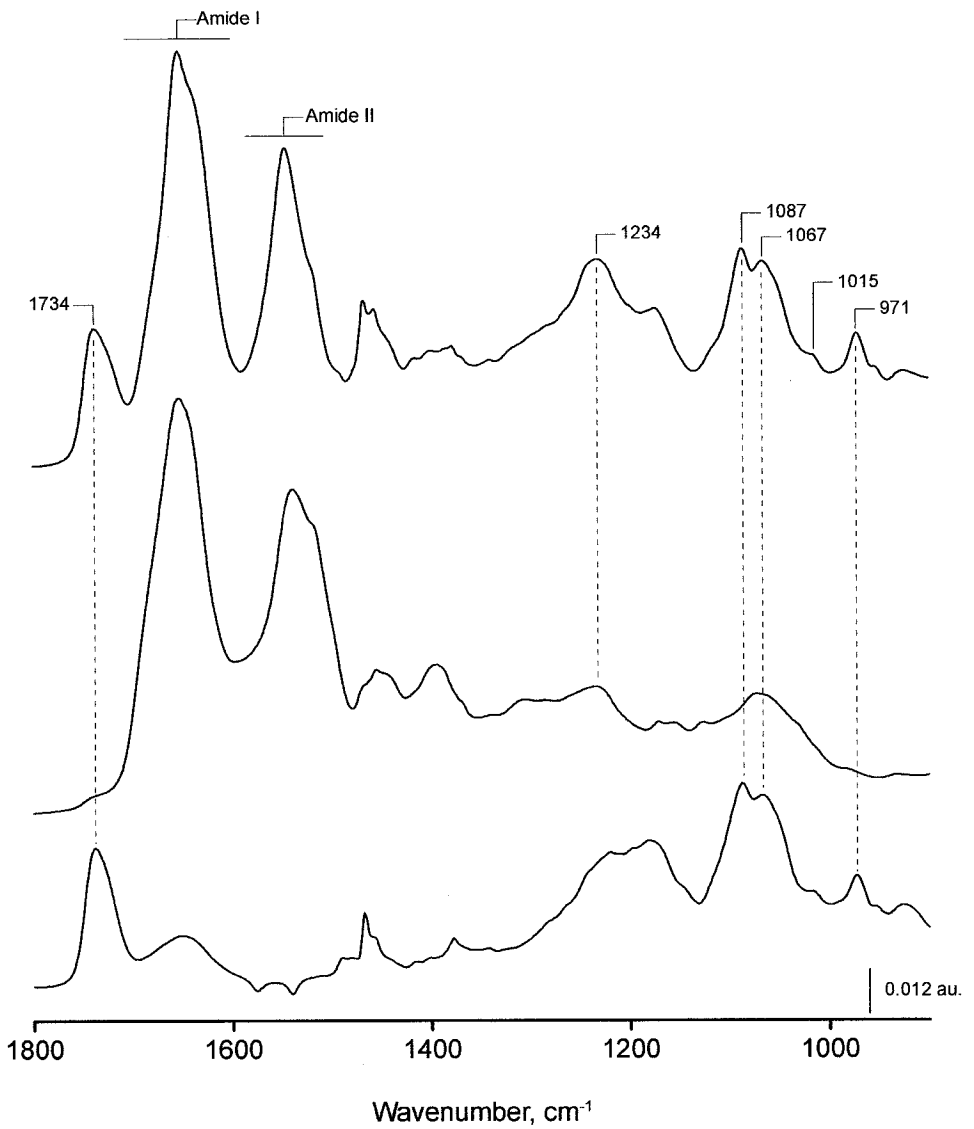
Amide I
Amide II
1734
1234
1087
1067
1015
971
0.012 au.
1800
1600
1400
1200
1000
Wavenumber, cm-1

stretching peak at 1020 cm^{-1}. Therefore, spectral band shape changes attributable to PA head group ionization state change in nAChR-reconstitutions should be visible and provide insight regarding the ionization state of PA within the nAChR-reconstitutions.

4.2.4 – Monitoring Ionization State of PA Head Groups in nAChR-Reconstitutions

Based on the ability to monitor ionization state in pure membrane titration experiments and the nAChR absorbing primarily in the amide region, I first examined the pH-dependence of phospholipid head groups in PC- and PC/PA-nAChR reconstitutions (Fig. 4.6). The samples used for these titrations were prepared using our reconstitution protocol and the titrations were performed within a week of the reconstitution in order to avoid loss of significant amounts of PA via hydrolysis to form DAG. Spectra recorded from the PC-nAChR reconstitutions exhibit no spectral band shape changes attributed to ionization state changes in the phosphate region in the titrations (Fig. 4.6A). The lack of spectral changes attributed to ionization state change in PC-nAChR reconstitutions correlates with the pure lipid bilayers. As expected, there are no pH-induced changes in the spectra as PC cannot undergo an ionization state change within the pH range.

Spectra were then recorded from PC/PA-nAChR reconstitutions over the pH range 4 to 10 (Fig. 4.6B). Surprisingly, the spectra recorded in these titrations exhibit no spectral band shape changes. The spectra exhibit consistent monoanionic-characteristic spectral band shapes in the phosphate region and complete absence of the dianionic PA stretching peaks, specifically at 1020 cm^{-1}. Comparison of the PC/PA-nAChR reconstitution spectra at all pH values to the spectra recorded from pure PC/PA 3:2 membranes at pH 4 reveal similar phosphate bands. I also recorded a titration over the smaller range 7 to 10, to exclude the

Figure 4.6

Phosphate Vibrational Region of Spectra Recorded at Varying pH values in nAChR-Reconstituted Membranes; pH titration: 4 to 10. A, Stacked spectra of PC-nAChR reconstitution. B, Stacked spectra of PC/PA-nAChR reconstitution. Each titration represented similarly to Figure 4.3. Minimal spectral changes observed at the peaks attributed to monoanionic and dianionic PA head groups observed. Spectra in each titration were scaled at the lipid ester carbonyl peak (~1735 cm^{-1}) to an absorbance intensity of 1. Titration shown for each membrane is a representative series of spectra. Each titration was repeated at least 4 times with different membrane films and different reconstitutions, and data shown are reproducible, representative titrations.

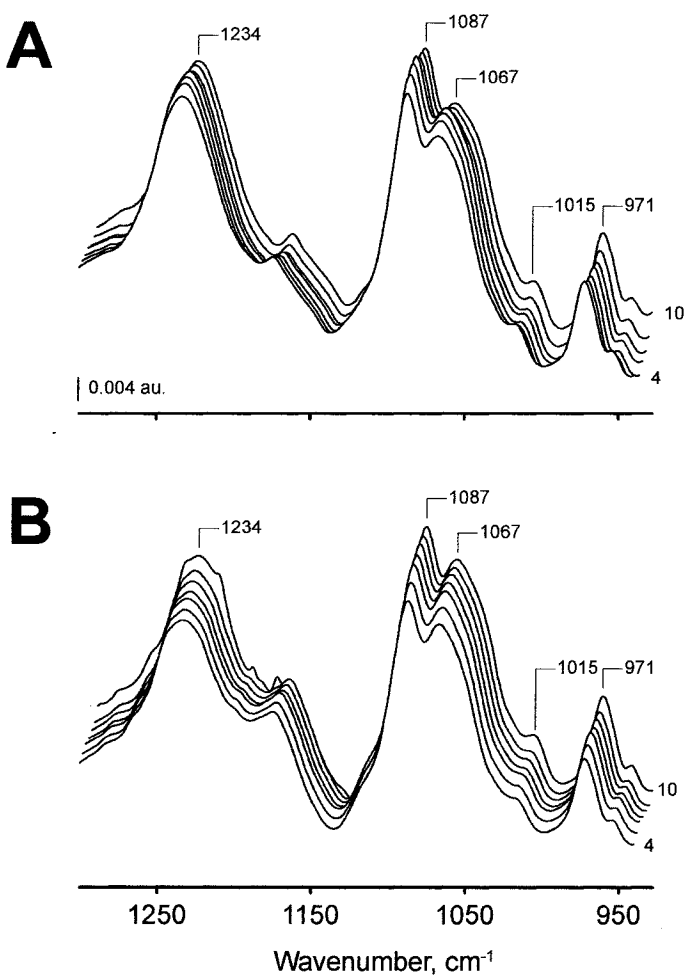
A
1234
1087
1067
1015
971
10
4
0.004 au.
B
1234
1087
1067
1015
971
10
4
1250
1150
1050
950
Wavenumber, cm-1

possibility of the low pH affecting the nAChR, and the titration spectra yielded similar phosphate band shapes. The spectra of the PC/PA-nAChR reconstitutions suggest stabilization of monoanionic PA head groups, regardless of the pH of the environment (no ionization state change visible up to pH 12; data not shown). These titrations were repeated several times, both with the same reconstitutions as well as freshly purified and reconstituted samples, to verify these findings, but in each case the spectra consisted of monoanionic-characteristic phosphate bands at each pH value. These findings are in direct contrast to those presented by Bhushan & McNamee (64). The results show that the nAChR does not stabilize the PA head group in the dianionic state. Furthermore, the dianionic state is not responsible for the efficacy of PA in stabilizing a functional nAChR.

As a further test, I examined the effects of the nAChR on the chemical properties of PA in a reconstituted PA membrane. The nAChR is stabilized in a moderately functional conformation compared to PC/PA-nAChR reconstitutions (Chapter 3). The pH-dependence of these membranes was found to be similar to that for the PC and PC/PA 3:2 membranes reconstituted with the nAChR in that there are no marker band intensity changes for monoanionic to dianionic PA head group ionization (Fig. 4.7A). The phosphate vibrational region of these spectra, however, appears substantially different from this region of spectra recorded from PA bilayers without the nAChR (Fig. 4.3B). The spectra contained bands with very weak intensities, and though there were some changes in the band shapes in this region with increasing pH, as mentioned the PA ionization marker bands, specifically the dianionic PA stretching peak at 1023 cm^{-1}, were absent. The spectra recorded from the nAChR-reconstituted PA membranes appeared to be dominated by the nAChR bands in this region from 1300-1000 cm^{-1}, suggesting a low amount of lipid head groups visible in these proteoliposomes.

Figure 4.7

FTIR Spectra of PA-nAChR Reconstitutions. A, Stacked spectra of phosphate vibrational region of pH titration of nAChR-reconstituted pure PA membranes. Spectrum at each pH value recorded at increasing pH value from front to back (pH 4 to 10). For comparison purposes, spectra presented on same scale as spectra in Figure 4.3B. Spectra scaled at the lipid ester carbonyl peak (~1735 cm^{-1}) to an absorbance intensity of 1. Titration shown is a representative series of spectra; Titration repeated 3 times with different membrane films and 2 different reconstitutions. B, Amide I (left) and II (right) regions of the PA-nAChR reconstitution. C, Lipid ester carbonyl profile of PA-nAChR reconstitution. Highlighted wavenumbers are attributed to the non-hydrogen-bonded ester carbonyl peak (1743 cm^{-1}) and the hydrogen-bonded ester carbonyl peak (1730 cm^{-1}). Spectra presented in B-left and C were deconvolved using GRAMS/AI software with deconvolution parameters: γ = 7, smoothing = 75%. Spectra of Amide II region shown without deconvolution. Spectra in B and C recorded in D_2O buffer.

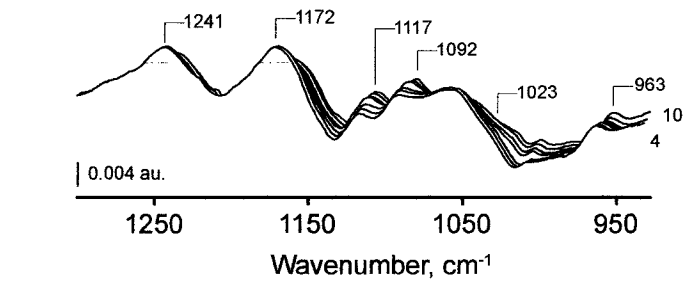
A
1241
1172
1117
1092
1023
963
10
4
0.004 au.
1250
1150
1050
950
Wavenumber, cm-1

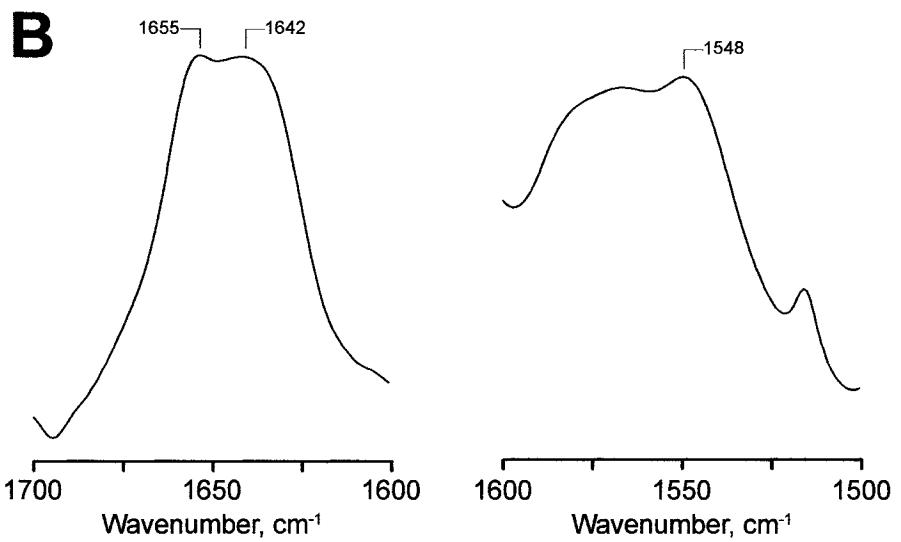
B
1655
1642
1548
1700
1650
1600
Wavenumber, cm-1
1600
1550
1500
Wavenumber, cm-1

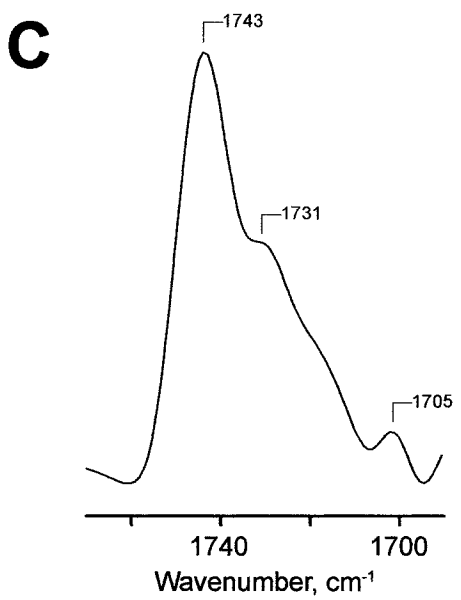
C
1743
1731
1705
1740
1700
Wavenumber, cm-1

One interesting feature of the FTIR spectra of the PA-nAChR reconstitutions is the lipid ester carbonyl profiles (Fig. 4.7C). The lipid ester carbonyl bands show a significantly larger intensity at the non-hydrogen bonded peak (1743 cm^{-1}) compared to the lipid ester carbonyl profiles of other reconstituted membrane systems (discussed in greater detail in next chapter). There are also extra peaks within the lipid ester carbonyl profile suggesting altered conformations of the lipid head groups, as seen in spectra recorded from PC/PS membranes with the nAChR. However, the peaks in PA-nAChR spectra do not appear at similar frequencies as in PC/PS-nAChR spectra. The lipid ester carbonyl profile here also reveals the lipid:protein ratio of these membranes, which was found to be higher than nAChR-reconstituted PC/PA 3:2 membranes (~150:1 mol:mol). This increased lipid:protein is intriguing given the weak intensity in the phosphate region of the spectra of the PA-nAChR reconstitutions. The amide I band shapes for the nAChR in the PA membrane are similar to those recorded from the nAChR in PC/PA 3:2 membranes, suggesting a similar extent of nAChR peptide hydrogen deuterium exchange in these membranes (13). The amide II band shapes of the nAChR in the PA membranes are also similar to those from PC/PA-nAChR reconstitutions. The amide I/II band shapes seen in these spectra generally correlate with the ability of the nAChR to undergo agonist-induced conformational change, as shown in previous studies (73). The interesting aspect is the significant differences between the lipid ester carbonyl profiles in the PA membranes compared to profiles recorded in other membranes that stabilize a functional nAChR. The analysis of the spectra indicates the similarities of the nAChR within these membranes, but hints at an altered head group conformation of the lipids in the PA-nAChR reconstitution proteoliposomes.

4.2.5 – Monitoring nAChR-Reconstituted Membrane Surface pH

In an attempt to examine the pH at the membrane surface, we used a pH-sensitive probe in order to monitor pH alterations at the membrane surface in the presence and absence of the nAChR (Fig. 4.8). Of the possible pH-sensitive probes, the pH-sensitivity of Fluorescein lies within the pH range examined for the titrations, and ionization of Fluorescein results in intense fluorescence. Fluorescein exhibits pH-dependent fluorescence when the neutral state ionizes to the anionic state, resulting in a strong fluorescence signal. As we wanted to examine the pH at membrane surface, we required a way to anchor the Fluorescein molecule within a short distance of the membrane surface. A Fluorescein-lipid probe where Fluorescein was covalently attached to the head group of PE (89-92), was used. Preliminary data collected with this lipid probe (CFPE) indicate that we can incorporate the probe into lipid vesicles and monitor the fluorescence signal resulting from increasing pH (Fig. 4.8B). The next step is to incorporate the probe into nAChR-reconstitutions, both PC-nAChR and PC/PA-nAChR, and examine the fluorescence and the pH-dependence. If the nAChR is causing reduced pH, the curve of fluorescence intensity at the emission maxima (Fig. 4.8C) would appear right-shifted, where the transition would occur at a higher buffer pH (*dashed line*). However, our early attempts to incorporate CFPE into nAChR-reconstituted proteoliposomes resulted in inconsistent data. Future work, including separation of CFPE-containing nAChR-reconstituted proteoliposomes from other liposomes and CFPE fluorescence in proteoliposomes with high lipid-to-protein ratios, will need to be completed in order to systematically address the possibility of determining the pH at the membrane surface in membrane protein reconstituted membranes.

Figure 4.8

pH-sensitive Fluorescent Probe, Fluorescein, Preliminary Findings. A, Structure of carboxyfluorescein-labeled DOPE (CFPE). Increasing pH leads to ionization of the Fluorescein molecule covalently attached to the head group of the phospholipid resulting in increased fluorescent signal. The Fluorescein molecule protrudes roughly 15Å from the membrane surface and should measure surface pH. B, Fluorescence emission spectra recorded from CFPE incorporated into PC (left) and PC/PA 3:2 (right) membranes. Increasing pH from 5 to 13 results in increasing fluorescence with emission maximum at roughly 526 nm. C, Plot of percent intensity vs. pH from emission spectra recorded from PC (open circles) and PC/PA 3:2 (open diamonds). The intensity at the emission maximum at each pH value was recorded and plotted as a percent of the intensity at pH after intensity reached maximum. Solid lines represent non-linear regression of data. Filled diamonds: theoretical data for PC/PA-nAChR reconstitution, with dashed line representing non-linear regression of said data.

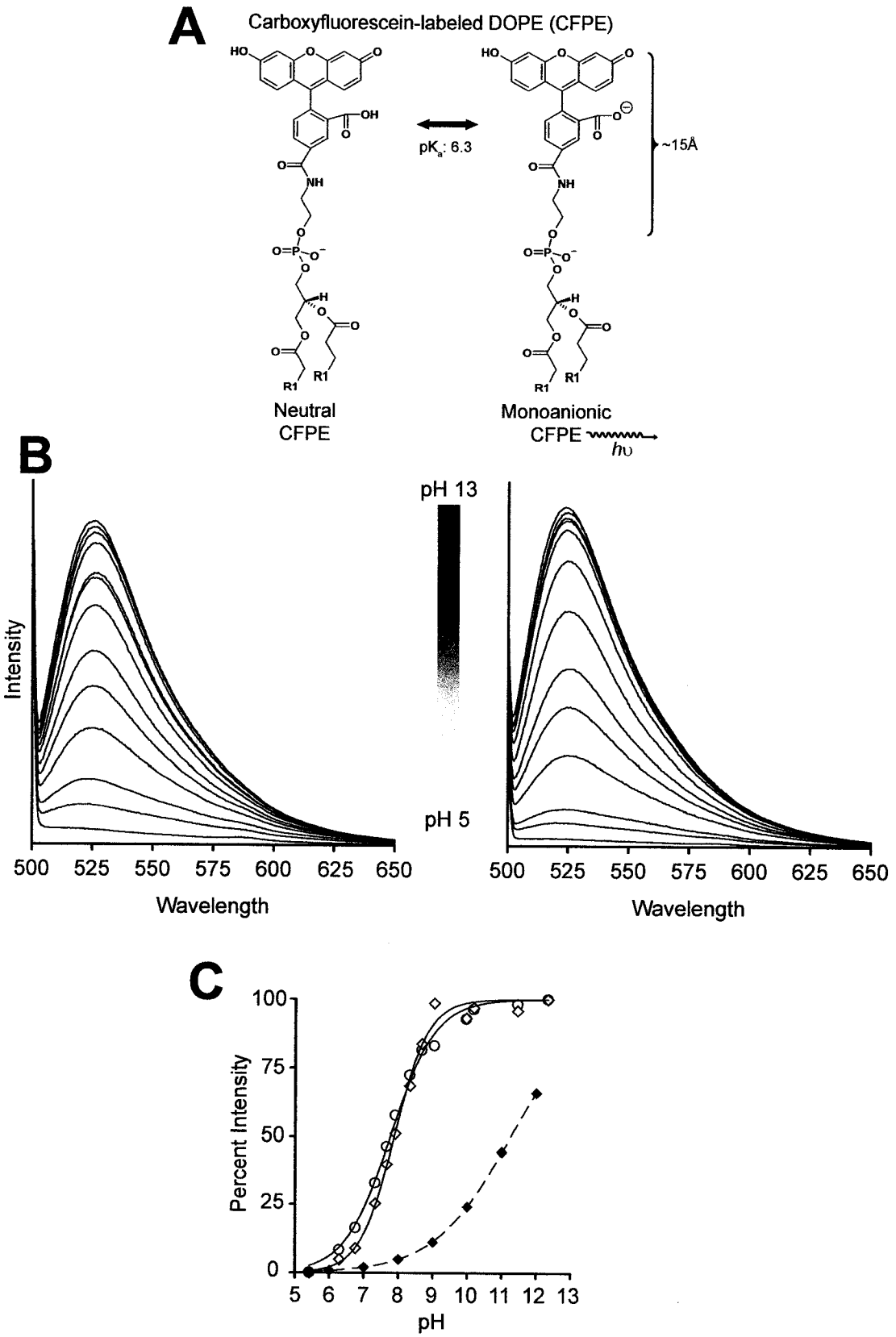
A
Carboxyfluorescein-labeled DOPE (CFPE)
pK$_a$: 6.3
~15Å
Neutral CFPE
Monoanionic CFPE
hυ
B
pH 13
pH 5
Intensity
500 525 550 575 600 625 650
Wavelength
500 525 550 575 600 625 650
Wavelength
C
Percent Intensity
100
75
50
25
0
5 6 7 8 9 10 11 12 13
pH

4.3 – Summary & Conclusions

In all of the pH titrations performed throughout this study, PC membranes, with and without the nAChR, were used as controls. These membranes are composed only of phospholipids which do not have ionizable head groups, thus the phospholipid head groups should not be susceptible to changes in the pH of the environment. Any spectral changes would therefore be an indication of general pH-induced membrane alterations, thereby hindering the analysis in PC/PA membranes and possibly in the PA membranes. In the PC membrane pH titrations, there were no changes in the phosphate region of the spectra that indicate head group ionization or membrane structural alterations (Fig. 4.3A). The apparent lack of spectral changes in the phosphate region combined with the lack of pH-induced lipid ester carbonyl band changes (see Chapter 5) suggest consistent PC membranes at each pH value throughout the titrations. Reconstitution of the nAChR into PC membranes results in spectra similar to the PC membranes in the absence of the nAChR, indicating the nAChR has little to no effect on the structural and chemical properties of these membranes. Spectra recorded from the PC-nAChR reconstitutions over the pH range 4 to 10 display no spectral changes suggestive of pH-dependent changes on membrane or protein structure (Fig. 4.6A). As expected, spectra recorded from PC membranes with and without the nAChR exhibit no indications of PC head group alterations throughout the titrations.

Spectra recorded from PA and PC/PA 3:2 membranes exhibit phosphate band shape changes as the pH of the system is increased (Fig. 4.3B, C). At low pH, the population of PA in these membranes is primarily monoanionic, which ionizes to increasingly dianionic as we increase the pH. These peaks appear slightly shifted between the 2 membranes due to the presence of contributing PC head group peaks in the PC/PA 3:2 membranes. Specifically,

the difference in peak frequency and broadness of the dianionic PA head group peak at 1020 cm^{-1} is due to the contributing small peak from PC at 1015 cm^{-1}, which is plainly visible in the PC-containing membranes. The difference in peak maximum and broadness are due to a contributing small peak from PC at 1015 cm^{-1} that is visible in PC/PA 3:2 membranes at pH 4. Spectra recorded from the pure PC membranes exhibit a small peak at 1015 cm^{-1} that experiences subtle intensity increases throughout the titrations. However, these changes are insignificant compared to PA and PC/PA 3:2 membrane intensity changes at the dianionic PA head group peak in this region. While it is thought that PA membranes might not form planar bilayers but something closer to that of a hexagonal phase structure (H_{II}) (93), spectral changes of marker monoanionic and dianionic PA head group bands were present in spectra recorded from the PA membranes.

The area and intensity of the dianionic PA head group peaks were compared in the PA and PC/PA 3:2 membranes by scaling the lipid ester carbonyl bands in all the spectra at each pH; The amount of lipid used in each titration was the same, thus scaling at the lipid ester carbonyl bands would account for any subtle variations in intensity between the spectral sets (due to film expansions, water penetration, etc). In PA membranes, the scaled intensity of the dianionic peak at pH 12 (full dianionic character, as determined qualitatively from the spectra) is only slightly more intense than the dianionic peak in PC/PA 3:2 membranes at pH 10 (full dianionic character). The small difference in intensity indicates that even in a membrane with 60% less PA, the intensity of an ionization state change is almost on par with a PA membrane, thus the intensity is not proportional to the percentage of PA in the membrane. Therefore, spectra of membranes with a decreased proportion of PA should still exhibit intensity at the marker bands suggesting PA head group ionization.

In PC/PA 3:2 membranes, the largest PA head group ionization state changes from monoanionic to dianionic occur between the pH range of 5 to 8 (Fig. 4.4, *open diamonds*), whereas PA membranes undergo the same ionization state changes in the pH range of 7 to 10 (*open squares*). The difference in the observed pK_a between these two membranes systems (~2.2 pH units) can be attributed to the presence of a large proportion of PC in the PC/PA 3:2 membranes. The possible explanation involves the electrostatic consideration of densely negatively charged lipids within short distances of each other. In the mixed PC/PA membranes, the negatively charged PA head groups are spaced out between the PC head groups, assuming a natural dilution of the phospholipids within the membrane system. In PA membranes, the absence of intervening neutral molecules separating the dense, negatively-charged head groups leads to an unfavorable membrane environment (Fig. 4.9). These unfavorable interactions increase significantly with rising pH and the subsequent increase in dianionic PA head groups. In both membrane systems, there is an inherent electrostatic barrier that prevents ionization of the head groups until there is a much lower concentration of hydrogen ions in the surrounding the membrane environment. Within the membranes with decreased amounts of PA and the presence of a neutral phospholipid this energy barrier is much lower, giving a decrease of 2 pH units in the apparent pK_a value for PA ionization in the mixed membranes compared to the PA membranes.

The primary objective of this study was to examine the importance of the ability of PA to exist in a dianionic state within a nAChR-reconstituted membrane. It had been suggested that this dianionic state of PA was instrumental in the efficacy of PA in stabilizing a functional nAChR. However, there were no spectral band shapes attributable to the dianionic PA head group in spectra recorded from the PC/PA-nAChR reconstitutions at any pH (Fig. 4.6B). Spectra recorded from the PC/PA-nAChR reconstitutions at every pH were

Figure 4.9

Electrostatic Interactions of PA Head Groups in Membranes without the nAChR. Top, increasing pH in pure PA bilayers results in the ionization of the monoanionic PA head groups (blue) to the dianionic state (red). The interactions between the small anionic head groups with 2 negative charges will be extremely unfavorable, resulting in large spaces between head groups or possibly a non-bilayer structure formation. Bottom, in mixed PC/PA bilayers, the anionic head groups of PA ionize from mono- to dianionic at a lower pH due to the presence of the larger, neutral PC head groups. The PC head groups occupy the space between the anionic PA head groups, and the natural dilution of membranes allows dianionic head groups to become spaced out even further in order to reduce the unfavorable interactions.

Pure PA Bilayers

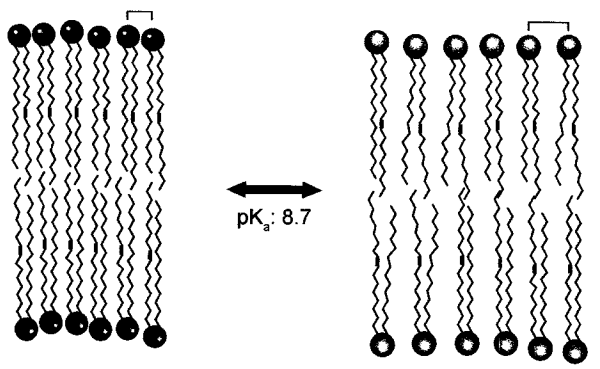

Moderately unfavorable

Extremely unfavorable

Lipids:

Dianionic POPA

Monoanionic POPA

POPC

Mixed PC/PA 3:2 Bilayers

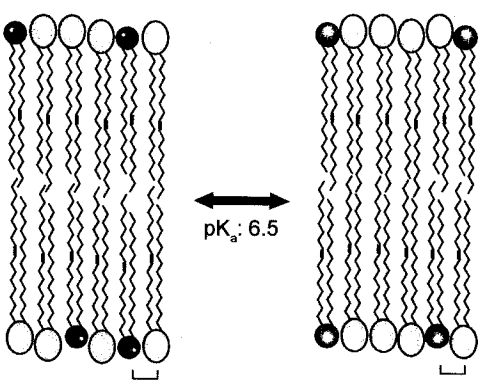

Minimal unfavorable head group interactions in both cases

similar to the PC/PA 3:2 membranes without the nAChR at low pH, at which there is primarily monoanionic PA (Fig. 4.3C, *front trace*). There was no observed intensity increases at 1020 cm^{-1}, which was seen in PC/PA 3:2 membranes as a slight broadening at first followed by increased intensity at 1020 cm^{-1}. The lack of increase at 1020 cm^{-1}, as well as the overall absence of changes in marker monoanionic and dianionic bands in the phosphate region, demonstrates that the nAChR stabilizes the monoanionic state of PA, rather than the dianionic state, contrary to previously suggested (64). Consistent with stabilization of the monoanionic head group of PA in PC/PA-nAChR reconstitutions the T_m of these reconstituted membranes at both pH 7 and 10 were similar, suggesting no increase of dianionic PA head group population within these nAChR-reconstituted membranes (Table 5.2). The similar T_m is indicative of consistent membrane chemical properties that affect the T_m (see Chapter 5), specifically PA head group ionization state. The dianionic state of the PA head group appears to be inconsequential in the efficacy of PA in stabilizing a functional nAChR in reconstituted membranes. Potential mechanism(s) behind the importance of this particular anionic lipid in stabilizing the functional conformation of the nAChR therefore remains to be elucidated (see Chapter 6).

Chapter 5: nAChR Modulation of Bilayer Physical Properties

5.1 – Introduction

The lipid composition of a nAChR-reconstituted membrane is an important determinant for preserving function a reconstituted system (58-62, 67, 72, 75). The importance of anionic lipids has been established, as well as the effect of neutral lipids combined with anionic lipids further increasing the functional level of the nAChR in reconstituted membranes (72). PA appears to be the most effective at modulating nAChR function in binary lipid mixtures with PC, while other lipids with different head group size and charge are not nearly as effective (76).

In the previous chapter, I showed that the unique ability of PA to exist in the dianionic state is not responsible for the efficacy of PA in stabilizing the functional conformation of the nAChR. In fact, I demonstrated that the nAChR stabilizes the monoanionic state of the PA head group in PC/PA 3:2 reconstituted membranes. In the previous chapter, I showed that PC/PA 3:2 membranes (without the nAChR) can contain populations of both mono- and dianionic PA head groups at a given pH. Given that these membranes contain a mixture of the monoanionic and dianionic PA head group states, it seemed likely that nAChR-induced stabilization of the monoanionic PA head group could lead to changes in membrane physical properties. The monoanionic state (with the lone negatively charged group) exhibits reduced electrostatic repulsion between the head groups than the dianionic state with its pair of negative charges. Stabilization of the monoanionic PA head group might thus account for the dramatic changes in the physical properties of

PC/PA membranes upon incorporation of the nAChR (73). As well, I showed in chapter 3 that the nAChR catalyzes the formation of DAG, which could factor into the altered bilayer physical properties in the PC/PA-nAChR reconstitutions.

At this point, the focus of my thesis work shifted towards addressing the mechanisms behind the observed alterations of the membrane physical properties that are observed upon incorporation of the nAChR into the membrane. The stabilization of the monoanionic state of the PA head group, the presence of DAG within the membrane, and increased concentrations of cations at the membrane surface were 3 factors that were considered to influence the bilayer properties. Each of these factors was shown to be partly responsible and when combined in pure lipid membranes, the bilayer physical properties mimicked the situation observed in the PC/PA-nAChR reconstitutions.

5.2 – Results

5.2.1 – Effects of the nAChR on Reconstituted Membranes

I first examined the physical properties of membranes with and without the nAChR, in order to validate the previous observations (Fig. 5.1A) (73). The phase transition temperature (T_m) of the lipids, a parameter related to the order of the lipid acyl chains, was first recorded. Upon cooling, the C-H stretching frequency of the lipid acyl chains shifts down roughly 2 cm^{-1} from 2853 to 2851 cm^{-1} as the lipids transition from the liquid crystal to the gel phase. Cooling curves for PC/PA 3:2 and PC membranes in *Torpedo* Ringer buffer show that these lipids undergo a liquid crystal to gel phase transition at different temperatures (Fig. 5.1A, *open circles*). The T_m for PC/PA 3:2 membranes is 13.1 ± 0.2°C while the PC membranes exhibit a T_m of -3.9 ± 1.8°C (Table 5.1). The presence of the nAChR (*filled circles*) in PC membranes leads to a slight increase in T_m to -1.8 ± 0.5°C, whereas the presence of the nAChR in PC/PA 3:2 membranes increases the T_m to 24.7 ± 0.2°C (*top*), an increase of 11.6°C. The increased T_m of the PC/PA-nAChR reconstitutions is evidence that the nAChR affects the thermal stability of these membranes, confirming the previous findings.

The lipid ester carbonyl bands provide qualitative information regarding the physical properties of membranes with and without the nAChR (73). Spectra recorded from both pure and reconstituted membranes exhibit lipid ester carbonyl bands typically composed of two component bands that correspond to hydrogen bonded (1729 cm^{-1}) and non-hydrogen-bonded (1741 cm^{-1}) lipid ester carbonyls (Fig. 5.1B). The intensities of these 2 component bands relative to each other are qualitative indicators of the amount of water penetrating into

Figure 5.1

Influence of the Presence of nAChR on Bilayer Physical Properties. A, Temperature dependence of the C-H stretching frequencies observed in spectra of membranes of PC/PA 3:2 (top) and PC (bottom) in the presence (filled circles) and absence of the nAChR (open circles). B, Carbonyl stretching region in deconvolved spectra of lipid membranes composed of PC/PA 3:2 (left) and PC (right) in the absence (trace i) and presence (trace ii) of the nAChR. The presence of the nAChR in PA-containing membranes leads to an increased amount of non-hydrogen bonded lipid ester carbonyl (1741 cm^{-1}) and a decrease in hydrogen-bonded ester carbonyl (1729 cm^{-1}) component bands, suggesting a change in water penetration into the membrane. Both the phase transition cooling curves and the lipid ester carbonyl profiles shown are representative data; Data shown are reproducible, and were collected at least 3 times to confirm consistency. Spectra shown in B scaled to 1 au. prior to deconvolution. Spectra deconvolved using parameters: $\gamma = 7$, smoothing = 75%.

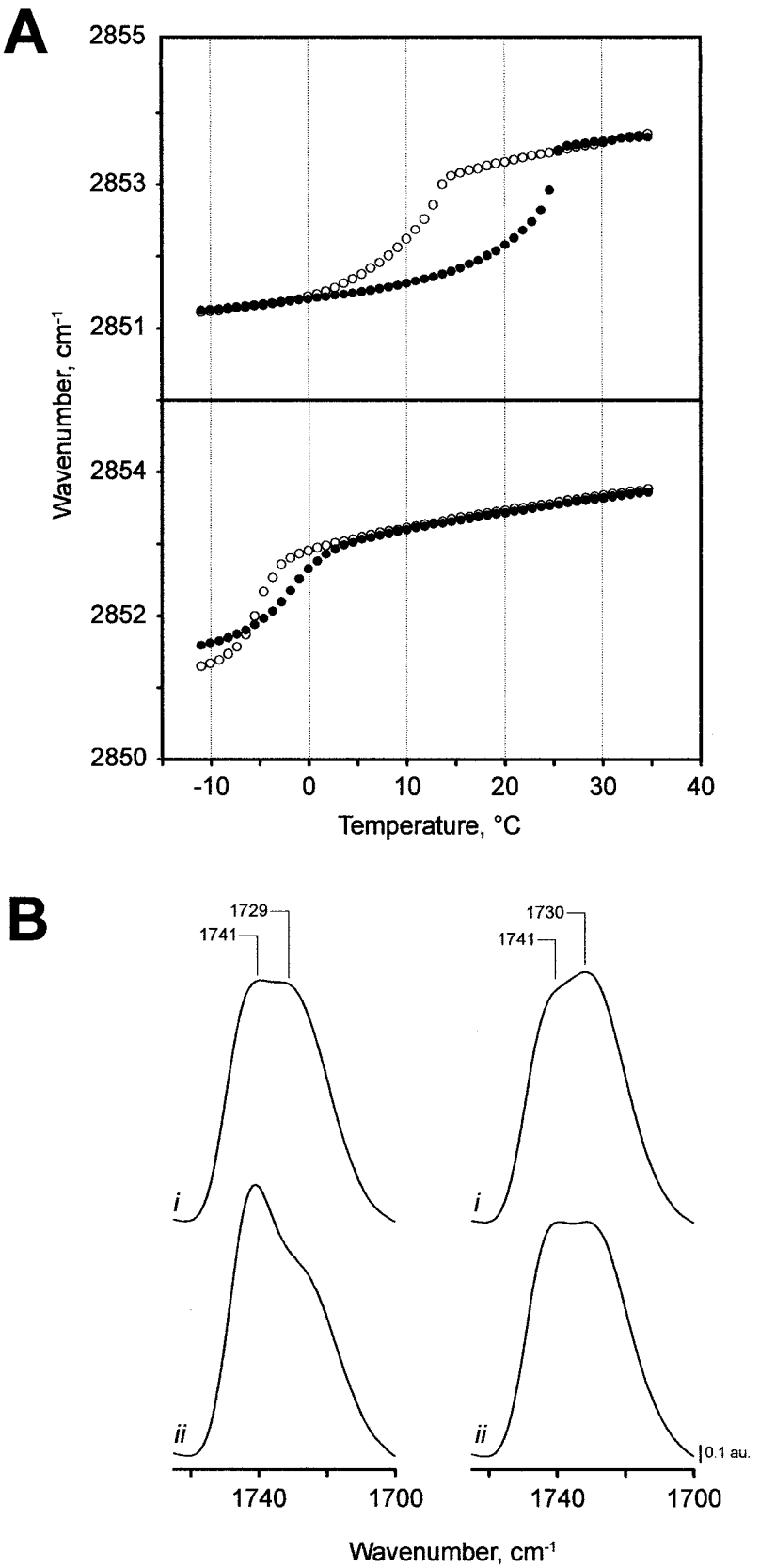
A
2855
2853
2851
2854
2852
2850
Wavenumber, cm-1
-10
0
10
20
30
40
Temperature, °C
B
1729
1741
1730
1741
i
i
ii
ii
0.1 au.
1740
1700
1740
1700
Wavenumber, cm-1

Table 5.1 - Gel-to-liquid Crystal Phase Transition Temperatures of Bilayers Under Varying Conditions

Gel-to-liquid crystal phase transition temperatures in the presence and absence of the nAChR

Membrane Lipid Composition	T_m of pure lipid (°C)	T_m of lipid + nAChR (°C)	Change in T_m with nAChR (°C)
PC	**-3.9 ± 1.8 (4)**	**-1.8 ± 0.5 (3)**	**2.1**
PC/PA 3:2	**13.1 ± 0.2 (4)**	**24.7 ± 0.2 (3)**	**11.6**

Gel-to-liquid crystal phase transition temperatures of the lipid bilayers at different pH values

	T_m at pH 4 (°C)	T_m at pH 7 (°C)	T_m at pH 10 (°C)	Change in T_m from 7 to 4 (°C)
PC	**-4.6 ± 0.4 (2)**	**-3.9 ± 1.8 (4)**	**-4.4 ± 1.6 (4)**	**-0.7**
PC/PA 3:2	**19.0 ± 0.0 (3)**	**13.1 ± 0.2 (4)**	**2.3 ± 0.0 (2)**	**5.9**

Gel-to-liquid crystal phase transition temperatures of the lipid bilayers at different Ionic Strengths

	T_m at 1X (°C)	T_m at 5X (°C)	T_m at 10X (°C)	Change in T_m from 1x to 10x (°C)
PC	**-3.9 ± 1.8 (4)**	**ND**	**0.7 ± 0.7 (2)**	**4.6**
PC/PA 3:2	**19.0 ± 0.0 (3)**	**23.6 ± 0.3 (3)**	**24.8 ± 0.4 (2)**	**4.8**

Gel-to-liquid crystal phase transition temperatures of PC bilayers with altered amounts of PA and/or DAG

	T_m with 33% PA (°C)	T_m with 33% DAG (°C)	T_m with 33% PA and DAG (°C)
PC	**2.9 ± 0.2 (3)**	**18.5 ± 0.5 (3)**	**20.7 ± 0.2 (3)**

the membrane head group region, thus an indicator of the membrane head group packing density (94).

Spectra recorded from the PC-nAChR reconstitutions exhibit roughly equal intensities at the hydrogen-bonded and non-hydrogen-bonded component bands (*right*). Incorporation of the nAChR into PC membranes leads to a slight decrease in the hydrogen-bonded component bands, suggesting a slight increase in lateral packing density. The lack of a substantial increase in the non-hydrogen-bonded component coupled with the minor change in the T_m of the membranes upon incorporation of the nAChR suggests that the presence of the nAChR only leads to minor changes in the lateral packing density of the PC membranes.

Spectra recorded from PC/PA 3:2 membranes also show roughly equal proportions of hydrogen-bonded and the non-hydrogen-bonded component bands. Upon incorporation of the nAChR, however, there is a substantial increase in the proportion of non-hydrogen-bonding lipid ester carbonyls (*left*). The larger non-hydrogen-bonded lipid ester carbonyl band is indicative of a low degree of water penetration into the interfacial region of the lipid bilayer and a higher lateral packing density, consistent with an increase in lateral tightening of the membrane upon nAChR reconstitution into only the PA-containing membranes, consistent with the effects on T_m. The interactions responsible for the altered physical properties in PA-containing bilayers reconstituted with the nAChR were not clear when this relationship was first discovered.

5.2.2 – PA head group ionization affects bilayer T_m

The nAChR stabilizes the monoanionic state of the PA head group in PC/PA 3:2 membranes and the altered head group ionization state could potentially affect the bilayer physical properties. To test this possibility, I examined the phase transition behaviour of membranes composed of PC/PA 3:2 and PC at varying pH (Fig. 5.2A). In PC/PA 3:2 membranes, increased pH results in a dramatic decrease in the T_m of the membrane (*top*). At low pH values, where the PA head groups are primarily in the monoanionic state, the T_m is 19.0 ± 0.0°C. At high pH values, where the PA head groups are primarily dianionic, the T_m was found to be 2.3 ± 0.0°C. Higher T_m suggests a more ordered and stable membrane at higher temperatures, requiring increased cooling to cause the transition from the liquid crystal to gel phase. PC membranes, however, exhibit no changes in T_m upon changes in pH (*bottom*). This is expected, though, as PC has no ionizable groups within this range. Clearly altered pH, and therefore altered head group ionization state within the bilayer, at the surface of PA-containing membranes can affect the T_m of the bilayer.

The lipid ester carbonyl band shapes were also examined at varying pH values (Fig. 5.2B). Spectra recorded from PC membranes show similar lipid ester carbonyl hydrogen-bonding component bands at varying pH values (*right*). The lack of alterations of the lipid ester carbonyl component bands in PC membranes agrees with the consistent T_m of PC membranes at different pH values. In contrast, spectra recorded from PC/PA 3:2 membranes indicate the lipid ester carbonyl component band patterns are influenced by pH (*left*). Consistent with the varying T_m, lipid ester carbonyl bands show a larger proportion of the non-hydrogen-bonded component at pH 4. As pH increases, the dianionic PA head group population increases and the proportion of non-hydrogen-bonded to hydrogen-bond lipid ester carbonyls shifts to primarily the hydrogen-bonded component band. The increased

Figure 5.2

Assessing the Physical Properties of Lipid Membranes without the nAChR at Varying pH. A, Temperature dependence of the C-H stretching frequencies observed in spectra of membranes of PC/PA 3:2 (top) and PC (bottom) at pH 4 (red circles), pH 7 (black circles) and pH 10 (blue circles). Curves for PC offset slightly for clarity, as they superimpose. B, Carbonyl stretching region in deconvolved spectra of lipid membranes composed of PC/PA 3:2 (left) and PC (right) at pH 10 (blue, trace i), pH 7 (black, trace ii) and pH 4 (red, trace iii). Spectra collected, scaled and deconvolved in similar manner as described in Figure 5.1.

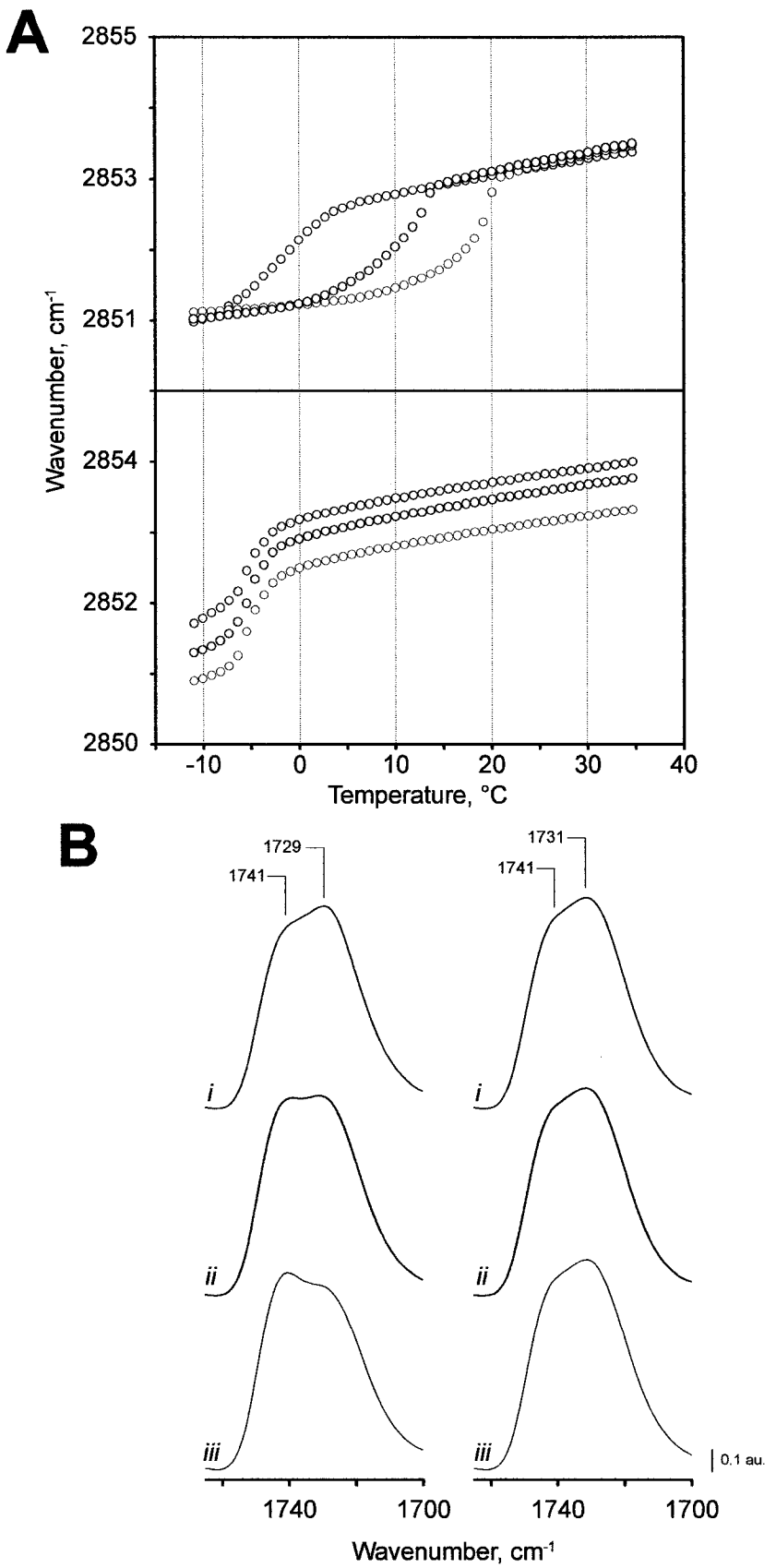
A
2855
2853
2851
2854
2852
2850
Wavenumber, cm-1
-10
0
10
20
30
40
Temperature, °C
B
1729
1741
1731
1741
i
ii
iii
0.1 au.
1740
1700
1740
1700
Wavenumber, cm-1

hydrogen-bonded component at high pH reflects increased water penetration into the head group region because the electrostatic repulsion between the dianionic PA head groups. The lipid ester carbonyl component bands and the T_m analysis of PC/PA 3:2 membranes reflect increased membrane stability and head group packing density, due to primarily monoanionic PA head groups present, possibly mimicking the situation in PC/PA-nAChR reconstitutions. However, stabilization of the monoanionic state in PC/PA 3:2 membranes results in a bilayer T_m of 19.0°C, which is 5.7°C below the T_m of the PC/PA-nAChR reconstitutions. Although the stabilization of the monoanionic state of PA may account for a large portion of the increased T_m upon incorporation of the nAChR, other factors are likely involved in the altered bilayer physical properties in PC/PA-nAChR reconstitutions.

5.2.3 – Environmental ionic strength affects bilayer T_m

The stabilization of the monoanionic state accounts for some of the changes in PC/PA 3:2 membrane physical properties in nAChR-reconstituted membranes though additional effects are observed. As previous work has suggested, membrane channel proteins such as the nAChR have the ability to increase the concentration of cations surrounding the receptor at the membrane surface (74, 95-97). In light of previous reports indicating ability of the nAChR to concentrate cations near its extramembranous domains, I examined if increased concentration of cations, similar to the decreased pH, at the membrane surface could affect the T_m and the lipid ester carbonyl bands of the PC/PA-nAChR reconstitutions.

I first examined the T_m of PC/PA 3:2 and PC membranes in buffers containing increased concentrations of all cations in *Torpedo* Ringer buffer (Na^+, K^+, Ca^{2+}, & Mg^{2+}) at pH 4 in an attempt to fully recreate the environment induced by the presence of the nAChR

in PC/PA-nAChR reconstitutions (Fig. 5.3A). The initial concentrations of the cations in *Torpedo* Ringer buffer are 250 mM, 5 mM, 3 mM and 2 mM for Na^+, K^+, Ca^{2+}, & Mg^{2+}, respectively. Interestingly, it appears that the T_m of both PC/PA 3:2 and PC membranes are influenced by increased concentrations of cations surrounding the membrane. In PC/PA 3:2 membranes at pH 4, increased concentrations of all cations in the buffer increased the T_m linearly up to five times the initial concentrations listed above, at which point the T_m reached 23.6 ± 0.3°C, and only increased to 24.8 ± 0.4°C upon increasing the concentration further to ten times the initial concentrations. The T_m of PC membranes increased to 0.7 ± 0.7°C upon increasing the cation concentrations to ten times that of *Torpedo* Ringer buffer, an increase of 4.6°C, similar to PC/PA 3:2 membranes. The increased T_m in PC membranes was observed with concentrations of all cations ten times higher than the standard concentrations. The observed bilayer T_m shift in these ionic strength experiments compared to the T_m shift upon nAChR incorporation suggests that the presence of the nAChR in PC membranes does not increase the concentrations of cations to the same degree as I used in these experiments. In PA-containing membranes, the increased cation concentration surrounding the lipid head groups combined stabilization of the monoanionic state of PA leads PC/PA 3:2 bilayers to undergo the phase transition at temperatures almost identical to PC/PA-nAChR reconstitutions.

Spectra recorded from PC/PA 3:2 membranes indicated that the lipid ester carbonyl component bands are also influenced by cation concentrations (Fig. 5.3B). Increasing cation concentrations, at pH 4, correlate with increased non-hydrogen-bonded lipid ester carbonyl component bands in PC/PA 3:2 membranes (*left*), which mimic the PC/PA-nAChR reconstitutions. Similar to the changes in pH, altered ion concentration leads to lipid ester carbonyl peaks (1741 and 1729 cm^{-1}) that are almost identical to the PC/PA-nAChR

Figure 5.3

Assessing the Physical Properties of Lipid Membranes without the nAChR at Varying Ionic Strength. A, Temperature dependence of the C-H stretching frequencies observed in spectra of membranes of PC/PA 3:2 (top) and PC (bottom) at pH 4 with 1x ionic strength (open diamonds), 5x ionic strength (grey filled diamonds) and 10x ionic strength (black filled diamonds) buffer. B, Carbonyl stretching region in deconvolved spectra of lipid membranes composed of PC/PA 3:2 (left) and PC (right) at pH 4 with 10x ionic strength (trace i), 5x ionic strength (trace ii) and 1x ionic strength (trace iii) buffer. Spectra collected, scaled and deconvolved in similar manner as described in Figure 5.1.

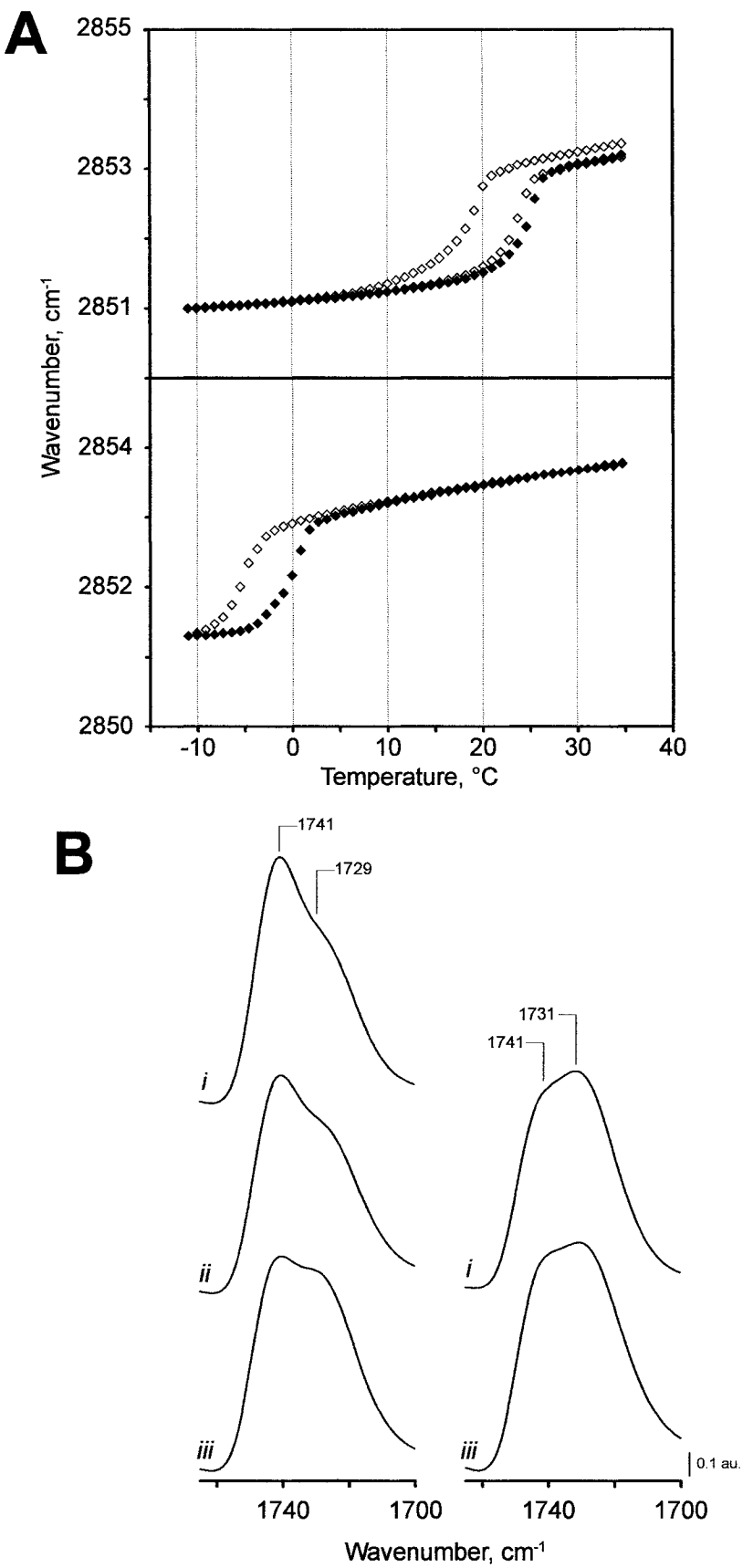
A
2855
2853
2851
2854
2852
2850
Wavenumber, cm-1
-10
0
10
20
30
40
Temperature, °C
B
1741
1729
1731
1741
i
ii
iii
i
iii
0.1 au.
1740
1700
1740
1700
Wavenumber, cm-1

reconstitutions. The spectra recorded from PC membranes indicate a subtle decrease in the hydrogen-bonded component band with increasing cation concentration, but at a much smaller amount than in PC/PA 3:2 membranes (*right*). The phase transition behaviour of pure lipid membranes is highly susceptible to both changing pH and ionic strength of the local environment, and altering these parameters can result in recreation of an environment similar to that induced in PC/PA-nAChR reconstitutions.

A series of experiments examining the T_m and lipid ester carbonyl bands of PC/PA 3:2 membranes in the presence of increased concentrations of individual cations was also performed. These experiments were aimed at determining the effects of different cations on the physical properties of the bilayers. Based on T_m values found, I determined that divalent cations, specifically calcium, affect bilayer T_m to a larger degree than monovalent cations (Table 5.2). A concentration of 30 mM Ca^{2+} resulted in a T_m of 22.7 ± 0.5°C, which was higher than if the concentration of Na^+ was increased from 250 mM to 2.5 M (21.4 ± 0.3°C). In correlation with the observed T_m values, the lipid ester carbonyl component bands in the presence of increased Ca^{2+} more closely resembled the PC/PA-nAChR reconstitution lipid ester carbonyl bands than did the increased Na^+ (data not shown). These findings were intriguing given reports indicating a possible nAChR-potentiator role of calcium (98-101). Overall, the results of varying the ionic strength suggest that the T_m shift observed upon reconstitution of the nAChR into PA-containing bilayers is partly due to the nAChR concentrating cations around its ligand binding intracellular domains, and the increased concentration of cations at the membrane surface alter the physical properties of the bilayer.

Table 5.2 - Gel-to-liquid Crysal Phase Transition Temperatures Under Varying Conditions (Part 2)

Gel-to-liquid crystal phase transition temperatures of lipid bilayers at increased concentrations of specific cations

Membrane Lipid Composition	T_m of 10x Monovalent Cations (°C)	T_m of 10x Divalent Cations (°C)	T_m of 10x Ca^{2+}, 1x other cations (°C)	T_m of 10x Mg^{2+}, 1x other cations (°C)
PC/PA 3:2	**21.4 ± 0.3 (4)**	**23.5 ± 1.3 (4)**	**22.7 ± 0.5 (3)**	**20.2 ± 0.6 (3)**

Gel-to-liquid crystal phase transition temperatures of nAChR-Reconstituted membranes at different pH values

	T_m at pH 4 (°C)	T_m at pH 7 (°C)	T_m at pH 10 (°C)	Change in T_m from 7 to 10 (°C)
PC/PA 3:2	**ND**	**24.7 ± 0.2 (3)**	**24.2 ± 1.6 (3)**	**-0.5**

Gel-to-liquid crystal phase transition temperatures of nAChR-Reconstituted membranes with increasing amounts of EDTA

	T_m after 2x EDTA washing (°C)	T_m after 4x EDTA washing (°C)	T_m after 8x EDTA washing (°C)	Change in T_m from no washing to 8x (°C)
PC/PA 3:2	**25.0 ± 0.1 (3)**	**24.2 ± 0.2 (3)**	**23.9 ± 0.3 (2)**	**-0.8**

5.2.4 – Presence of DAG affects bilayer T_m

The presence of DAG in the nAChR-reconstituted samples containing PA could also be affecting the physical properties of the bilayers, as well as the reason PA-containing membranes are able to stabilize a functional nAChR upon reconstitution. The physical properties of bilayers capable of stabilizing function have been deemed an important aspect of the lipid membrane modulating the functional state of the nAChR. The presence of DAG could be playing an unforeseen role in these PA-containing membranes that has not yet been examined. In order to address the possibility of DAG affecting the physical properties of bilayers, the phase transition behaviour of membranes containing different amounts of DAG and PA was examined (Fig. 5.4A). I also examined the effect of a decreased amount of PA within a PC membrane. In PC/PA 3:1 membranes, the T_m of the membrane was found to be 2.9 ± 0.2°C, compared to the T_m of 13.1 ± 0.2°C in PC/PA 3:2 membranes (Table 5.1). Compensating for the decrease in PA with a correlated amount of DAG results in a drastic increase in the T_m of these membranes; the T_m of PC/PA/DAG 3:1:1 membranes was found to be 20.7 ± 0.2°C. The presence of DAG alone in a membrane (PC/DAG 3:1) resulted in a T_m similar to a PC/PA 3:2 membrane: 18.5 ± 0.5°C. These phase transition curves were obtained at a standard pH of 7, at which we expect to find a mixture of both dianionic and monoanionic PA head groups.

As was observed with the varying pH and ion concentrations, spectra recorded from membranes containing different amounts of DAG exhibit lipid ester carbonyl bands that correlate with the changes in T_m observed upon inclusion of DAG within the membranes (Fig. 5.4B). In the PC/PA 3:1 membranes, which displayed a significantly lower T_m, the lipid ester carbonyl profile shows an increased portion of the hydrogen-bonded component

Figure 5.4

Assessing the Physical Properties of Lipid Membranes without the nAChR with Varying Amounts of DAG. A, Temperature dependence of the C-H stretching frequencies observed in spectra of membranes of PC/PA 3:1 (open triangles), PC/DAG 3:1 (grey filled triangles) and PC/PA/DAG 3:1:1 (black filled triangles) at pH 7. B, Carbonyl stretching region in deconvolved spectra of lipid membranes composed of PC/PA/DAG 3:1:1 (trace i), PC/DAG 3:1 (trace ii) and PC/PA 3:1 (trace iii) at pH 7. Spectra collected, scaled and deconvolved in similar manner as described in Figure 5.1.

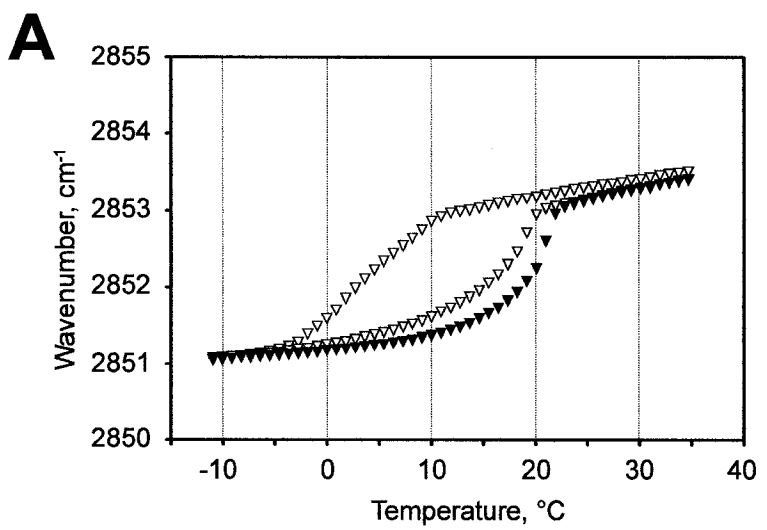
A
2855
2854
2853
2852
2851
2850
Wavenumber, cm-1
-10
0
10
20
30
40
Temperature, °C

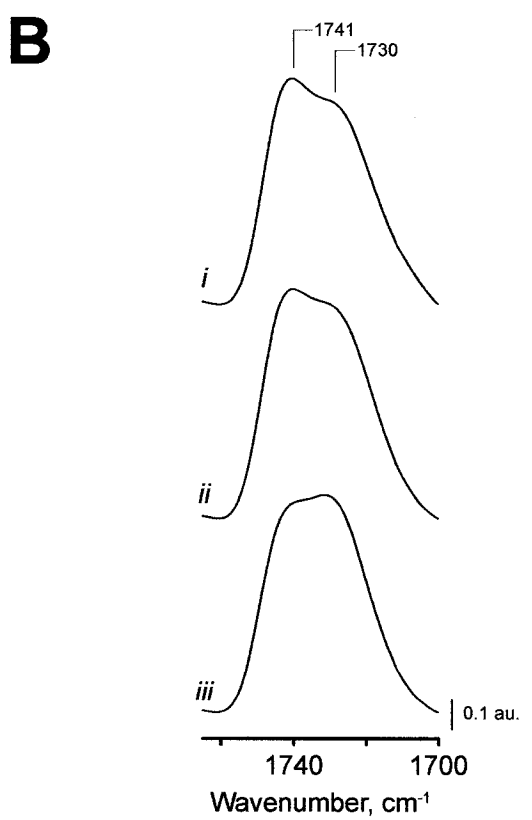
B
1741
1730
i
ii
iii
0.1 au.
1740
1700
Wavenumber, cm-1

band compared to the non-hydrogen-bonded band, suggestive of a decreased head group packing in these membranes. In the DAG-containing membranes, the increased T_m values reflect a more stable membrane, which is supported by the lipid ester carbonyl bands. The PC/DAG 3:1 membrane shows an increased portion of the non-hydrogen-bonded component, while the PC/PA/DAG 3:1:1 shows a further increase in the intensity of the non-hydrogen-bonded band, consistent with the high T_m of these membrane mixtures. It is clear that the presence of DAG within a PC or a PC/PA membrane has significant effects on the physical properties of the bilayer. However, the effects of the DAG within these membranes are hard to fully elucidate, as there are also contributing effects on the physical properties of the bilayer due to the nAChR-induced environment at the membrane surface. It is clear, however, that these "simple" membrane systems into which the nAChR is incorporated display complex interactions between the membrane physical and chemical properties and the structure and function of the nAChR, and the effects of the various parameters examined herein are interwoven and may all be important in stabilizing a functional nAChR in these membranes.

5.3 – Summary & Conclusions

There is a reciprocal coupling observed between PA and the nAChR. PA is particularly effective at stabilizing a functional conformation of the nAChR in reconstituted membranes, and the nAChR influences the physical properties of PA-containing membranes (Fig. 5.1). PC/PA 3:2 membranes, in which the nAChR is functional, undergo a significant increase in the T_m, from 13.1 to 24.7°C, and thus the stability or ordering of the membrane upon reconstitution of the nAChR. The spectra recorded from the PC/PA-nAChR reconstitutions also exhibit lipid ester carbonyl bands consistent with decreased hydrogen-bonding of the lipid ester carbonyl groups compared to the pure membranes. In contrast, the presence of the nAChR in PC membranes displayed minimal effects on the physical properties of the bilayers. While the coupling between PA-containing membranes and the nAChR has been observed prior to this study (73), there has been no clear explanation proposed. The explanation, however, could lie in the ability of the nAChR to alter the surrounding environment coupled with the formation of DAG within the PC/PA-nAChR reconstitutions.

The ability of the nAChR to concentrate cations (and protons) could be responsible for the altered bilayer physical properties in PC/PA-nAChR reconstitutions compared to the pure lipids. As discussed in the previous chapter, the monoanionic PA head group is stabilized in PC/PA-nAChR reconstitutions. Stabilization of the monoanionic state (decreasing the pH of the surrounding membrane environment to pH 4) in PC/PA 3:2 membranes leads to an increase in T_m of the bilayer to 19.0°C (Fig. 5.2; Table 5.1). The T_m changes with decreasing pH are attributable to the PA head groups changing from dianionic to monoanionic within the membrane since the T_m of PC membranes (no ionizable head

groups) was consistent at all pH values. Stabilization of the monoanionic state, however, does not fully account for the increased T_m of the membrane reconstituted with the nAChR as the T_m of PC/PA 3:2 membranes at pH 4 is not as high as the nAChR-reconstituted PC/PA 3:2 membranes. However, in PC/PA 3:2 membranes, at pH 4, increased concentrations of cations results in an increase in the bilayer T_m to 24.8°C, close to that of the PC/PA-nAChR reconstitutions (Fig. 5.3). The standard *Torpedo* Ringer buffer contains a variety of cations, and I examined the extent to which the different ions influenced the T_m of PC/PA 3:2 membranes (Table 5.2). Increased concentrations of divalent cations seemed to exhibit the largest effect on the T_m of the membranes without the nAChR. Increased NaCl (2.5 M), for example, had less of an effect on T_m than increased Ca^{2+} (30 mM). This finding was interesting given that calcium has been implicated as a potentiator of nAChR function (98-100). However, despite the enhanced effects of divalent cations, increases in all cation concentrations in combination with decreases in local pH were required to mimic the T_m of PC/PA-nAChR reconstitutions.

The lipid ester carbonyl bands in spectra recorded from pure PC/PA 3:2 membranes in varying pH and ionic strength exhibit dependency on the environment surrounding the membrane. Decreasing the pH from 7 to 4 resulted in lipid ester carbonyl bands in spectra recorded from pure membranes with increased intensity at the non-hydrogen-bonded peak, but the intensity did not rival that of the PC/PA-nAChR reconstitutions. However, increasing the cation concentration in combination with decreasing the pH surrounding PC/PA 3:2 membranes resulted in spectra similar to those of the reconstituted membranes. Spectra recorded from PC/PA 3:2 membranes surrounded by increased protons (decreased local pH) and high cation concentrations leads to lipid ester carbonyl bands with similar proportions of the hydrogen-bonded and non-hydrogen-bonded peaks as those of the PC/PA-

nAChR reconstitutions. While the general class of anionic lipids has been implicated in the ability to stabilize a functional nAChR, the bi-directional coupling between membrane physical properties and the functional conformation of the nAChR is only seen in PA-containing membranes (and to a lesser degree PG-containing membranes). The similarities between PA and PG, however, suggest that the chemical and structural properties of these particular lipids are required within a reconstituted membrane to mediate the bi-directional coupling.

The presence of DAG within PC/PA-nAChR reconstitutions led to consideration of the effect of DAG on the physical properties of lipid membranes. The formation of DAG in nAChR-reconstitutions, which correlates with a decrease in the amount of PA, had not been seen previously, and therefore the influence of a lipid with no phosphate head group had not been considered. Interestingly, PC/PA 3:1 membranes exhibit a much lower T_m than the PC/PA 3:2 membranes. The decreased amount of PA resulted in a drop of roughly 10°C compared to the PC/PA 3:2 membranes, which indicates a non-linear increase in T_m due to the presence of PA in a PC bilayer. The presence of DAG with or without PA, however, resulted in increased T_m within the lipid bilayers. The PC/PA/DAG 3:1:1 membranes, mimicking a possible nAChR-reconstitution lipid composition following the formation of a significant amount of DAG from the PA, exhibit a T_m of 20.7°C while the PC/DAG 3:1 membranes exhibit a T_m of 18.5°C. Spectra recorded from both the PC/PA/DAG and PC/DAG membranes exhibit lipid ester carbonyl band shapes consistent with physical properties resembling those of the PC/PA-nAChR reconstitutions. The formation of DAG in the PC/PA-nAChR reconstitutions results in altered physical properties, and the presence of DAG could be partly responsible for the observed bi-directional coupling, along with the influence of local pH and surrounding cation concentrations.

The presence of DAG in PC/PA-nAChR reconstitutions influences the physical properties of the bilayer, although as the formation is time-dependent and the altered physical properties are seen immediately, the effect of DAG is not as influential as the situation examined here. The experiments include ~25% and 20% DAG, but the TLC analysis in chapter 3 suggests that the amount of DAG is as little as 5% in PC/PA-nAChR reconstitutions. Based on the experiments performed herein, 5% DAG (formed from 5% of the PA population) within the membrane would result in altered bilayer physical properties, though the changes would not be as dramatic as those observed here.

Chapter 6: General Discussion

6.1 – nAChR influence on reconstituted PA-containing membranes

The anionic lipid PA is very effective in a reconstituted PC membrane at stabilizing a functional nAChR (see Chapter 3) (58, 59, 61, 72, 73). While the specific mechanistic and/or structural reasoning behind the effectiveness of PA in influencing nAChR function has not been elucidated, an interesting aspect of the PC/PA-nAChR reconstitutions is the observed bi-directional coupling between the nAChR functional capabilities and the physical properties of the PA-containing, reconstituted membranes (73, 74). The presence of the nAChR in PC/PA 3:2 membranes leads to increased T_m and reduced water penetration into the head group region of the bilayer, consistent with increased packing density of the lipid head groups. This observed bi-directional coupling was initially observed in PA-containing membranes but now it appears that the coupling occurs to varying degrees in other anionic lipid-containing membranes, and seems related to the ability of said membrane to stabilize a functional conformation of the nAChR. Initial discovery of this relationship between the nAChR and bilayer physical properties did not provide a rationale for this lipid-selective influence of the nAChR on the bilayer properties (73). In this study, I examined the possibility that the bi-directional coupling is a result of the nAChR affecting its extramembranous ionic environment, leading to alteration of the physical properties of its membrane environment.

The stabilization of the monoanionic state of PA occurs in nAChR-reconstituted membranes. While the mechanism of monoanionic PA influencing function is not yet

understood (a mechanism is proposed in section 6.4), it appears that the monoanionic state stabilization is involved in the bi-directional coupling. As previously mentioned, it has been previously shown that cation-selective channel proteins, such as the nAChR and KcsA, possess the ability to concentrate cations around the vicinity of these membrane channel proteins (74, 95-97). The increased concentration of cations proximal to the entrance of the conduction pathways of these channel proteins facilitates the rapid conduction of cations across the membrane. Included with the increased cations at the surface, protons could also be increased in concentration around the channel proteins, resulting in a decreased pH at the membrane surface; generally the entrance to the pores of channel proteins are found close to the surface of the membrane (24, 102-104). Decreased pH at the membrane surface of PC/PA-nAChR reconstitutions would lead to stabilization of the monoanionic PA head group. The apparent pK_a of the PA head group shifts to a pH value higher than 12, as the monoanionic state of the PA head group was stabilized at all pH values examined (up to 12). The pK_a of the head groups could be unchanged but the concentrating effect of the nAChR results in pH values at the membrane surface below the known pK_a. As shown in chapter 4, we are currently examining the possibility of assaying the pH at the membrane surface.

The stabilization of the monoanionic state leads to altered physical properties of the bilayer. PC/PA 3:2 membranes exhibited altered physical properties when the surrounding environment pH was decreased. The properties observed were close to those of the PC/PA-nAChR reconstitutions, but not identical. Membranes composed of PC and other anionic lipids, such as PG and PS, which do not possess ionizable head groups in the pH range examined, exhibit moderate to minimal altered bilayer physical properties upon the incorporation of the nAChR; In the case of PG, there are moderate changes (discussed below) but in the case of PS there are minimal alterations of bilayer physical properties (76).

As these other anionic lipids contain no ionizable groups near physiological pH values, but exhibit altered physical properties with the nAChR, there are likely additional factors involved.

6.2 – DAG in PA-containing nAChR-Reconstituted Membranes

The reduced pH at the membrane surface could affect the PA head groups in an alternate manner than only changing the ionization state of the head groups. The formation of DAG could be a result of hydrolysis of the PA head groups, removing the phosphate group resulting in DAG with the same lipid acyl chains (the lipid species identified by TLC analysis) (Fig. 6.1). Ester hydrolysis occurs readily at lower pH (5-6) therefore the phosphate group may be removed without enzymatic activity (105). The time-dependent formation of DAG could also be due to phospholipase activity of the nAChR similar to phospholipase C, which cleaves the ester linkage of the lipid head groups (106). There are parts of the nAChR structure that were not resolved in the structure presented by Unwin (8), such as the cytoplasmic domain, that could contain phospholipase-activity motifs, thereby endowing the nAChR with the inherent ability to enzymatically influence its surrounding environment. However, a section of the resolved structure with an unidentified function could also be responsible for the phospholipase activity on the lipid head groups. Enzymatically altering its surrounding environment leading to membrane physical properties "optimal" for functional activity might be the mechanism by which the nAChR functions *in vivo* and/or in the reconstituted membranes.

Regardless of the mechanism of formation, the presence of DAG in PC/PA membranes results in increased T_m and lipid ester carbonyl bands similar to the PC/PA-

Figure 6.1

Locations of Cleavage Sites of Various known Phospholipases. Phospholipids can be cleaved in different locations by phospholipases (PL): D, removes the choline group from phospholipid head group of PC, leaving PA; C, removes the head group including the phosphate molecule, creating diacylglycerol; A1 and A2, removes the acyl chains by cleaving the bonds to their respective glycerol oxygen group. The reaction of PLC is shown as we suspect the formation of DAG, through action similar to that of PLC *in vivo*, from PA releasing dihydrogen phosphite.

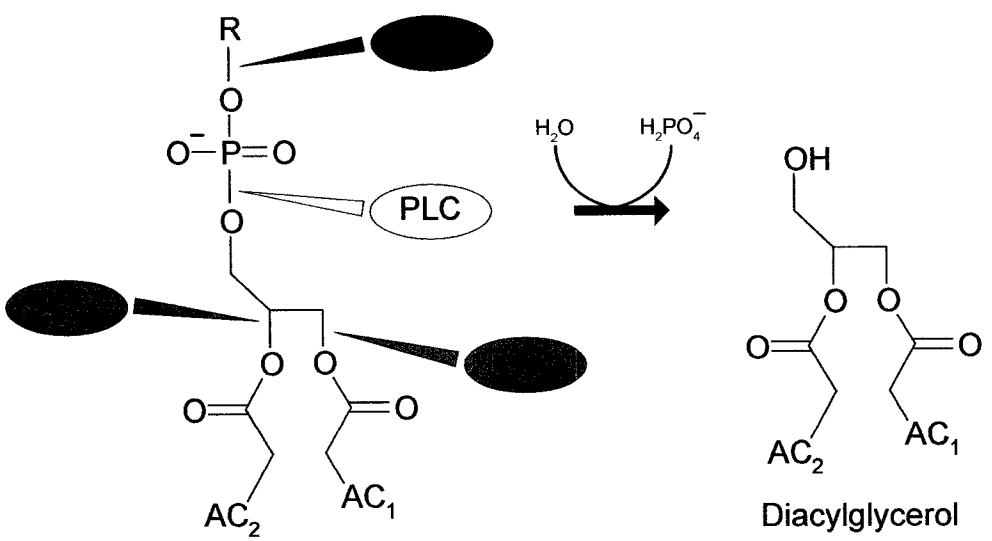
R
O
O⁻—P=O
O
PLC
O
O
O
O
AC2
AC1
H2O
H2PO4⁻
OH
O
O
O
O
AC2
AC1
Diacylglycerol

nAChR reconstitutions. The presence of DAG is yet another factor of the lipid environment that is likely influenced by the nAChR, creating an environment with altered physical properties. Interestingly, DAG formation only occurs in PA-containing membranes, suggesting that the head groups of other anionic lipids are not removed, by any mechanism, in the presence of the nAChR. TLC analysis of PG- and PS-containing nAChR-reconstituted membranes suggests no formation of DAG, which could be related to the moderate and subtle changes in the physical properties of the bilayers upon reconstitution of the nAChR, respectively (76). The nAChR might only be able to alter PA head groups, while the larger PG and PS head groups hinder the phospholipase-like activity. Indications are that both reduced pH and DAG formation influence bilayer physical properties, but there are still further additional factors involved.

6.3 – Cation Concentration of the nAChR

The final factor examined is the presence of increased cation concentrations at the surface of the membrane, which as mentioned is important for the rapid conduction of cations, but has also been shown to affect the T_m of lipid membranes (88). The cations at the surface appear to interact with the membranes as extensive washing of the nAChR-reconstituted membranes with EDTA results in minimal reduction of the T_m of the bilayers. The interaction of the cations with the membranes hints that cations are influencing properties of the membranes. In PC/PA 3:2 membranes, increased concentrations of cations resulted in increased T_m and lipid ester carbonyl bands similar to the PC/PA-nAChR reconstitutions when coupled with the reduced surface pH. However, we also found that increasing the concentration of cations 10x that of the normal *Torpedo* Ringer buffer

surrounding PC membranes lead to increases in T_m similar to that of the PC/PA membranes. This effect is not, however, seen in PC membranes upon reconstitution of the nAChR. Interestingly, the moderate T_m changes in PG-containing membranes and the absence of bilayer physical properties changes in PS-containing membranes upon reconstitution could be related to the altered T_m in PC bilayers seen at ten times the ionic strength of standard *Torpedo* Ringer buffer.

PG, like PA, has a head group with a single negative charge and no positive charges, resulting in its anionic head group. PS, however, contains a positive charge and 2 negative charges resulting in the net anionic head group. PC, like PS, has a positive charge and only one countering negative charge, giving it a zwitterionic head group. These head group charge distributions likely play a contributing role to the concentration of cations in the nAChR-reconstituted membranes (Fig. 6.2). In pure PC membranes, the zwitterionic head group does not contribute significantly, while the PS head group contributes minimally due to the head group charge distribution. In contrast, the charge distribution of PG and PA head groups contribute to the negative surface potential of the membrane. When combined with the negative surface potential of the nAChR concentrations of cations at the surface of the PC/PA-nAChR reconstitutions compared to other anionic lipid-containing reconstitutions is significantly higher.

Overall, the nAChR substantially alters its surrounding environment, but the complete alteration of the surrounding environment is only seen in the PC/PA-nAChR reconstitutions (Fig. 6.3). The reduced pH at the membrane surface results in stabilization of the monoanionic state of the PA head group, which results in increased T_m of the bilayers. Included with the effect on the ionization state of the PA head group, the PA head groups can have their phosphate group removed in the presence of the nAChR resulting in the presence

Figure 6.2

Concentrating Effects of PC Bilayers and PC/Anionic Lipid Binary Membranes. PC head groups are zwitterionic with their positive charge located at the surface of the bilayer, thus creating a neutral (or weakly positive) surface potential – the compensating negative charge is likely deep enough in the membrane to have minimal effect on the surface potential. PC/PS bilayers likely have a weakly negative surface potential due to their net negatively charged head group, but the charge distribution results in a weakly attractive surface to cations. PC/PG bilayers possess an overall negative surface potential stronger than PC/PS bilayers due to the absence of positive charges in the lipid head groups. However, the negatively charged phosphate groups are not on the surface, thus the PC head groups reduce the negative surface potential. PC/PA bilayers would result in the largest negative surface potential as the negatively charged head groups would be at the surface with the PC head groups, adding to the concentrating ability of these bilayers.

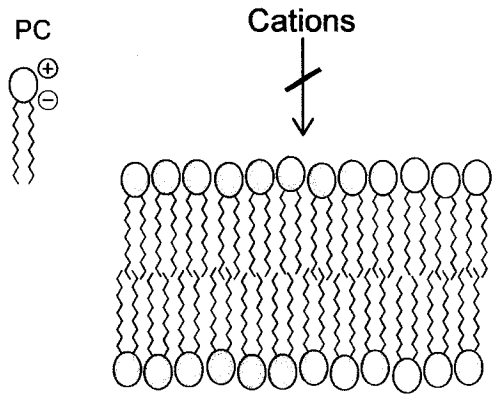

Pure PC Bilayer
Overall neutral surface potential

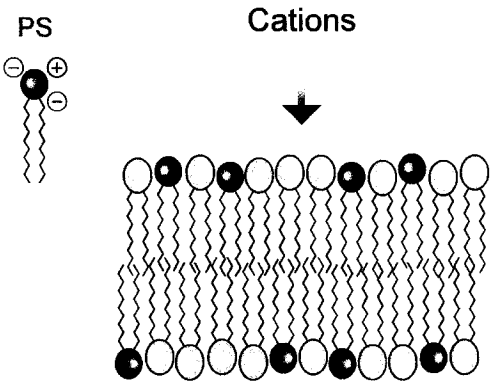

PC/PS 3:2
Overall minimal negative surface potential

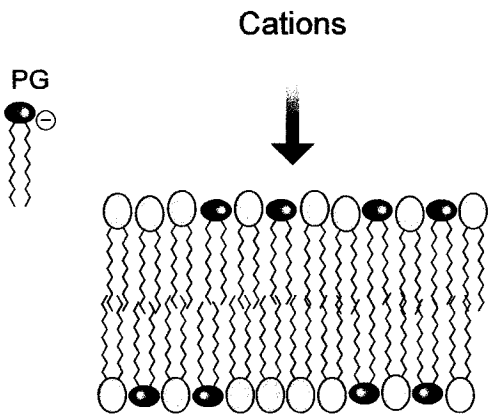

PC/PG 3:2
Overall moderate negative surface potential

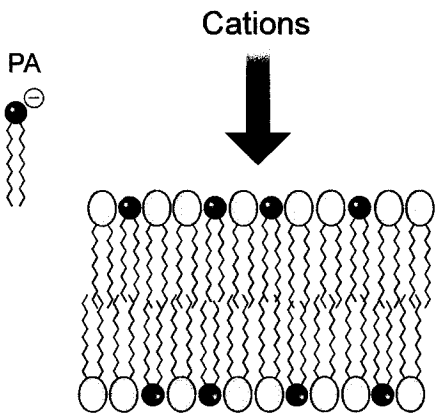

PC/PA 3:2
Overall strong negative surface potential

Figure 6.3

Environment Created in PC/PA-nAChR Reconstitutions as a Result of the Effect of the nAChR coupled with the Negative Surface Potential of the Bilayer. The electrostatic potential map of the nAChR is shown, red and blue regions indicating negatively charged and positively charged regions, respectively. Overall, the nAChR surface on both the LBD and ICD exhibits a negative surface potential, increasing the concentration of cations (green: cations; light blue: protons) at the membrane surface and the entrance to the pore. As a result, the lipid head groups are tightly packed and the pH at the membrane surface is decreased. The decreased pH results in some the formation of DAG (brown lipid head groups) from the monoanionic PA (blue). CFPE (red triangle attached to cyan PE head group) would experience the reduced pH at the surface and therefore produce no significant fluorescence signal. Bars at left and right indicate concentration of cations and protons increasing as one approaches the membrane. The zoomed-in region (top) is a representation of one nAChR found within our reconstituted proteoliposomes (bottom), and each nAChR would create a similar environment in the proteoliposome. PDB accession code: 2BG9 (8).

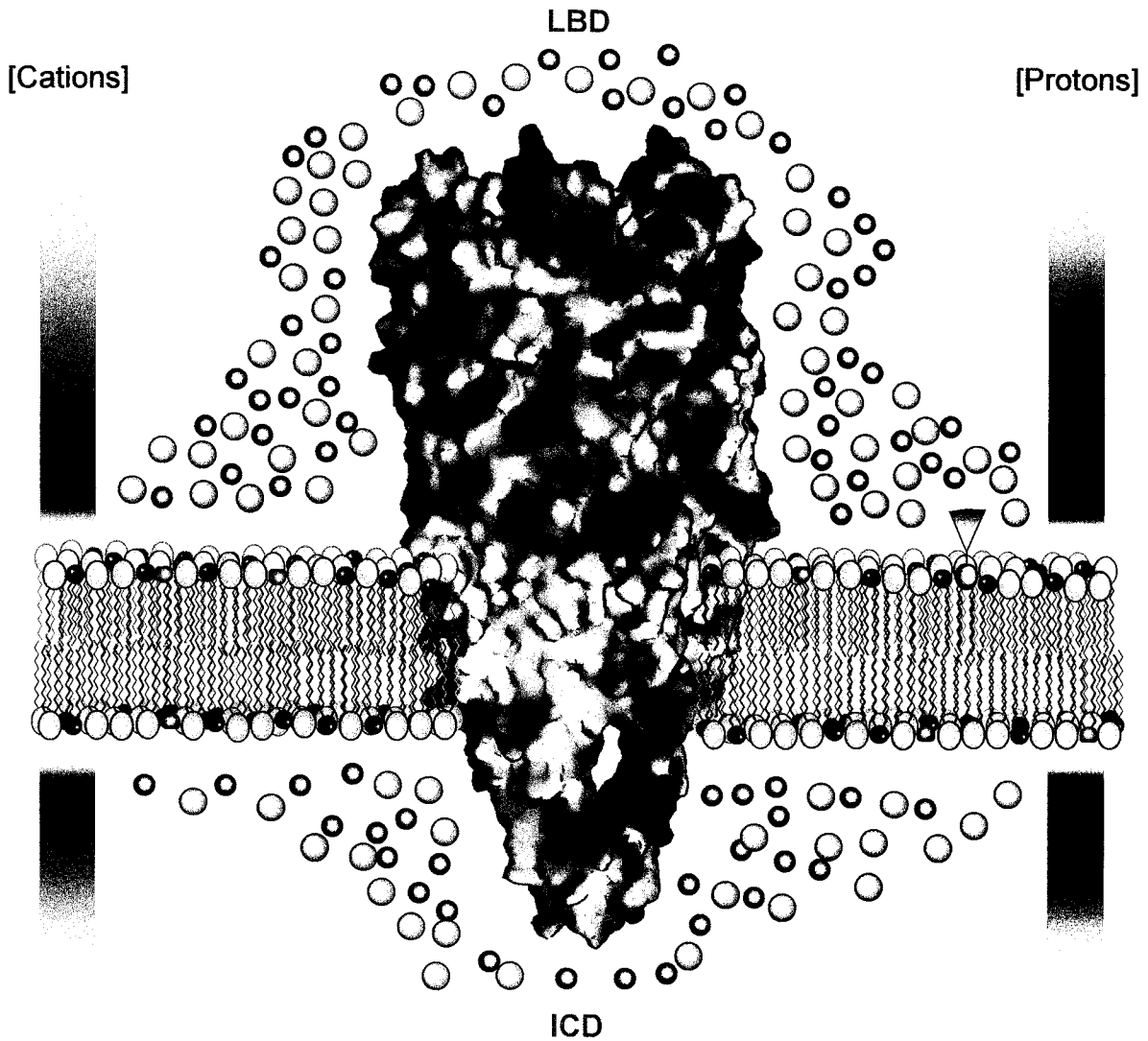
LBD
[Cations]
[Protons]
ICD

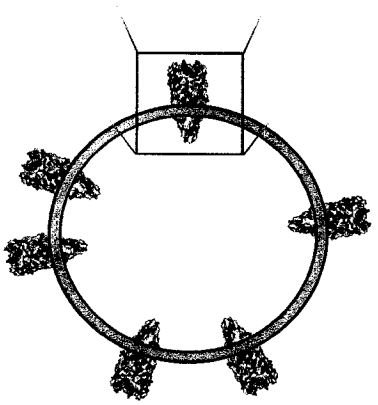

of DAG within these PC/PA-nAChR reconstitutions. The presence of DAG, however it is produced, increases the T_m of the bilayers, and reduces the water penetration into the head group region of the bilayers. The concentration of cations at the membrane surface due to the large negative surface potential of the nAChR, as well as the plethora of negatively charged PA head groups within the membrane, increases the local concentration of cations raising the T_m and reducing the hydrogen-bonding of the lipid ester carbonyls. Membranes containing PG instead of PA display moderately altered physical properties, possibly due to the inability of the PG head groups to be removed to produce DAG or the altered charge distribution of the head groups. Membranes with other anionic lipids exhibit minimal alterations of bilayer physical properties as a result of no formation of DAG and reduced cation-concentrating effects of the membrane compared to those of PA-containing nAChR-reconstituted membranes. The bi-directional coupling between nAChR functional capabilities and the bilayer physical properties appears to be an interplay of the induced environment at the membrane surface due to the negative surface potential of the nAChR and the reconstituted membrane itself, which could mirror the environment created at the neuromuscular junctions *in vivo*.

The ability of the nAChR to influence its lipid environment through altering the ionic environment surrounding its extramembranous domains may be important for the formation of nAChR micro-domains or lipid rafts. The nAChR has been suggested to be found within lipid rafts within the post-synaptic membrane (107, 108). Alterations of the nAChR environment through concentrating cations at the membrane surface and reducing the membrane surface pH could lead to significant changes in the lipids found within rafts. By altering the physical properties of membrane lipids found in the rafts thereby affecting its functional equilibrium, the nAChR could be described as "self-modulating." Altering the

strength of synaptic communication by changing its surrounding environment, depending on the situation, the cation-concentrating ability of the nAChR could be viewed as one of the most important functional aspects of the nAChR. Rafts and/or micro-domains have also been shown to be involved in signaling processes resulting in the beginning of different signaling cascades. The ability of the nAChR to modulate the raft environment suggests that the nAChR may be involved in the commencement of signaling *in vivo* (106, 107). However, rafts and the nAChR remains a controversial topic, as clear evidence of the presence of the nAChR within these rafts has yet to be demonstrated consistently. In order to substantiate the possibility that the nAChR is influencing the formation or the local environment of lipid rafts (outside the membrane), it must first clearly be shown that the nAChR is regularly found within lipid rafts at synapses.

6.4 – PA-Specific Binding Sites on the nAChR

Based on past and contemporary studies examining anionic lipids, PA is now considered an essential lipid in stabilizing a functional nAChR in reconstituted membranes (59, 62, 72, 73). More recent reports, including this study, have attempted to elucidate the possible key element of PA that endows PA with its inherent efficacy in stabilizing the functional state of the nAChR. An attractive possibility is the existence of specific PA-nAChR interactions that occur at the nAChR within the transmembrane domain influencing the agonist-induced response. Jones & McNamee used brominated lipids and determined that there exists multiple annular and non-annular binding sites for lipids, specifically PA and cholesterol (and its analogues), respectively (68). However, locations of these sites have not been identified, nor have any more recent papers unequivocally corroborated the

existence of PA-specific binding sites upon the nAChR or how specific head group interactions would result in stabilization of a functional nAChR. Despite the controversy regarding the existence of these sites, it is accepted that PA retains an innate ability to influence the function of the nAChR. Studies have indicated that the head group carrying the negative charge is not responsible for stabilizing function upon reconstitution (72-74). Also, we have examined anionic lipids with differing head group sizes and find that PG, with a single negative charge and moderately larger head group than PA, moderately stabilizes the nAChR in a functional state upon reconstitution. In light of these findings, armed with a recent model from our laboratory (83) and the recently published high-resolution model of the nAChR, I examined the possible existence of binding sites for small, anionic (with one negative charge) lipid head groups on the nAChR and their potential involvement in nAChR function.

The recent model suggests that the M4 helix of the nAChR plays a role in coupling agonist binding to channel gating in the functional nAChR (83). The proximity of the C-terminal end of M4 to the Cys-loop in the functional nAChR is theorized to be dependent on the composition of the lipid membrane. In PC membranes, which stabilize a non-functional conformation of the nAChR, M4 is uncoupled from the 3 remaining helices, and the coupling between the domains is abolished. The lipids that stabilize function could fulfill a scaffolding role, ensuring that the C-terminal end of M4 is in contact with the Cys-loop, thereby coupling the agonist binding domain to the transmembrane domain, allowing translation of agonist binding to channel gating (Fig. 6.4). The presence of particular lipids within the membrane is considered essential for maintaining M4 in a conformation that couples these 2 domains, and their functions, resulting in stabilization of the conformation of the functional nAChR (83).

Figure 6.4

The Uncoupled State of the nAChR in PC-nAChR Reconstitutions. A, Scheme of the equilibrium between the functional resting state and the uncoupled state of the nAChR. The resting state, R, exists in functional membranes (native *Torpedo*, PC/PA 3:2 and PC/PA/Chol 3:1:1), while the uncoupled state has been characterized in pure PC membranes. The uncoupled state is thus named due to a lack of functional and structural coupling between the agonist binding domain and the ligand binding domain. B, Schematic model of the coupled, resting state and the uncoupled state of the α-subunit. The C-terminal end of the M4 helix (orange) of the nAChR in the PC/PA 3:2 membrane, left, is coupled to the other helices and the Cys-loop (green) thereby maintaining the communication between the agonist binding and transmembrane domains. The M4 helix of the uncoupled state in pure PC membranes, right, is separated from the remaining helices resulting in uncoupling of the 2 domains (adapted from (83)).

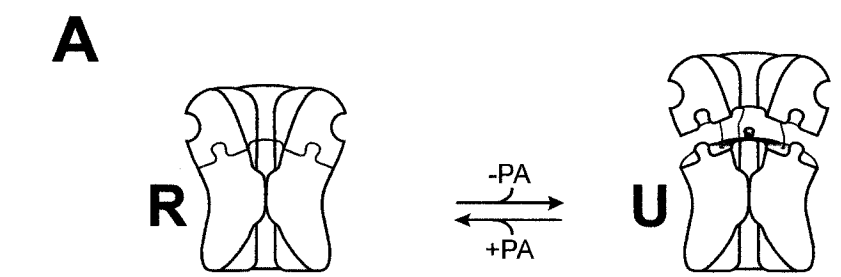
A
R
-PA
+PA
U

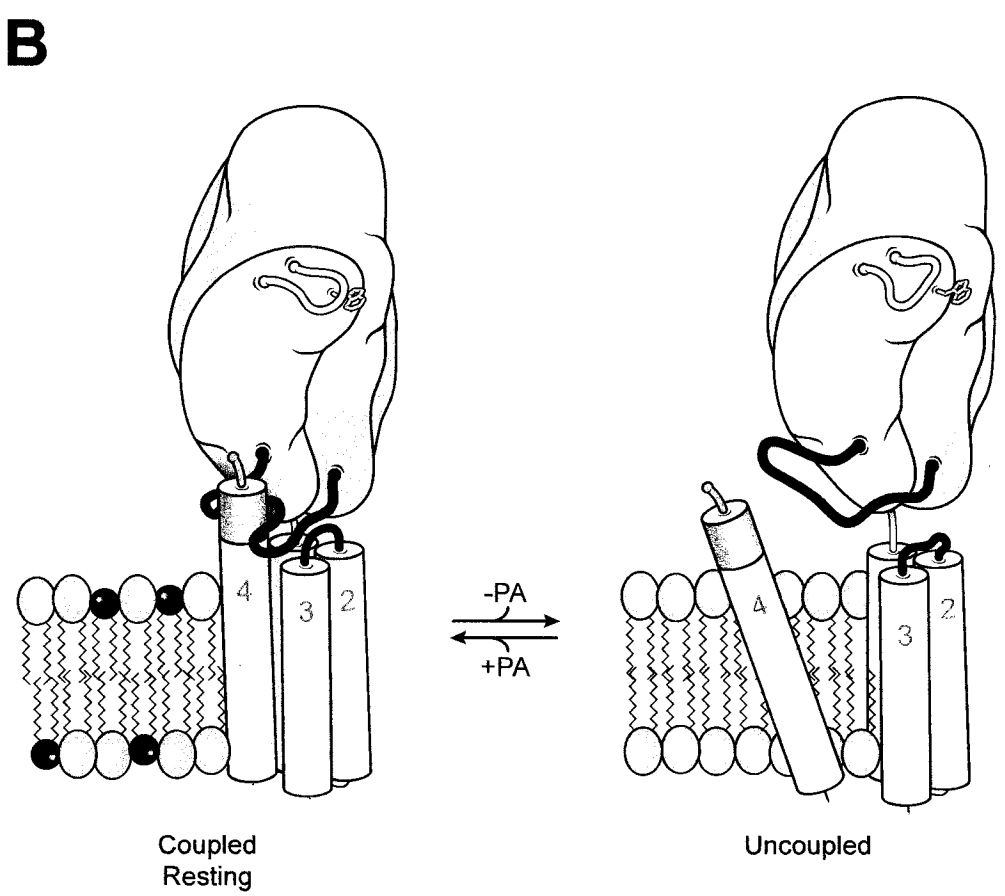
B
4
3
2
-PA
+PA
4
3
2
Coupled
Resting
Uncoupled

From Unwin's model, we can see that there are a number of lipid-exposed residues in the transmembrane domain of the nAChR that could be involved in formation of a binding site for lipid head groups (8). These residues are polar and/or positively charged (due to the reduced surface pH the ASP/GLU residues are likely neutral and polar), which would form favorable interactions with the polar head group of PA. The proposed binding sites could accommodate small, anionic lipid head groups (like that of PA), as well as slightly larger head groups (like that of PG). The first set of residues is located on the intracellular side of the transmembrane domain in the α-subunit. I chose to focus on the α-subunit since agonist binding occurs in the α-subunit therefore structural coupling of M4 to the Cys-loop is believed to occur within the α-subunit effectively translating agonist binding to gating of the transmembrane pore. As the resolution of the structure is 4Å, some of the residue side chains might be in altered conformations from what is shown in the reconstituted membranes containing PA. The intracellular anionic lipid binding site between M4 and M1 is likely formed by the following residues: Y234, T237, D238 and D407 (Fig. 6.5). By binding the small, anionic PA head group to this proposed site, the PA head group could act as a scaffold between the base of the M4 helix and M1, thereby maintaining the functional conformation of M4 (see below). On the extracellular side of the membrane, a 2nd set of residues might also form a PA binding site between the extracellular ends of M4 and M3: K276, Y277, E432 and S434. Both of the proposed sites consist of polar side chains that could form a favorable, polar pocket for the head groups of PA, effectively occluding the polar side chains from the hydrophobic membrane. The observation that PG, which possesses a monoanionic head group, results in a moderately functional nAChR (76) further suggests that the dianionic state of the PA head group is inconsequential, as the singly charged PG is moderately

Figure 6.5

Residues Proposed to Compose the Anionic Lipid Binding Sites. Left, α-subunit of the nAChR shown in cartoon representation with the residues involved in the M1-M4 intracellular anionic lipid binding site shown as blue spheres. Since M4 is the outermost helix, the M2 helix (opposite side from M4) forms the channel lining. Right, The residues involved in the M3-M4 extracellular anionic lipid binding site. The orientation of the residues is speculated, based on the 4Å model (8). In both cases, the binding sites are proposed to be located between the highlighted helices, causing the PA (or PG) to act as a scaffold between the helices, allowing coupling of the agonist binding and transmembrane domains via M4 interactions with the Cys-loop. PDB accession code: 2BG9 (8).

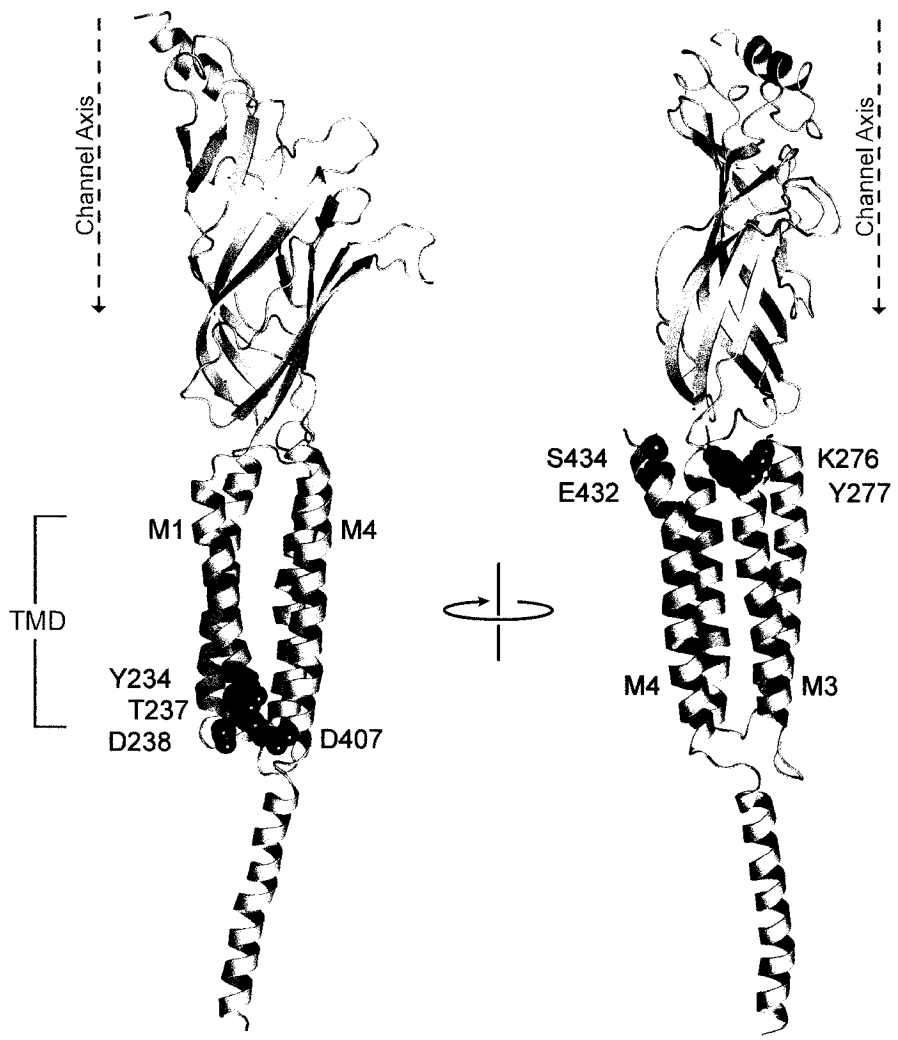
Channel Axis
M1
M4
TMD
Y234
T237
D238
D407
S434
E432
K276
Y277
M4
M3
Channel Axis

effective. The binding sites would form favorable interactions between the small, anionic head group of PA/PG and the nAChR. These interactions would bridge the association between the TMD helices, ensuring the retention of the functional conformation of the M4 helix leading to the coupled, resting nAChR (Fig. 6.4).

Previous reports indicated that the anionic charge of lipid head groups alone is not sufficient for stabilizing a coupled nAChR. However, PG, with its smaller head group and no countering positive charge, stabilizes a moderate level of function in reconstituted membranes (Fig. 6.6). The moderate function suggests that the anionic lipid binding sites proposed above could accommodate PG with its particular charge distribution and head group size, both of which are similar to PA (Fig. 6.2). However, the fit is not ideal indicating that M4 could be coupling the 2 domains together but not with the same efficiency as when PA is bound between the helices. In the case of PG-containing membranes, M4 could be interacting with the Cys-loop but relatively loosely compared to PA-containing membranes. PS is another anionic lipid that possesses a net negative charge on the head group and a slightly larger head group, but it possesses a positively charged group. With its different charge distribution, the head group of PS likely cannot bind to the proposed sites. Therefore in PC/PS membranes M4 does not associate with the other helices due to lack of the anionic lipids at the proposed sites, resulting in an uncoupled nAChR. Other anionic lipids, which have even larger head groups than PS, would result in steric hindrance between M4 and M1/M3 leading to M4 uncoupling from the remaining helices of the transmembrane domain thus an uncoupled, non-functional nAChR. The uncoupled state was characterized in PC membranes since biochemical data of the nAChR in PC membranes were inconsistent with both the desensitized state and the resting state, thus a novel conformation was hypothesized (83). The head group of PC is zwitterionic, with the negatively charged phosphate group

Figure 6.6

The Anionic Lipid Binding Sites Accommodate PA and PG Resulting in the Coupled, Resting State of the nAChR. In PC/PA 3:2 membranes, the nAChR is in the coupled resting state as PA (blue head group) binds to the anionic lipid binding site (Red triangles on M4 and M3). On the opposite side of M4, the intracellular anionic lipid binding site would also be occupied by PA (not shown). In PC (yellow) and PS (purple) membranes, the lipid head groups do not bind to these sites, due to the presence of the positive charges, and larger head group size. In the PG (green) membranes, the slightly larger PG head groups result in subtle hindrance but still bind to the anionic lipid binding sites, resulting in a moderately functional (coupled) nAChR.

PC/PA 3:2

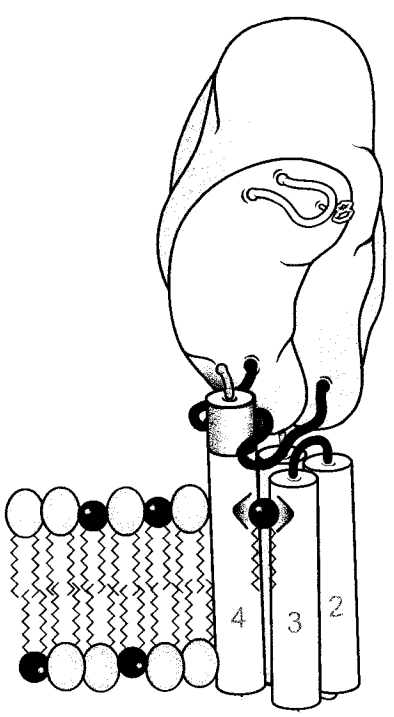

PC

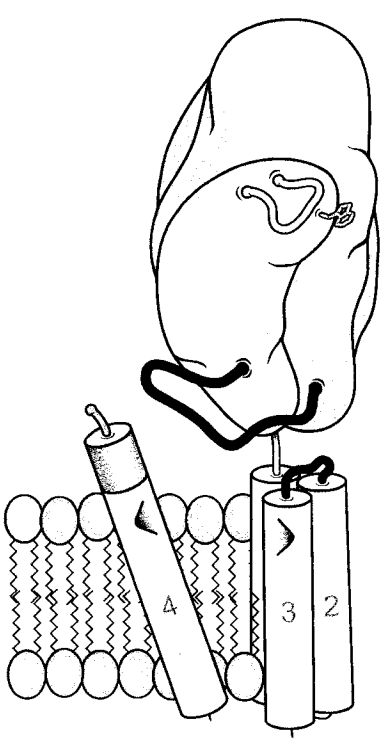

PC/PG 3:2

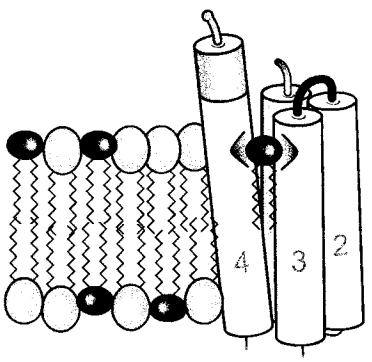

Moderately
Coupled

PC/PS 3:2

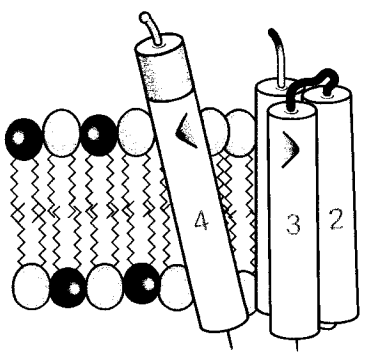

Uncoupled

countered by the choline group. The larger, neutral head group would not bind to the anionic lipid binding sites proposed here, ensuring complete uncoupling of the nAChR domains.

A point of interest for the interaction of M4 to the other helices via this proposed lipid binding sites is the improved function in PC/PA/Chol 3:1:1 membranes compared to PC/PA 3:2 membranes. If PA binding to the anionic lipid binding sites was sufficient for stabilizing a fully functional nAChR, then the presence of Chol should not result in the enhanced function, as determined by difference spectroscopy and ethidium fluorescence (72-74). So what role is Chol playing in the enhanced coupling of the nAChR? The answer could lie in the existence of steroid potentiation sites that have been found on other members of the Cys-loop receptor superfamily. Steroid potentiation sites have been located on $GABA_A$ receptors; binding of endogenous neurostreroids to these transmembrane potentiation sites results in enhanced $GABA_A$ function in electrophysiology traces (109). The sites lie within the transmembrane domains, and the neurosteroids gain access to the sites through the membrane. Binding of these neurosteroids would be similar to how Chol interacts with the nAChR, thereby facilitating the coupling of M4 to M1/M3. Chol non-annular sites have been suggested in the past, and these sites could play a role in Chol potentiating nAChR function via enhanced coupling between the 2 domains. A recent study suggested Chol binds to sites embedded within the nAChR. These sites could be similar to the $GABA_A$ potentiator sites (110). PA binding to the anionic lipid binding sites combined with Chol binding could result in the improved function by forming a scaffold between M4 and M1/M3, allowing the C-terminal end of M4 to fully couple the 2 domains via Cys-loop interactions.

A number of residues in the lipid-exposed region of the α-subunit have been shown to affect the function of the nAChR (111-113). However, the residues mentioned above have not yet been examined at this level of detail. An early step towards establishing the presence of these sites composed of the residues suggested would be mutating the residues and examining electrophysiological traces of the mutant nAChRs. While this would not automatically indicate these residues are indeed binding the anionic lipids present resulting in the coupled, resting state of the nAChR, altered nAChR function in the mutants would suggest that these residues play a role in coupling binding to gating, and therefore it can be extrapolated that the binding of lipids to these residues is somehow altered compared to the wild-type nAChR. If these mutations provide qualitative information regarding the involvement of these residues, further steps must be taken in order to establish the existence of these residues. Structural information, as in high-resolution crystallography or cryo-electron microscopy, would be crucial in establishing the existence of the proposed anionic lipid binding sites, which would require co-crystallization of lipids bound to the sites. As eukaryotic nAChR and Cys-loop receptors remain resistant to crystallography, the structural information will remain unavailable, hindering the work towards proving the existence of these sites. Studies using labeled or radiolabeled lipids could be beneficial if they provide the intricate level of detail required to suggest specific locations of the binding sites. Brominated lipids have been used to establish the existence of these sites, but site-specific labeling would be required in order to obtain data unequivocally showing that the residues mentioned are involved in specific interactions between PA and the nAChR. As PA is found in low amounts within biological membranes, establishing specific PA-nAChR interactions could represent a missing piece of the puzzle of the mechanism of the functional nAChR.

REFERENCE LIST

1. Jones, S., S. Sudweeks, and J.L. Yakel. 1999. Nicotinic receptors in the brain: correlating physiology with function. *Trends Neurosci* 22:555-561.

2. Levin, E.D., and B.B. Simon. 1998. Nicotinic acetylcholine involvement in cognitive function in animals. *Psychopharmacology (Berl)* 138:217-230.

3. Abbott, L.F., and W.G. Regehr. 2004. Synaptic computation. *Nature* 431:796-803.

4. Cohen, S., and M.E. Greenberg. 2008. Communication between the synapse and the nucleus in neuronal development, plasticity, and disease. *Annu Rev Cell Dev Biol* 24:183-209.

5. Sine, S.M., and A.G. Engel. 2006. Recent advances in Cys-loop receptor structure and function. *Nature* 440:448-455.

6. Ashcroft, F.M. 2006. From molecule to malady. *Nature* 440:440-447.

7. Greer, P.L., and M.E. Greenberg. 2008. From synapse to nucleus: calcium-dependent gene transcription in the control of synapse development and function. *Neuron* 59:846-860.

8. Unwin, N. 2005. Refined structure of the nicotinic acetylcholine receptor at 4A resolution. *J Mol Biol* 346:967-989.

9. Karlin, A. 2002. Emerging structure of the nicotinic acetylcholine receptors. *Nat Rev Neurosci* 3:102-114.

10. Maehle, A.H., C.R. Prull, and R.F. Halliwell. 2002. The emergence of the drug receptor theory. *Nat Rev Drug Discov* 1:637-641.

11. Langley, J.N. 1907. On the contraction of muscle, chiefly in relation to the presence of "receptive" substances: Part I. *J Physiol* 36:347-384.

12. Monod, J., J. Wyman, and J.P. Changeux. 1965. On The Nature Of Allosteric Transitions: A Plausible Model. *J Mol Biol* 12:88-118.

13. Changeux, J.P., M. Kasai, and C.Y. Lee. 1970. Use of a snake venom toxin to characterize the cholinergic receptor protein. *Proc Natl Acad Sci U S A* 67:1241-1247.

14. Changeux, J.P., M. Kasai, M. Huchet, and J.C. Meunier. 1970. [Extraction from electric tissue of gymnotus of a protein presenting several typical properties characteristic of the physiological receptor of acetylcholine]. *C R Acad Sci Hebd Seances Acad Sci D* 270:2864-2867.

15. Heidmann, T., and J.P. Changeux. 1978. Structural and functional properties of the acetylcholine receptor protein in its purified and membrane-bound states. *Annu Rev Biochem* 47:317-357.

16. Claudio, T., and M.A. Raftery. 1977. Immunological comparison of acetylcholine receptors and their subunits from species of electric ray. *Arch Biochem Biophys* 181:484-489.

17. Schmidt, J., and M.A. Raftery. 1972. Use of affinity chromatography for acetylcholine receptor purification. *Biochem Biophys Res Commun* 49:572-578.

18. Schmidt, J., and M.A. Raftery. 1973. Purification of acetylcholine receptors from Torpedo californica electroplax by affinity chromatography. *Biochemistry* 12:852-856.

19. Weill, C.L., M.G. McNamee, and A. Karlin. 1974. Affinity-labeling of purified acetylcholine receptor from Torpedo californica. *Biochem Biophys Res Commun* 61:997-1003.

20. Noda, M., H. Takahashi, T. Tanabe, M. Toyosato, S. Kikyotani, Y. Furutani, T. Hirose, H. Takashima, S. Inayama, T. Miyata, and S. Numa. 1983. Structural homology of Torpedo californica acetylcholine receptor subunits. *Nature* 302:528-532.

21. Mishina, M., T. Kurosaki, T. Tobimatsu, Y. Morimoto, M. Noda, T. Yamamoto, M. Terao, J. Lindstrom, T. Takahashi, M. Kuno, and et al. 1984. Expression of functional acetylcholine receptor from cloned cDNAs. *Nature* 307:604-608.

22. Popot, J.L., and J.P. Changeux. 1984. Nicotinic receptor of acetylcholine: structure of an oligomeric integral membrane protein. *Physiol Rev* 64:1162-1239.

23. daCosta, C.J. 2006. A Structural Role for Lipids in Coupling Ligand Binding to Channel Gating in a Neurotransmitter Receptor. In Biochemistry, Microbiology and Immunology. University of Ottawa, Ottawa. 236.

24. Doyle, D.A., J. Morais Cabral, R.A. Pfuetzner, A. Kuo, J.M. Gulbis, S.L. Cohen, B.T. Chait, and R. MacKinnon. 1998. The structure of the potassium channel: molecular basis of K+ conduction and selectivity. *Science* 280:69-77.

25. Jiang, Y., A. Lee, J. Chen, V. Ruta, M. Cadene, B.T. Chait, and R. MacKinnon. 2003. X-ray structure of a voltage-dependent K+ channel. *Nature* 423:33-41.

26. Long, S.B., E.B. Campbell, and R. Mackinnon. 2005. Crystal structure of a mammalian voltage-dependent Shaker family K+ channel. *Science* 309:897-903.

27. Long, S.B., X. Tao, E.B. Campbell, and R. MacKinnon. 2007. Atomic structure of a voltage-dependent K+ channel in a lipid membrane-like environment. *Nature* 450:376-382.

28. Smit, A.B., N.I. Syed, D. Schaap, J. van Minnen, J. Klumperman, K.S. Kits, H. Lodder, R.C. van der Schors, R. van Elk, B. Sorgedrager, K. Brejc, T.K. Sixma, and W.P. Geraerts. 2001. A glia-derived acetylcholine-binding protein that modulates synaptic transmission. *Nature* 411:261-268.

29. Brejc, K., W.J. van Dijk, R.V. Klaassen, M. Schuurmans, J. van Der Oost, A.B. Smit, and T.K. Sixma. 2001. Crystal structure of an ACh-binding protein reveals the ligand-binding domain of nicotinic receptors. *Nature* 411:269-276.

30. Paterson, D., and A. Nordberg. 2000. Neuronal nicotinic receptors in the human brain. *Prog Neurobiol* 61:75-111.

31. Dougherty, D.A. 1996. Cation-pi interactions in chemistry and biology: a new view of benzene, Phe, Tyr, and Trp. *Science* 271:163-168.

32. Czajkowski, C., and A. Karlin. 1995. Structure of the nicotinic receptor acetylcholine-binding site. Identification of acidic residues in the delta subunit within 0.9 nm of the 5 alpha subunit-binding. *J Biol Chem* 270:3160-3164.

33. Fu, D.X., and S.M. Sine. 1994. Competitive antagonists bridge the alpha-gamma subunit interface of the acetylcholine receptor through quaternary ammonium-aromatic interactions. *J Biol Chem* 269:26152-26157.

34. Hansen, S.B., T.T. Talley, Z. Radic, and P. Taylor. 2004. Structural and ligand recognition characteristics of an acetylcholine-binding protein from Aplysia californica. *J Biol Chem* 279:24197-24202.

35. Miyazawa, A., Y. Fujiyoshi, and N. Unwin. 2003. Structure and gating mechanism of the acetylcholine receptor pore. *Nature* 423:949-955.

36. Purohit, P., A. Mitra, and A. Auerbach. 2007. A stepwise mechanism for acetylcholine receptor channel gating. *Nature* 446:930-933.

37. Jha, A., D.J. Cadugan, P. Purohit, and A. Auerbach. 2007. Acetylcholine receptor gating at extracellular transmembrane domain interface: the cys-loop and M2-M3 linker. *J Gen Physiol* 130:547-558.

38. Thompson, A.J., C.L. Padgett, and S.C. Lummis. 2006. Mutagenesis and molecular modeling reveal the importance of the 5-HT3 receptor F-loop. *J Biol Chem* 281:16576-16582.

39. Beckstein, O., and M.S. Sansom. 2006. A hydrophobic gate in an ion channel: the closed state of the nicotinic acetylcholine receptor. *Phys Biol* 3:147-159.

40. Xiu, X., A.P. Hanek, J. Wang, H.A. Lester, and D.A. Dougherty. 2005. A unified view of the role of electrostatic interactions in modulating the gating of Cys loop receptors. *J Biol Chem* 280:41655-41666.

41. Lummis, S.C., D.L. Beene, L.W. Lee, H.A. Lester, R.W. Broadhurst, and D.A. Dougherty. 2005. Cis-trans isomerization at a proline opens the pore of a neurotransmitter-gated ion channel. *Nature* 438:248-252.

42. Lee, W.Y., and S.M. Sine. 2005. Principal pathway coupling agonist binding to channel gating in nicotinic receptors. *Nature* 438:243-247.

43. Eldefrawi, M.E., A.T. Eldefrawi, S. Seifert, and R.D. O'Brien. 1972. Properties of lubrol-solubilized acetylcholine receptor from Torpedo electroplax. *Arch Biochem Biophys* 150:210-218.

44. Sobel, A., M. Weber, and J.P. Changeux. 1977. Large-scale purification of the acetylcholine-receptor protein in its membrane-bound and detergent-extracted forms from Torpedo marmorata electric organ. *Eur J Biochem* 80:215-224.

45. Edelstein, S.J., W.B. Beyer, A.T. Elderfrawi, and M.E. Elderfrawi. 1975. Molecular weight of the acetylcholine receptors of electric organs and the effect of Triton X-100. *J Biol Chem* 250:6101-6106.

46. Epstein, M., and E. Racker. 1978. Reconstitution of carbamylcholine-dependent sodium ion flux and desensitization of the acetylcholine receptor from Torpedo californica. *J Biol Chem* 253:6660-6662.

47. Changeux, J.P., T. Heidmann, J.L. Popot, and A. Sobel. 1979. Reconstitution of a functional acetylcholine regulator under defined conditions. *FEBS Lett* 105:181-187.

48. Nelson, N., R. Anholt, J. Lindstrom, and M. Montal. 1980. Reconstitution of purified acetylcholine receptors with functional ion channels in planar lipid bilayers. *Proc Natl Acad Sci U S A* 77:3057-3061.

49. Dalziel, A.W., E.S. Rollins, and M.G. McNamee. 1980. The effect of cholesterol on agonist-induced flux in reconstituted acetylcholine receptor vesicles. *FEBS Lett* 122:193-196.

50. Anholt, R., J. Lindstrom, and M. Montal. 1981. Stabilization of acetylcholine receptor channels by lipids in cholate solution and during reconstitution in vesicles. *J Biol Chem* 256:4377-4387.

51. Lee, A.G. 2004. How lipids affect the activities of integral membrane proteins. *Biochim Biophys Acta* 1666:62-87.

52. Barrantes, F.J. 2004. Structural basis for lipid modulation of nicotinic acetylcholine receptor function. *Brain Res Brain Res Rev* 47:71-95.

53. Gonzalez-Ros, J.M., M. Llanillo, A. Paraschos, and M. Martinez-Carrion. 1982. Lipid environment of acetylcholine receptor from Torpedo californica. *Biochemistry* 21:3467-3474.

54. Schiebler, W., and F. Hucho. 1978. Membranes rich in acetylcholine receptor: characterization and reconstitution to excitable membranes from exogenous lipids. *Eur J Biochem* 85:55-63.

55. Demel, R., G. Schiavo, B. de Kruijff, and C. Montecucco. 1991. Lipid interaction of diphtheria toxin and mutants. A study with phospholipid and protein monolayers. *Eur J Biochem* 197:481-486.

56. Ochoa, E.L., A.W. Dalziel, and M.G. McNamee. 1983. Reconstitution of acetylcholine receptor function in lipid vesicles of defined composition. *Biochim Biophys Acta* 727:151-162.

57. Ellena, J.F., M.A. Blazing, and M.G. McNamee. 1983. Lipid-protein interactions in reconstituted membranes containing acetylcholine receptor. *Biochemistry* 22:5523-5535.

58. Fong, T.M., and M.G. McNamee. 1986. Correlation between acetylcholine receptor function and structural properties of membranes. *Biochemistry* 25:830-840.

59. Sunshine, C., and M.G. McNamee. 1992. Lipid modulation of nicotinic acetylcholine receptor function: the role of neutral and negatively charged lipids. *Biochim Biophys Acta* 1108:240-246.

60. Rankin, S.E., G.H. Addona, M.A. Kloczewiak, B. Bugge, and K.W. Miller. 1997. The cholesterol dependence of activation and fast desensitization of the nicotinic acetylcholine receptor. *Biophys J* 73:2446-2455.

61. Ryan, S.E., C.N. Demers, J.P. Chew, and J.E. Baenziger. 1996. Structural effects of neutral and anionic lipids on the nicotinic acetylcholine receptor. An infrared difference spectroscopy study. *J Biol Chem* 271:24590-24597.

62. Sunshine, C., and M.G. McNamee. 1994. Lipid modulation of nicotinic acetylcholine receptor function: the role of membrane lipid composition and fluidity. *Biochim Biophys Acta* 1191:59-64.

63. Baenziger, J.E., K.W. Miller, and K.J. Rothschild. 1993. Fourier transform infrared difference spectroscopy of the nicotinic acetylcholine receptor: evidence for specific protein structural changes upon desensitization. *Biochemistry* 32:5448-5454.

64. Bhushan, A., and M.G. McNamee. 1993. Correlation of phospholipid structure with functional effects on the nicotinic acetylcholine receptor. A modulatory role for phosphatidic acid. *Biophys J* 64:716-723.

65. Baenziger, J.E., K.W. Miller, M.P. McCarthy, and K.J. Rothschild. 1992. Probing conformational changes in the nicotinic acetylcholine receptor by Fourier transform infrared difference spectroscopy. *Biophys J* 62:64-66.

66. Baenziger, J.E., K.W. Miller, and K.J. Rothschild. 1992. Incorporation of the nicotinic acetylcholine receptor into planar multilamellar films: characterization by fluorescence and Fourier transform infrared difference spectroscopy. *Biophys J* 61:983-992.

67. McCarthy, M.P., and M.A. Moore. 1992. Effects of lipids and detergents on the conformation of the nicotinic acetylcholine receptor from Torpedo californica. *J Biol Chem* 267:7655-7663.

68. Jones, O.T., and M.G. McNamee. 1988. Annular and nonannular binding sites for cholesterol associated with the nicotinic acetylcholine receptor. *Biochemistry* 27:2364-2374.

69. Butler, D.H., and M.G. McNamee. 1993. FTIR analysis of nicotinic acetylcholine receptor secondary structure in reconstituted membranes. *Biochim Biophys Acta* 1150:17-24.

70. Fong, T.M., and M.G. McNamee. 1987. Stabilization of acetylcholine receptor secondary structure by cholesterol and negatively charged phospholipids in membranes. *Biochemistry* 26:3871-3880.

71. Methot, N., C.N. Demers, and J.E. Baenziger. 1995. Structure of both the ligand- and lipid-dependent channel-inactive states of the nicotinic acetylcholine receptor probed by FTIR spectroscopy and hydrogen exchange. *Biochemistry* 34:15142-15149.

72. Baenziger, J.E., M.L. Morris, T.E. Darsaut, and S.E. Ryan. 2000. Effect of membrane lipid composition on the conformational equilibria of the nicotinic acetylcholine receptor. *J Biol Chem* 275:777-784.

73. daCosta, C.J., A.A. Ogrel, E.A. McCardy, M.P. Blanton, and J.E. Baenziger. 2002. Lipid-protein interactions at the nicotinic acetylcholine receptor. A functional coupling between nicotinic receptors and phosphatidic acid-containing lipid bilayers. *J Biol Chem* 277:201-208.

74. daCosta, C.J., I.D. Wagg, M.E. McKay, and J.E. Baenziger. 2004. Phosphatidic acid and phosphatidylserine have distinct structural and functional interactions with the nicotinic acetylcholine receptor. *J Biol Chem* 279:14967-14974.

75. Hamouda, A.K., M. Sanghvi, D. Sauls, T.K. Machu, and M.P. Blanton. 2006. Assessing the lipid requirements of the Torpedo californica nicotinic acetylcholine receptor. *Biochemistry* 45:4327-4337.

76. daCosta, C.J., S.A. Medaglia, N. Lavigne, C.L. Carswell, and J.E. Baenziger. 2009. The Role of Anionic Lipids in the Bi-directional Interaction between the Nicotinic Acetylcholine Receptor and its Environment. In Submitted.

77. Bligh, E.G., and W.J. Dyer. 1959. A rapid method of total lipid extraction and purification. *Can J Biochem Physiol* 37:911-917.

78. Furimsky, A., N. Vuong, H. Xu, P. Kumarathasan, M. Xu, W. Weerachatyanukul, M. Bou Khalil, M. Kates, and N. Tanphaichitr. 2005. Percoll gradient-centrifuged capacitated mouse sperm have increased fertilizing ability and higher contents of sulfogalactosylglycerolipid and docosahexaenoic acid-containing phosphatidylcholine compared to washed capacitated mouse sperm. *Biol Reprod* 72:574-583.

79. daCosta, C.J., and J.E. Baenziger. 2003. A rapid method for assessing lipid:protein and detergent:protein ratios in membrane-protein crystallization. *Acta Crystallogr D Biol Crystallogr* 59:77-83.

80. Herz, J.M., D.A. Johnson, and P. Taylor. 1987. Interaction of noncompetitive inhibitors with the acetylcholine receptor. The site specificity and spectroscopic properties of ethidium binding. *J Biol Chem* 262:7238-7247.

81. Methot, N., and J.E. Baenziger. 1998. Secondary structure of the exchange-resistant core from the nicotinic acetylcholine receptor probed directly by infrared spectroscopy and hydrogen/deuterium exchange. *Biochemistry* 37:14815-14822.

82. Baenziger, J.E., S.E. Ryan, M.M. Goodreid, N.Q. Vuong, R.M. Sturgeon, and C.J. daCosta. 2008. Lipid composition alters drug action at the nicotinic acetylcholine receptor. *Mol Pharmacol* 73:880-890.

83. daCosta, C.J., and J.E. Baenziger. 2009. A lipid-dependent Uncoupled Conformation of the Acetylcholine Receptor. Submitted.

84. Tamm, L.K., and S.A. Tatulian. 1997. Infrared spectroscopy of proteins and peptides in lipid bilayers. *Q Rev Biophys* 30:365-429.

85. Pavia, D.L., G.M. Lampman, and G.S. Kriz. 1996. Introduction to Spectroscopy: A Guide for Students of Organic Chemistry. Harcourt Brace College Publishers, Orlando, Florida. 463. pp.

86. Sanchez-Ruiz, J.M., and M. Martinez-Carrion. 1988. A Fourier-transform infrared spectroscopic study of the phosphoserine residues in hen egg phosvitin and ovalbumin. *Biochemistry* 27:3338-3342.

87. Demel, R.A., C.C. Yin, B.Z. Lin, and H. Hauser. 1992. Monolayer characteristics and thermal behaviour of phosphatidic acids. *Chem Phys Lipids* 60:209-223.

88. Trauble, H., and H. Eibl. 1974. Electrostatic effects on lipid phase transitions: membrane structure and ionic environment. *Proc Natl Acad Sci U S A* 71:214-219.

89. Knight, C.G., and T. Stephens. 1989. Xanthene-dye-labelled phosphatidylethanolamines as probes of interfacial pH. Studies in phospholipid vesicles. *Biochem J* 258:683-687.

90. Soucaille, P., M. Prats, J.F. Tocanne, and J. Teissie. 1988. Use of a fluorescein derivative of phosphatidylethanolamine as a pH probe at water/lipid interfaces. *Biochim Biophys Acta* 939:289-294.

91. Petrossian, A., A.B. Kantor, and J.C. Owicki. 1985. Synthesis and characterization of a highly fluorescent peptidyl-phosphatidylethanolamine. *J Lipid Res* 26:767-773.

92. Thelen, M., G. Petrone, P.S. O'Shea, and A. Azzi. 1984. The use of fluorescein-dipalmitoylphosphatidylethanolamine for measuring pH-changes in the internal compartment of phospholipid vesicles. *Biochim Biophys Acta* 766:161-168.

93. Yaeagle, P.L., editor. 2005. The Structure of Biological Membranes. CRC Press, Boca Raton, Florida. 180-183 pp.

94. Hubner, W., H.H. Mantsch, F. Paltauf, and H. Hauser. 1994. Conformation of phosphatidylserine in bilayers as studied by Fourier transform infrared spectroscopy. *Biochemistry* 33:320-326.

95. Moczydlowski, E., O. Alvarez, C. Vergara, and R. Latorre. 1985. Effect of phospholipid surface charge on the conductance and gating of a Ca2+-activated K+ channel in planar lipid bilayers. *J Membr Biol* 83:273-282.

96. Bell, J. 1985. Protons decrease the single channel conductance of the sarcoplasmic reticulum K+ channel in neutral and negatively charged bilayers. *Biophys J* 48:349-353.

97. Bell, J.E., and C. Miller. 1984. Effects of phospholipid surface charge on ion conduction in the K+ channel of sarcoplasmic reticulum. *Biophys J* 45:279-287.

98. Guo, X., and R.A. Lester. 2007. Regulation of nicotinic acetylcholine receptor desensitization by Ca2+. *J Neurophysiol* 97:93-101.

99. McLaughlin, J.T., J. Fu, A.D. Sproul, and R.L. Rosenberg. 2006. Role of the outer beta-sheet in divalent cation modulation of alpha7 nicotinic receptors. *Mol Pharmacol* 70:16-22.

100. Lindstrom, J. 2006. Potentiation of acetylcholine receptors by divalent cations. *Mol Pharmacol* 70:5-7.

101. Galzi, J.L., S. Bertrand, P.J. Corringer, J.P. Changeux, and D. Bertrand. 1996. Identification of calcium binding sites that regulate potentiation of a neuronal nicotinic acetylcholine receptor. *Embo J* 15:5824-5832.

102. Jasti, J., H. Furukawa, E.B. Gonzales, and E. Gouaux. 2007. Structure of acid-sensing ion channel 1 at 1.9 A resolution and low pH. *Nature* 449:316-323.

103. Bocquet, N., L. Prado de Carvalho, J. Cartaud, J. Neyton, C. Le Poupon, A. Taly, T. Grutter, J.P. Changeux, and P.J. Corringer. 2007. A prokaryotic proton-gated ion channel from the nicotinic acetylcholine receptor family. *Nature* 445:116-119.

104. Lunin, V.V., E. Dobrovetsky, G. Khutoreskaya, R. Zhang, A. Joachimiak, D.A. Doyle, A. Bochkarev, M.E. Maguire, A.M. Edwards, and C.M. Koth. 2006. Crystal structure of the CorA Mg2+ transporter. *Nature* 440:833-837.

105. Clayden, J., N. Greeves, S. Warren, and P. Wothers. 2001. Organic Chemistry. New York, NY. 346-350 pp.

106. Wymann, M.P., and R. Schneiter. 2008. Lipid signalling in disease. *Nat Rev Mol Cell Biol* 9:162-176.

107. Allen, J.A., R.A. Halverson-Tamboli, and M.M. Rasenick. 2007. Lipid raft microdomains and neurotransmitter signalling. *Nat Rev Neurosci* 8:128-140.

108. Zhu, D., W.C. Xiong, and L. Mei. 2006. Lipid rafts serve as a signaling platform for nicotinic acetylcholine receptor clustering. *J Neurosci* 26:4841-4851.

109. Hosie, A.M., M.E. Wilkins, H.M. da Silva, and T.G. Smart. 2006. Endogenous neurosteroids regulate GABAA receptors through two discrete transmembrane sites. *Nature* 444:486-489.

110. Brannigan, G., J. Henin, R. Law, R. Eckenhoff, and M.L. Klein. 2008. Embedded cholesterol in the nicotinic acetylcholine receptor. *Proc Natl Acad Sci U S A* 105:14418-14423.

111. Ortiz-Miranda, S.I., J.A. Lasalde, P.A. Pappone, and M.G. McNamee. 1997. Mutations in the M4 domain of the Torpedo californica nicotinic acetylcholine receptor alter channel opening and closing. *J Membr Biol* 158:17-30.

112. Lee, Y.H., L. Li, J. Lasalde, L. Rojas, M. McNamee, S.I. Ortiz-Miranda, and P. Pappone. 1994. Mutations in the M4 domain of Torpedo californica acetylcholine receptor dramatically alter ion channel function. *Biophys J* 66:646-653.

113. Bouzat, C., F. Gumilar, M. del Carmen Esandi, and S.M. Sine. 2002. Subunit-selective contribution to channel gating of the M4 domain of the nicotinic receptor. *Biophys J* 82:1920-1929.

CONTRIBUTION OF COLLABORATORS

- Jon Labriola: Performed the Fln and CFPE experiments in vesicles without nAChR, and performed the preliminary work on the nAChR-reconstituted proteoliposomes with incorporated CFPE.
- Nadine Lavigne: Performed several purification and reconstitutions for the experiments described.
- Shuzhi Wang: Performed several purification and reconstitutions for the experiments described, as well as a large portion of the TLC plates aimed at identifying the contaminants/impurities.

CURRICULUM VITAE

NAME:
STURGEON, Raymond M., MSc. Candidate
Member of the School of Graduate Studies and Research
University of Ottawa

DEGREES:
B.Sc. (honours), Biochemistry, University of Ottawa, Canada, 2005.

WORK EXPERIENCE:

1. Teaching Assistant for *Protein Structure and Function* at the University of Ottawa (course code: BCH3125). January to April, 2006-2008. Meeting with students, both individually and in organized tutorial sessions, answering questions regarding subject material. Marking of assignments, quizzes and midterms.

2. Summer student in laboratory of Dr. John E. Baenziger at the University of Ottawa. May to September, 2004. General and specialized laboratory work performed as preparation for honours research project for 4th year studies.

3. Inventory Controller, Nortel Networks. November 1999 to January 2004. Duties ranged from project-oriented tasks and customer service to inventory tracking and categorization. Both part-time (15 hours/week) and full-time (40 hours/week) experience.

ACHIEVEMENTS:

1. Poster presentation at the **52nd Annual Biophysical Society Meeting** (refereed) in Long Beach, Calif. U.S.A. Feb, 2008.

2. 2nd place (Biochemistry Master's Student) in Graduate Poster Session, 2006.

3. Graduated, Honours Biochemistry, University of Ottawa, 2005.

4. 2nd place (Biochemistry Section) in 4th Year Honours Thesis Poster Presentation, 2005.

PUBLICATIONS:

Articles published in refereed journals

1. John E. Baenziger, Stephen E. Ryan, Michael M. Goodreid, Ngoc Q. Vuong, Raymond M. Sturgeon, and Corrie J. B. daCosta. **Lipid composition alters drug action at the nicotinic acetylcholine receptor.** (2008). *Mol Pharm* **73**, 880-890.

Refereed abstracts

1. Raymond M. Sturgeon and John E. Baenziger. **Interplay of Cations, Anionic Lipids and Lipid-Protein Interactions at the Nicotinic Acetylcholine Receptor.** Biophysical Society Meeting Abstracts. *Biophysical Journal, Supplement*, Abstract, 1406-Pos.

Non-refereed contributions

1. R. Michel Sturgeon and John. E. Baenziger. **Role of Lipid Ionization in Nicotinic Receptor-lipid Interactions** *(Honours Thesis).*

2. R. Michel Sturgeon and John E. Baenziger. Poster Presentation (Fourth Year). **Role of Lipid Ionization in Nicotinic Receptor-lipid Interactions** *(Honours Thesis).*